Functional Analysis of *MDY2*, a Novel Gene Required for

Mating of the Yeast *Saccharomyces cerevisiae*

INAUGURAL-DISSERTATION

zur

Erlangung des Doktorgrades

der

Mathematisch-Naturwissenschaftlichen Fakultät

der Heinrich-Heine-Universität Düsseldorf

vorgelegt von

Zheng HU

aus Hangzhou, China

Düsseldorf 2004

Gedruckt mit der Genehmigung der Mathematisch-Naturwissenschaftlichen Fakultät der Heinrich-Heine-Universität Düsseldorf

Referent: Prof. Dr. C. P. Hollenberg

Korreferent: Prof. Dr. Th. Lisowsky

Korreferent: Priv.-Doz. Dr. M. Ramezani Rad

Tag der mündlichen Prüfung: 25. Mai 2004

Contents

3 Results   40

1. Introduction

One of the oldest questions in biology is how cells sense and discriminate between various environmental stimuli and then translate these inputs into an appropriate intracellular response (review Dohlman and Thorner, 2001). In the *S. cerevisiae*, environmental stimuli of various kinds can induce a diversity of processes including mating and spore formation, as well as developmental responses triggered by starvation, high extracellular osmilarity and damage to the cell wall (review Herskowitz, 1995). Among these, the mating process is one of the best studied examples of a cellular response to an environmental stimulus (Elion, 2001).

1.1 Mating process of *S. cerevisiae*

Haploid *S. cerevisiae* cells occur in two mating types, **a** cells and α cells, which depend on the genetic constitution at the *MAT* locus. Haploid cells can also switch mating type by transferring genetic information from one of two silent storage sites, termed *HML* and *HMR*, into the *MAT* locus. Haploid cells signal to each other by means of peptide pheromones. *MAT*α cells secrete α-factor, whereas *MAT***a** cells secrete **a**-factor. Mature extracellular α-factor is a 13-residue peptide and is generated from larger precursors that are encoded by two genes, *MFα1* and *MFα2*. The majority of extracellular α-factor is derived from *MFα1* (review Fuller *et al.*, 1988). Mature extracellular **a**-factor is a 12-residue peptide that carries two posttranslational modifications. The bioactive **a**-factor is also generated from precursors that are encoded by two genes, *MFA1* and *MFA2*. The majority of extracellular **a**-factor is derived from the product of the *MFA1* gene (Anderegg *et al.*, 1988; Michaelis and Herskowitz, 1988; review Sprague and Thorner, 1992). In yeast, **a**-factor and α-factor are released from the cells by two very different routes. α-Factor is produced as a larger prepro-α-factor that is translocated into the endoplasmic reticulum, processed to its mature form in the Golgi compartment, and released from cells in secretory vesicles (Fuller *et al.*, 1988; Brake *et al.*, 1989; Roberg *et al.*, 1997). However, pro-**a**-factor is produced and processed in the cytosol (Boyartchuk and Rine, 1998; Schmidt *et al.*, 2000) and secreted by Ste6, a dedicated ATP-binding cassette transporter that resides in the plasma membrane (Kuchler *et al.*, 1993; Michaelis, 1993; Kolling and Hollenberg, 1994; Kolling and Losko, 1997; Ketchum *et al.*, 2001).

The receptors for **a**-factor and α-factor are encoded by *STE3* in *MAT*α cells and *STE2* in *MAT***a** cells respectively, and they are members of the large family of G-protein-coupled receptors characterized by seven transmembrane domains (Sprague *et al.*, 1983; Burkholder and Hartwell, 1985). The binding of pheromone to receptor stimulates three major responses: (1) transcriptional induction of genes involved in mating, (2) arrest of the cells in G_1 phase, and (3) morphological changes (review Herskowitz, 1995). The targets affected include many genes whose functions are required for

pheromone production and the pheromone response and genes that encode products which facilitate or actually participate in cell pairing, cell cycle arrest and subsequent recovery from the arrested state, and for the morphological events required for mating (Sprague and Thorner, 1992). One of the earliest effects of pheromone reception is that cell cycle progression is blocked at a position in the division cycle late in the G_1 phase. This is prior to bud emergence, spindle pole body duplication, and the initiation of DNA synthesis (Pringle and Hartwell, 1981). Morphological changes ensue because mating cells can sense the direction from which the pheromone emanating from a mating partner impinges upon them; the receiving cell then undergoes polarized growth, forming a projection that is directed towards the source. This response is termed chemotropism and is thought to involve the generation of an internal landmark that reflects the direction of incidence of the

a-Factor

α-Factor

a-Cells (1n)   **α -Cells (1n)**

Cell Cycle Arrest

Shmoo

Zygote

Budding Zygote

Diploid Cells (2n)
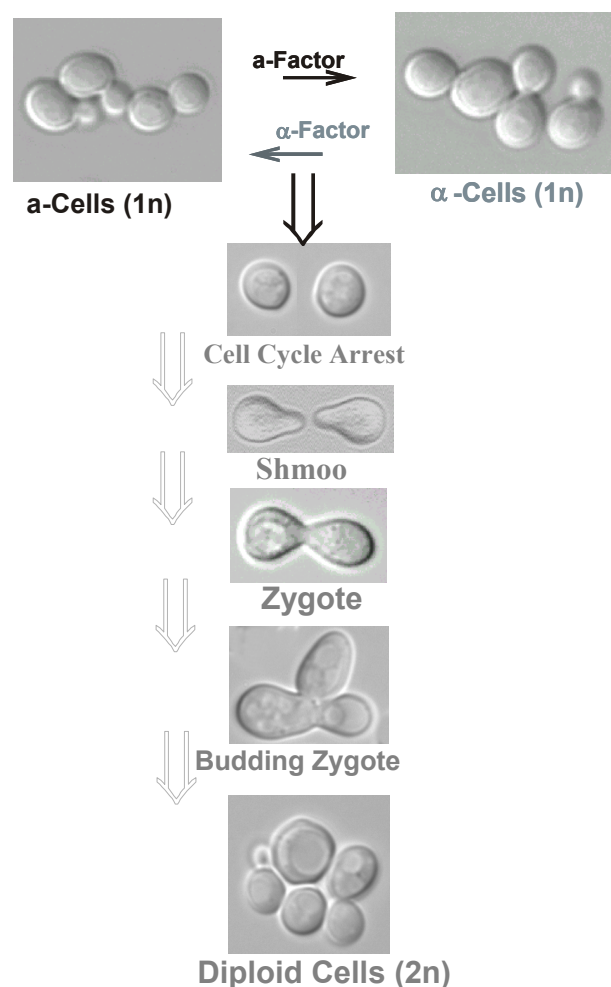
Fig1.1.
Schematic diagram of the mating process of yeast *S. cerevisiae*

external pheromone signal, and this overrides the internal spatial cues that normally control bud formation (Arkowitz, 1999; Chant, 1999). Formation of projections is mediated by the actin cytoskeleton and by many other proteins (e.g., Spa2, Pea2, Bem1, and Cdc42) that normally control bud emergence, giving rise to an asymmetric organization of the cytoskeleton, secretory system, plasma membrane and cell wall along the axis defined by the pheromone source (Herskowitz *et al*, 1995; Roemer *et al*, 1996). Formation of the mating projection concentrates the components involved

in cell adhesion (agglutinins), signalling (pheromones and pheromone receptors), and fusion (Fus2) in the area of future cell contact and fusion. The proteins (α-factor, **a**-factor, Ste2, Ste3) that function specifically in these processes are all highly localized to the mating projections or their tips (Sprague and Thorner, 1992; Elion, 1995). Polarized mating cells, which are referred to as "shmoos", signal to one another through the projection, and thereby mutually direct growth to a site of cell contact and fusion. Many cell polarization-related genes also function in the cell fusion pathway, as indicated by the cell fusion defects observed in strains that are mutant for such genes (e.g., *SPA2*, *PEA2*, *BNI1*, *RVS161, PRM1*) (Dorer *et al.*, 1997; Heiman and Walter, 2000). Cell fusion usually occurs at the tips of the projections by formation of a conjugation tube or bridge. Nuclear fusion (karyogamy) is the last stage in the mating process and involves at least two major steps. First, cytoplasmic microtubules emanating from the spindle pole body (SPB) bring the nuclei into close proximity, in a process called congression. The second step, karyogamy, entails the fusion of the nuclear membranes (review Rose, 1996). Then the zygote undergoes meiosis, and subsequently re-enters the vegetative cell cycle.

Although the cytological events involved in yeast mating have been well described, the molecular components and mechanisms important for mating cell morphogenesis, cell fusion and nuclear fusion are not well understood. Further work will be necessary to identify all the genes which are required for mating in yeast. In this study a strategy was devised to identify mating-specific genes using a reversed genetic method that depends on assessing the mating phenotype of a collection of single gene deletion mutants. To detect genes that produce a weak phenotype, we determined the mating efficiency of each deletion mutant in *MAT***a** and *MAT*α cells crossed with a wild-type strain and the bilateral mating efficiency of a cross between the same deletants. Single gene deletion mutants with reduced mating efficiency were initially identified in the context of the EUROFAN project. The characterization of single gene deletion mutants with respect to pheromone production, pheromone response, morphogenesis, cell fusion and nuclear fusion revealed the specific defect(s) of mutants and provided additional insights into each gene's function in the mating process.

1.2 Pheromone response pathway of *S. cerevisiae*

S. cerevisiae uses mitogen-activated protein kinase (MAPK) cascades to respond to a wide variety of signals that regulate cellular responses. A typical MAPK cascade consists of three kinases: a MAP kinase kinase kinase (MAPKKK or MEKK), a MAP kinase kinase (MAPKK or MEK), and a MAP kinase (MAPK). When such a cascade is activated, the MAPKKK first phosphorylates the MAPKK, which in turn phosphorylates the MAPK (review Gustin *et al.*, 1998). In *S. cerevisiae*, five MAPK signalling pathways have been identified, which regulate mating, the osmotic-stress response, cell-wall integrity, filamentous growth, and spore wall formation (Herskowitz, 1995; Gustin *et al.*, 1998). There are also indications that a MAPK signaling pathway involving the reaction sequence: the *S. cerevisiae* Sho1→Ste20/Ste50→Ste11→Ste7→Kss1 contributes to the maintenance of cell wall

integrity in vegetative cells (Lee and Elion, 1999; Cullen *et al*., 2000). The *S. cerevisiae* mating pheromone response pathway represents a well-characterized MAPK signaling pathway that controls the formation of diploid cells from two haploid cells (Bardwell *et al*., 1994). The pheromone receptors (Ste2 and Ste3) each have seven transmembrane domains; the third intracellular loop is involved in G-protein coupling, and the cytoplasmic carboxy-terminal domain mediates ligand-induced endocytosis and desensitization (Leberer *et al.*, 1997; Hicke, 1999). Binding of pheromone to its cognate receptor (Ste2 or Ste3) leads to exchange of GDP for GTP on $G\alpha$ and dissociation of the heterotrimeric G-protein (G_α, G_β and G_γ). The $G_{\beta\gamma}$ heterodimer can then interact with its downstream effectors Ste20 and Ste5 (Whiteway *et al*., 1995; Leeuw *et al*., 1998). Ste20 is a PAK (p21-activated kinase)-related protein kinase, which phosphorylates the MAPKKK Ste11 (Wu *et al*., 1995; Pryciak and Huntress, 1998; Drogen *et al*., 2000).
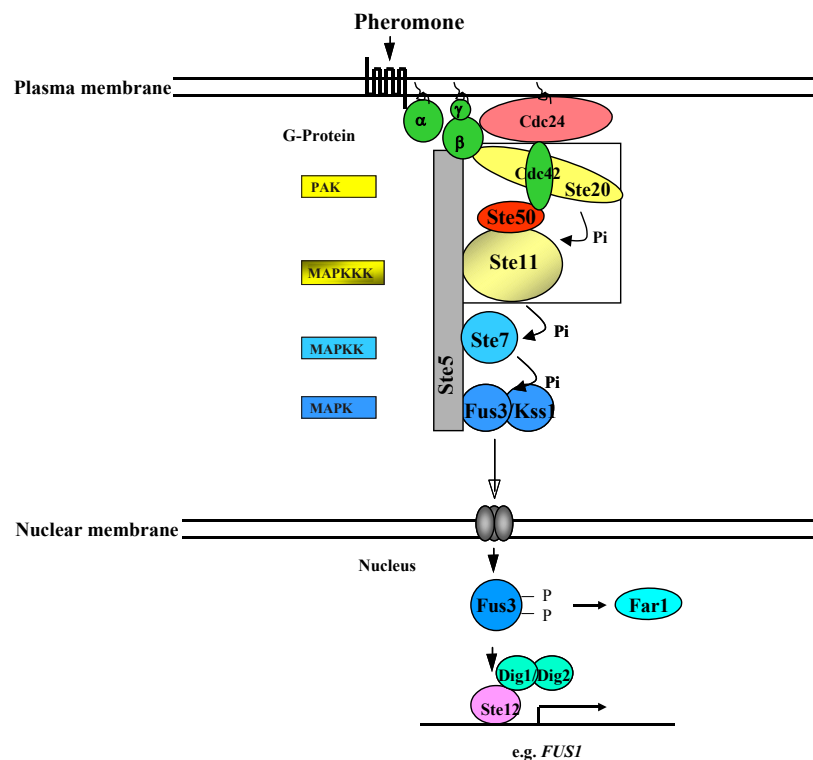
Fig 1.2 Schematic diagram of the mating pheromone response pathway of *S. cerevisiae*

Ste50 is associated with Ste11, and acts as an adaptor that links the G protein-associated Cdc42-Ste20 kinase complex to the effector MAPKKK Ste11 (Ramezani-Rad, 2003). Ste5 acts as a scaffold upon which the protein kinases Ste11 (the MAPKKK), Ste7 (the MAPKK), and Fus3 and Kss1 (MAPKs) can assemble and be efficiently activated. Results from a variety of experiments suggest that Ste5 must shuttle in and out of the nucleus to enable it to be recruited to the plasma membrane and activate Fus3 (Mahanty *et al*., 1999). Whether Ste5 migrates into and out of the nucleus alone or in a complex with the MAPK cascade kinases is not yet known (Elion, 2001; Van Drogen *et al*., 2001). Activation of the MAPKs Fus3 and Kss1 (which show partial functional overlap) results in the phosphorylation

of numerous substrates, including pathway components such as Far1, the transcription factor Ste12, and the Ste12 repressors Dig1 and Dig2. Fus3-dependent phosphorylation leads to the stabilization of Far1 (review Dohlman and Thorner, 2001; Zeitlinger *et al*., 2003). Phosphorylation of the transcriptional repressors Dig1 and Dig2 by Fus3 is thought to trigger their dissociation from the transcriptional activator Ste12 (Cook *et al*., 1996, Tedford *et al*., 1997). Activated Ste12 in turn is thought to induce transcription of the mating-specific genes. Deletion of both MAPKs (Fus3 and Kss1), but not either one alone, abolishes Ste12-dependent induction of mating genes in response to pheromone (Breitkreutz *et al*., 2001; Roberts *et al*., 2000).

In this study, a novel gene, *MDY2*, was characterized. Phenotypic analysis of *mdy2* mutants indicated that *MDY2* is required for mating in *S. cerevisiae*, and influences the pheromone-induced formation of the mating projection and, to a lesser extent, pheromone-induced G_1 arrest. The effects of overexpression of *MDY2* confirmed that the gene plays an important role in the regulation of the mating pheromone response pathway.

1.3 The Ste5 scaffold

The *STE5* gene was identified in screens for mutants that were unable to mate or undergo G_1 arrest in the presence of mating pheromone (Mackay and Manney, 1974; Hartwell, 1980). Subsequent cloning of the *STE5* gene and analysis of strains harboring *ste5* null mutations demonstrated that the Ste5 protein positively regulates mating (Leberer *et al*., 1993; Mukai *et al*., 1993). Subsequently, epistasis tests provided evidence for its essential role in signalling, and indicated that it functions between Ste20 and Ste11 (MAPKKK) in the MAPK cascade (Blinder *et al*., 1989; Leberer *et al*., 1993; Hasson *et al*., 1993). Ste5 was then defined as a scaffold upon which the protein kinases Ste11, Ste7, Fus3 and Kss1 can assemble and be efficiently activated. Elion and co-workers have suggested that Ste5 selectively associates with Ste11, Ste7 and binds to the MAPK cascade kinases through separable binding sites (Choi *et al*., 1994; Kranz *et al*., 1994), and that Ste5 binds the kinases simultaneously. This conclusion is based on co-sedimentation of the kinases from the wild type in a glycerol gradient and the lack of such a co-sedimentation pattern upon removal of Ste5 (Elion, 1995; Choi *et al*., 1999).

The recruitment of Ste5 to Gβγ at the plasma membrane is regulated, and involves the prior shuttling of Ste5 through the nucleus. Localization studies show that Ste5 is found both in the cytoplasm and in the nucleus (Pryciak and Huntress, 1998; Mahanty *et al*., 1999; Kunzler *et al*., 2001), and undergoes rapid recruitment to the plasma membrane in the presence of mating pheromone and cycloheximide (Mahanty *et al*., 1999), subsequently accumulating at the tip of the emerging mating projection (Pryciak and Huntress, 1998; Mahanty *et al*., 1999). The cytoplasmic pool of Ste5 shuttles continuously into and out of the nucleus, and nuclear shuttling requires the Kap95 (Rsl1) import receptor and the Msn5 (Ste21 or Kap142) export receptor (Mahanty *et al*., 1999).

Elion (2001) has proposed that Ste5 exists in two forms: (1) a less active, folded or closed monomer or dimer in which the RING-H2 domain is not available to bind Gβγ and signalling is repressed; and (2) an open, active dimer of parallel strands in which the RING-H2 domain binds to Gβγ and interactions involving the N- and C-termini drive head to tail multimerization of adjacent Ste5 dimers (Fig 1.3). This event might result in a global rearrangement that could position the kinases for recognition by Ste20. Moreover, simple concentration of the kinases by multimerization of Ste5 might itself be sufficient to drive activation of the MAPK independently of any contribution by Gβγ and Ste20 (Robinson *et al*., 1998; Kieran *et al*., 1999).
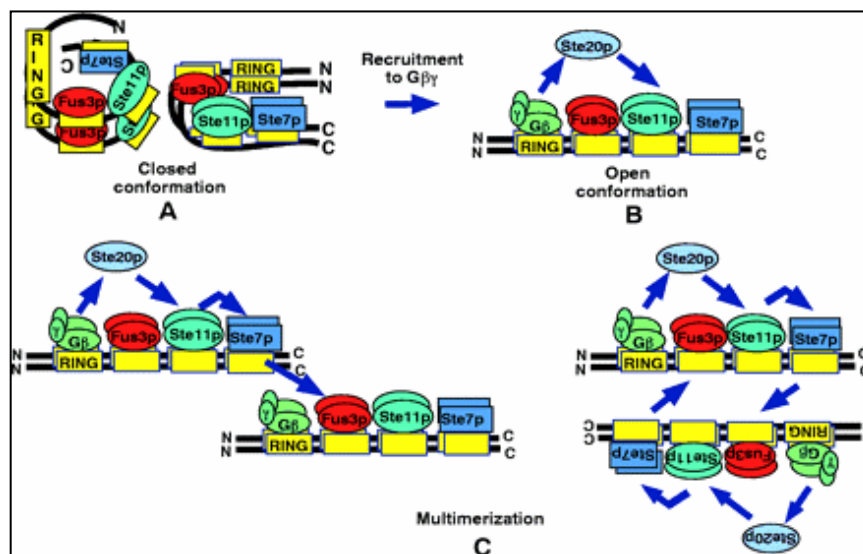
Fig 1.3. Ste5 oligomerization/recruitment model (Elion, 2001). (A) a Ste5 dimer can exist with a protected RING-H2 domain as a fold dimer of parallel strands or dimer of anti-parallel strands. (B) An open dimer of parallel strands in which the RING-H2 domain is accessible to homo-dimerize and bind Gβγ. (C) Higher-order oligomers can form through N- to C-terminal interactions, the binding of Gβγ driving the formation of higher-order oligomers at the plasma membrane by interfering with intramolecular interactions. Two types of high-order oligomer are shown: tandem head-to-tail oligomers and stacked anti-parallel oligomers.

Recent evidence shows that oligomerization indeed affects Ste5 activity and localization. The majority of Ste5 is monomeric (perhaps <1% of Myc-tagged Ste5 is oligomerized) and oligomerization is tightly regulated. The key determinant of oligomerization is the RING-H2 domain. Fusing GST to Ste5 greatly increases the size of the pool of oligomers, and Ste5-GST is more efficiently exported from the nucleus and is retained by Ste11 in the cytoplasm. Mutational analysis suggests that the leucine-rich domain limits the accessibility of the RING-H2 domain, and inhibits export from the nucleus and recruitment to the cytoplasmic membrane, in addition to promoting association with, and activation of, Ste11. Thus it appears that oligomerization of Ste5 positively regulates nuclear shuttling, recruitment to the membrane, association with signalling components, and

the ability to activate the MAPK cascade, and that the activation of Ste5 involves a conformational switch from an inactive monomer to an active dimer (Wang and Elion, 2003).

In this study, I have used two-hybrid assays to look for interaction between Mdy2 and Ste5, and the effect of Mdy2 upon the Ste5 scaffold was also investigated. It is shown that Mdy2 interacts with Ste5 and that there is a much higher level of GST-Ste5, but not of Myc-Ste5, in the *mdy2* mutant than in the wild-type strain in the absence or presence of α-factor. Mdy2 was also found to interact with Fus3, and the next section discusses the function of Fus3 in more detail.

1.4 The MAPK Fus3

The MAPKs Fus3 and Kss1 are Ser/Thr-specific protein kinases, which play partially overlapping roles in the mating response. *FUS3* was first identified as a $cdc2^+$/CDC28 related kinase, and is required both for the arrest of cells in G_1 and for mating (Elion *et al*., 1990). *fus3* null mutants are defective in G_1 arrest whereas *kss1* null mutants are not, suggesting that Fus3 plays a more important role in the control of G_1 arrest than Kss1 (Elion *et al*., 1990, 1991; Cherkasova *et al*., 1999). The defect of *fus3* null mutants in G_1 arrest is due to the fact that activation of the cyclin-dependent kinase inhibitor Far1 is almost completely dependent on phosphorylation by Fus3, and thus Fus3 is the major kinase required for the repression of G_1/S cyclin genes and thus for cell cycle arrest (Tyers and Futcher, 1993; Cherkasova *et al*., 1999). Fus3 also plays essential roles in projection formation, partner selection, and cell fusion that are not shared by Kss1 (Elion *et al*., 1990; Farley *et al*., 1999). That Fus3 is more critical than Kss1 for the response to mating pheromone is consistent with the fact that *FUS3* is expressed predominantly in haploids and is induced by mating pheromone (Elion *et al*., 1990), whereas the *KSS1* gene is constitutively expressed in both haploids and diploids (Ma *et al*., 1995).

During vegetative growth, Fus3 is largely unphosphorylated and inactive (Gartner *et al*., 1992; Elion *et al*., 1993). In the presence of mating pheromone, Fus3 is rapidly phosphorylated and activated by Ste7.   Activated Fus3, like other MAP kinases from stimulated eukaryotic cells, is highly phosphorylated on tyrosine and threonine residues that are conserved among all members of this protein kinase family (Gartner *et al*., 1992; Elion *et al*., 1993; Errede *et al*., 1993; review Nishida and Gotoh, 1993). The activation of Fus3 can be viewed as a two-step process. First, autophosphorylation results in the formation of a small quantity of tyrosine-phosphorylated Fus3.   Second, signal transduction leading to the activation of Fus3 proceeds through Ste11 to Ste7, which in turn phosphorylates both the unphosphorylated and tyrosine-phosphorylated form of Fus3.   As autophosphorylation of Fus3 occurs only on tyrosine, Ste7-dependent phosphorylation of the threonine residue is absolutely required for Fus3 activation and efficient phosphorylation of target substrates, including Ste12 and Far1 (Elion *et al*., 1993).   Once Fus3 is activated by Ste7-dependent phosphorylation, a number of factors help to limit the active lifetime of the MAPK. One particularly

important mechanism involves the dephosphorylation of either Tyr or Thr, which inactivates Fus3. Fus3 is inactivated by at least three phosphatases (Msg5, Ptp2 and Ptp3), presumably to allow cells to recover and re-enter the mitotic cycle in the absence of mating pheromone (Doi *et al*., 1994; Zhan *et al*., 1997; review Dohlman and Thorner, 2001).

The subcellular localization of the MAPK Fus3 has recently been examined (Van Drogen *et al*., 2001; Blackwell *et al*., 2003). Van Drogen *et al*. (2001) reported that, in vegetatively growing cells, Fus3-GFP was predominantly nuclear, but a small fraction was dispersed throughout the cytoplasm. In cells treated with α-factor, Fus3-GFP localized transiently at shmoo tips, whereas Ste5-GFP binds in a stable manner. In addition, FRAP (fluorescence recovery after photobleaching) analyses suggest that Fus3-GFP shuttles between nucleus and cytoplasm in an α-factor- and phosphorylation-independent manner (Van Drogen *et al*., 2001). Therefore, these authors suggest a dynamic model for the activation of the MAPK module in response to pheromones (Fig 1.4).
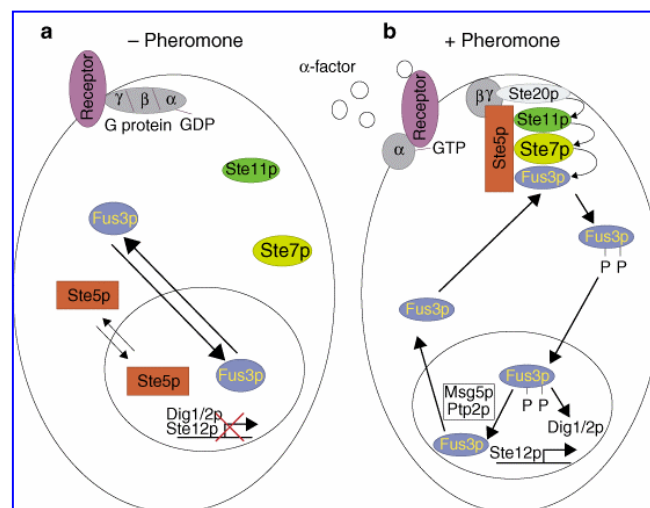
Fig 1.4. A model for the dynamic behaviour of Ste5 and Fus3 in response to pheromone (Van Drogen *et al*., 2001). **a**, in the absence of pheromone, the MAPK Fus3 and its scaffold Ste5 shuttle rapidly between the nucleus and the cytoplasm, in contrast to Ste11 and Ste7, which are predominantly cytoplasmic. In the nucleus, the Dig proteins are bound to Ste12 to prevent transcription of mating specific genes. **b**, in the presence of pheromone, Ste5 associates with Gβγ at the plasma membrane and in turns recruits Ste11, Ste7 and the MAPK Fus3. Ste20 activates the MAPK cascade by phosphorylating Ste11. Phosphorylated Fus3 rapidly dissociates from Ste5, and translocates into the nucleus where it phosphorylates Dig1 and Dig2, leading to activation of the transcription factor Ste12.

More recently, it has been reported that Gpa1, which codes for the alpha-subunit of the receptor-coupled G protein, binds directly to the mating-specific MAPK Fus3 (Metodiev, *et al*., 2002). Disruption of this interaction by mutation confers increased sensitivity to pheromone and a defect in Gpa1-mediated adaptation. These findings raise the question of whether Gpa1 regulates cell sensitivity to pheromone by affecting the localization of Fus3. Because MAPK signalling modules connect signalling elements located at the plasma membrane to response effectors in the nucleus, it has been presumed that, upon activation, MAPKs must be transported from the cytoplasm into the nucleus. Although some MAPKs clearly undergo signal-induced nuclear translocation (Kaffman and

O'Shea, 1999; Reiser *et al*., 1999), others constitutively shuttle between the cytoplasm and nucleus and show less obvious nuclear concentration when activated (Van Drogen *et al*., 2001). To test the possibility that Gpa1 down-regulates the mating signal by affecting the localization of Fus3, Blackwell *et al*. (2003) created a Fus3-GFP protein. It was found that, in vegetative cells, Fus3-GFP was localized in both the cytoplasm and the nucleus. The addition of pheromone to cells stimulated a measurable increase in the ratio of nuclear to cytoplasmic Fus3-GFP. The accumulation of Fus3-GFP in the nuclei of stimulated cells was inhibited by overexpression of Gpa1 or the dual-specificity phosphatase Msg5, and the effects of Gpa1 and Msg5 were found to be partially interdependent. All these properties suggest that Gpa1 and Msg5 work in concert to down-regulate the mating signal, and that they do so by inhibiting the pheromone-induced increase in the concentration of Fus3 in the nucleus. Kap104 is required for the G_α/phosphatase-mediated effect on Fus3 localization (Blackwell *et al*., 2003).

To determine how *MDY2* functions within the signal transduction pathway, I looked for interactions between Mdy2 and proteins known to be involved in the mating pheromone response pathway using two-hybrid assays. The results demonstrated that Mdy2 interacts *in vivo* with Fus3, as well as Ste5, Ste7, Kss1, and Cdc24. In addition to the results of the two-hybrid assays, Mdy2 was shown to interact specifically with Fus3 by pull down analysis. A difference in modification of the Myc-Fus3 fusion protein between the wild-type *MDY2* strain and the *mdy2* mutant suggests in addition that Mdy2 is probably required for the stabilization of the phosphorylated MAPK Fus3.

1.5 The aim of this study

Whereas the cytological events that occur during mating in yeast have been well described, relatively few components are known to be specifically involved in the various steps in the mating process. The limited number of genes currently known to function in these processes suggested that a search for new genes required for mating might yield additional components of the mating pathway.

In the first part of this study, a deletion library was screened using a semi-quantitative mating assay and complementation tests to identify new genes required for mating of *S. cerevisiae*. The single-gene deletion mutants were then analysed for pheromone production, pheromone response, morphogenesis, cell fusion and nuclear fusion in order to specifically pinpoint the defects in the mating mutants.

In the second and main part of my study the function of *MDY2*, a novel gene which required for the mating of *S.cerevisiae*, was further analysed. Phenotypic analysis of *mdy2* deletion mutants, overexpression of *MDY2,* the investigation of the subcellular localization of Mdy2, and the characterization of Mdy2 interaction partners in the pheromone response pathway and its role in protein modification were used to unravel the function of Mdy2 in the MAPK signalling pathway during the mating response in *S. cerevisiae*.

2. Materials and Methods

2.1 Materials

2.1.1   Yeast strains and media

2.1.1.1 *S. cerevisiae* strains

All yeast strains listed in Table 2.1 were derivatives of FY1679 which had been selected in systematic screens of EUROFAN single-gene disruptants for defects in mating.

Table 2.1. Strains of *S. cerevisiae* used in this study

Strain[*]	Genotype**			
10001A	*MAT***a**	*ura3-52 his3Δ200 leu2Δ1 YOL088c(2,834)::kanMX4*		
10001B	*MAT*α	*ura3-52 trp1Δ63 YOL088c(2,834)::kanMX4*		
10002A	*MAT***a**	*ura3-52 trp1Δ63 YOL087c(5,3348)::kanMX4*		
10002B	*MAT*α	*ura3-52 his3Δ200 leu2Δ1 YOL087c(5,3348)::kanMX4*		
10003A	*MAT***a**	*ura3-52 his3Δ200 trp1Δ63 YOR311c(2,873)::kanMX4*		
10003B	*MAT*α	*ura3-52 leu2Δ1 YOR311c(2,873)::kanMX4*		
10009A	*MAT***a**	*ura3-52 trp1Δ63 YBR041w(43,847)::kanMX4*		
10009B	*MAT*α	*ura3-52 leu2Δ1 YBR041w(43,847)::kanMX4*		
10018A	*MAT***a**	*ura3-52 his3Δ200 YNL054w(4,3495)::kanMX4*		
10018B	*MAT*α	*ura3-52 his3Δ200 YNL054w(4,3495)::kanMX4*		
10023A	*MAT***a**	*ura3-52 his3Δ200 leu2Δ1 YNL214w(55,630)::kanMX6*		
10023B	*MAT*α	*ura3-52 trp1Δ63 YNL214w(55,630)::kanMX6*		
10032A	*MAT***a**	*ura3-52 his3Δ200 trp1Δ63 YJL199c(-110,337)::kanMX6*		
10032B	*MAT*α	*ura3-52 leu2Δ1 YJL199c(-110,337)::kanMX6*		
10035A	*MAT***a**	*ura3-52 leu2Δ1 YOL101c(4,935)::kanMX4*		
10035B	*MAT*α	*ura3-52 his3Δ200 trp1Δ63 YOL101c(4,935)::kanMX4*		
10039A	*MAT***a**	*ura3-52 his3Δ200 leu2Δ1 YNL196c(4,895)::kanMX4*		
10039B	*MAT*α	*ura3-52 trp1Δ63 YNL196c(4,895)::kanMX4*		
10068A	*MAT***a**	*ura3-52 trp1Δ63 YJL047c(69,842)::kanMX4*		
10068B	*MAT*α	*ura3-52 his3Δ200 leu2Δ1 YJL047c(69,842)::kanMX4*		
10115A	*MAT***a**	*ura3-52 leu2Δ1 YBL042c(11,1902)::kanMX4*		
10115B	*MAT*α	*ura3-52 his3Δ200 trp1Δ63 YBL042c(11,1902)::kanMX4*		
10121A	*MAT***a**	*ura3-52 leu2Δ1 YNL164c(4,989)::kanMX4*		
10121B	*MAT*α	*ura3-52 his3Δ200 trp1Δ63 YNL164c(4,989)::kanMX4*		
10141A	*MAT***a**	*ura3-52 his3Δ200 YLR077w(97,1751)::kanMX-loxP*		
10141B	*MAT*α	*ura3-52 leu2Δ1 trp1Δ63 YLR077w(97,1751)::kanMX-loxP*		

*All strains were constructed in the FY1679 background. **The numbers in parentheses indicate the endpoints of the deletions.

Table 2.1 (continued)

Strain*	Genotype**
10145A	*MAT***a** *ura3-52 leu2Δ1* *trp1Δ63 YNR021w(386,1215)::kanMX-loxP*
10145B	*MAT*α *ura3-52 his3Δ200 trp1Δ63 YNR021w(386,1215)::kanMX-loxP*
10185A	*MAT***a** *ura3-52 leu2Δ1* *YBL036c(21,687)::kanMX6*
10185B	*MAT*α *ura3-52 his3Δ200 trp1Δ63 YBL036c(21,687)::kanMX6*
10188A	*MAT***a** *ura3-52 leu2Δ1* *YBL029w(114,1082)::kanMX6*
10188B	*MAT*α *ura3-52 his3Δ200 trp1Δ63 YBL029w(114,1082)::kanMX6*
10190A	*MAT***a** *ura3-52 his3Δ200 trp1Δ63 YBL025w(114,1082)::kanMX6*
10190B	*MAT*α *ura3-52 leu2Δ1* *YBL025w(114,1082)::kanMX6*
10250A	*MAT***a** *ura3-52 his3Δ200 leu2Δ1* *trp1Δ63 YGL100w(1,1050)::kanMX4*
10250B	*MAT*α *ura3-52 his3Δ200 leu2Δ1* *trp1Δ63 YGL100w(1,1050)::kanMX4*
10303A	*MAT***a** *ura3-52 trp1Δ63* *YGL133w(3,3496)::kanMX4*
10303B	*MAT*α *ura3-52 his3Δ200 leu2Δ1* *YGL133w(3,3496)::kanMX4*
10312A	*MAT***a** *ura3-52 his3Δ200 leu2Δ1* *YNL107w(1,678)::kanMX4*
10312B	*MAT*α *ura3-52 trp1Δ63* *YNL107w(1,678)::kanMX4*
10319A	*MAT***a** *ura3-52 his3Δ200 trp1Δ63 YLR104w(4,397)::kanMX4*
10319B	*MAT*α *ura3-52 his3Δ200 leu2Δ1* *YLR104w(4,397)::kanMX4*
10349A	*MAT***a** *ura3-52 his3Δ200 trp1Δ63 YBR078w(638,1738)::kanMX4*
10349B	*MAT*α *ura3-52 leu2Δ1* *trp1Δ63 YBR078w(638,1738)::kanMX4*
10359A	*MAT***a** *ura3-52 trp1Δ63 YNL097c(1,987)::kanMX4*
10359B	*MAT*α *ura3-52 his3Δ200 leu2Δ1* *trp1Δ63 YNL097c(11,987)::kanMX4*
10372A	*MAT***a** *ura3-52 his3Δ200 leu2Δ1* *trp1Δ63 YBL048w(12,786)::pINA-KAN*
10372B	*MAT*α *ura3-52 his3Δ200 leu2Δ1* *trp1Δ63 YBL048w(12,786)::pINA-KAN*
10373A	*MAT***a** *ura3-52 his3Δ200 leu2Δ1* *YNL059c(4,1329)::kanMX4*
10373B	*MAT*α *ura3-52 leu2Δ1* *YNL059c(4,1329)::kanMX4*
10380A	*MAT***a** *ura3-52 leu2Δ1* *trp1Δ63 YBR283c(4,1446)::kanMX4*
10380B	*MAT*α *ura3-52 leu2Δ1* *YBR283c(4,1446)::kanMX4*
10505A	*MAT***a** *ura3-52 leu2Δ1* *trp1Δ63 YNL119w(200,1284)::kanMX4*
10505B	*MAT*α *ura3-52 leu2Δ1* *trp1Δ63 YNL119w(200,1284)::kanMX4*
10565A	*MAT***a** *ura3-52 his3Δ200 trp1Δ63 YNL331c(6,1045)::kanMX4*
10565B	*MAT*α *ura3-52 his3Δ200 leu2Δ1* *YNL331c(6,1045)::kanMX4*
10566A	*MAT***a** *ura3-52 his3Δ200 trp1Δ63 YLL057c(1,1244)::kanMX4*
10566B	*MAT*α *ura3-52 YLL057c(1,1244)::kanMX4*

*All strains were constructed in the FY1679 background. **The numbers in parentheses indicate the endpoints of the deletions.

Table 2.1 (continued)

Strain*	Genotype**
10016A	*MAT**a*** *ura3-52 his3Δ200 YNL058c(4, 948)::kanMX4*
10016B	*MAT*α *ura3-52 YNL058c(4, 948)::kanMX4*
10058A	*MAT**a*** *ura3-52 his3Δ200 YBR016w(2, 124)::kanMX4*
10058B	*MAT*α *ura3-52 leu2Δ1 trp1Δ63 YBR016w(2, 124)::kanMX4*
10070A	*MAT**a*** *ura3-52 his3Δ200 YJL058c(4, 489)::kanMX4*
10070B	*MAT*α *ura3-52 leu2Δ1 trp1Δ63 YJL058c(4, 489)::kanMX4*
10143A	*MAT**a*** *ura3-52 leu2Δ1 trp1Δ63 YNR018w(-60, 675)::kanMX-loxP*
10143B	*MAT*α *ura3-52 his3Δ200 trp1Δ63 YNR018w(-60, 675)::kanMX-loxP*
10165A	*MAT**a*** *ura3-52 his3Δ200 trp1Δ63 YOL111c(-10, 623)::kanMX4*
10165B	*MAT*α *ura3-52 leu2Δ1 YOL111c(-10, 623)::kanMX4*
10166A	*MAT**a*** *ura3-52 his3Δ200 YOL072w(2, 1395)::kanMX4*
10166B	*MAT*α *ura3-52 leu2Δ1 trp1Δ63 YOL072w(2, 1395)::kanMX4*
10171A	*MAT**a*** *ura3-52 his3Δ200 trp1Δ63 YDL005c(-47, 1310)::kanMX4*
10171B	*MAT*α *ura3-52 leu2Δ1 trp1Δ63 YDL005c(-47, 1310)::kanMX4*
10419A	*MAT**a*** *ura3-52 leu2Δ1 trp1Δ63 YDR063w(4, 447)::kanMX4*
10419B	*MAT*α *ura3-52 his3Δ200 leu2Δ1 trp1Δ63 YDR063w(4, 447)::kanMX4*
10423A	*MAT**a*** *ura3-52 his3Δ200 leu2Δ1 trp1Δ63 YDR072c(4, 1544)::kanMX4*
10423B	*MAT*α *ura3-52 his3Δ200 leu2Δ1 trp1Δ63 YDR072c(4, 1544)::kanMX4*
10424A	*MAT**a*** *ura3-52 his3Δ200 leu2Δ1 YJL134w(25, 1196)::kanMX4*
10424B	*MAT*α *ura3-52 leu2Δ1 trp1Δ63 YJL134w(25, 1196)::kanMX4*
10425A	*MAT**a*** *ura3-52 his3Δ200 leu2Δ1 YJL145w(4, 882)::kanMX4*
10425B	*MAT*α *ura3-52 leu2Δ1 trp1Δ63 YJL145w(4, 882)::kanMX4*
10426A	*MAT**a*** *ura3-52 his3Δ200 leu2Δ1 YJL146w(4, 1407)::kanMX4*
10426B	*MAT*α *ura3-52 leu2Δ1 trp1Δ63 YJL146w(4, 1407)::kanMX4*
10427A	*MAT**a*** *ura3-52 his3Δ200 leu2Δ1 YJL147c(4, 1146)::kanMX4*
10427B	*MAT*α *ura3-52 leu2Δ1 trp1Δ63 YJL147c(4, 1146)::kanMX4*
10428A	*MAT**a*** *ura3-52 his3Δ200 leu2Δ1 YJL148w(4, 699)::kanMX4*
10428B	*MAT*α *ura3-52 leu2Δ1 trp1Δ63 YJL148w(4, 699)::kanMX4*
10429A	*MAT**a*** *ura3-52 his3Δ200 leu2Δ1 YJL149w(4, 1989)::kanMX4*
10429B	*MAT*α *ura3-52 leu2Δ1 trp1Δ63 YJL149w(4, 1989)::kanMX4*
10430A	*MAT**a*** *ura3-52 trp1Δ63 YDL202w(1, 744)::kanMX4*
10430B	*MAT*α *ura3-52 leu2Δ1 YDL202w(1, 744)::kanMX4*

*All strains were constructed in the FY1679 background. **The numbers in parentheses indicate the endpoints of the deletions.

Table 2.1 (continued)

Strain*	Genotype**
10431A	*MAT**a*** *ura3-52 his3Δ200 leu2Δ1 YDL201w(1, 859)::kanMX4*
10431B	*MATα ura3-52 his3Δ200 leu2Δ1 YDL201w(1, 859)::kanMX4*
10434A	*MAT**a*** *ura3-52 his3Δ200 leu2Δ1 trp1Δ63 YDL189w(238, 1607)::kanMX4*
10434B	*MATα ura3-52 his3Δ200 leu2Δ1 trp1Δ63 YDL189w(238, 1607)::kanMX4*
10438A	*MAT**a*** *ura3-52 his3Δ200 leu2Δ1 trp1Δ63 YJL122w(4, 525)::kanMX4*
10438B	*MATα ura3-52 YJL122w(4, 525)::kanMX4*
10446A	*MAT**a*** *ura3-52 his3Δ200 leu2Δ1 trp1Δ63 YDL018c(4, 674)::kanMX4*
10446B	*MATα ura3-52 leu2Δ1 trp1Δ63 YDL018c(4, 674)::kanMX4*
10454A	*MAT**a*** *ura3-52 his3Δ200 leu2Δ1 trp1Δ63 YOR109w(4, 3321)::kanMX4*
10454B	*MATα ura3-52 his3Δ200 YOR109w(4,3321)::kanMX4*
10458A	*MAT**a*** *ura3-52 leu2Δ1 trp1Δ63 YNL100w(4, 622)::kanMX4*
10458B	*MATα ura3-52 his3Δ200 leu2Δ1 trp1Δ63 YNL100w(4, 622)::kanMX*
10459A	*MAT**a*** *ura3-52 his3Δ200 leu2Δ1 trp1Δ63 YNL099c(4, 714)::kanMX4*
10459B	*MATα ura3-52 leu2Δ1 YNL099c(4, 714)::kanMX4*
10470A	*MAT**a*** *ura3-52 his3Δ200 leu2Δ1 YBR217w(158, 558)::kanMX4*
10470B	*MATα ura3-52 YBR217w(158, 558)::kanMX4*
10475A	*MAT**a*** *ura3-52 leu2Δ1 trp1Δ63 YDL158c(1, 308)::kanMX4*
10475B	*MATα ura3-52 his3Δ200 YDL158c(1, 308)::kanMX4*
10489A	*MAT**a*** *ura3-52 his3Δ200 leu2Δ1 YDL048c(1, 1517)::kanMX4*
10489B	*MATα ura3-52 leu2Δ1 YDL048c(1, 1517)::kanMX4*
10495A	*MAT**a*** *ura3-52 leu2Δ1 YOL151w(4, 877)::kanMX4*
10495B	*MATα ura3-52 leu2Δ1 trp1Δ63 YOL151w(4, 877)::kanMX4*
10496A	*MAT**a*** *ura3-52 leu2Δ1 YOL124c(4, 1286)::kanMX4*
10496B	*MATα ura3-52 leu2Δ1 trp1Δ63 YOL124c(4, 1286)::kanMX4*
10614A	*MAT**a*** *ura3-52 trp1Δ63 YDL231c(1, 3470)::kanMX4*
10614B	*MATα ura3-52 trp1Δ63 YDL231c(1, 3470)::kanMX4*
10615A	*MAT**a*** *ura3-52 his3Δ200 leu2Δ1 trp1Δ63 YLL051c(47, 2154)::kanMX4*
10615B	*MATα ura3-52 trp1Δ63 YLL051c(47, 2154)::kanMX4*
10623A	*MAT**a*** *ura3-52 his3Δ200 YGL085w(10, 822)::kanMX4*
10623B	*MATα ura3-52 leu2Δ1 trp1Δ63 YGL085w(10, 822)::kanMX4*
10659A	*MAT**a*** *ura3-52 leu2Δ1 YNL080c(4, 1049)::kanMX4*
10659B	*MATα ura3-52 trp1Δ63 YNL080c(4, 1049)::kanMX4*

*All strains were constructed in the FY1679 background. **The numbers in parentheses indicate the endpoints of the deletions.

Table 2.1 (continued)

Strain*	Genotype**
10674A	*MAT**a** ura3-52 trp1Δ63 YJR074w(,)::kanMX4*
10674B	*MAT*α *ura3-52 leu2Δ1 YJR074w(,)::kanMX4*
10624A	*MAT**a** ura3-52 leu2Δ1 trp1Δ63 YGR016w(9, 570)::kanMX4*
10624B	*MAT*α *ura3-52 his3Δ200 trp1Δ63 YGR016w(9, 570)::kanMX4*
10740A	*MAT**a** ura3-52 leu2Δ1 YNL323w(38, 1207)::kanMX2*
10740B	*MAT*α *ura3-52 trp1Δ63 YNL323w(38, 1207)::kanMX2*

*All strains were constructed in the FY1679 background. **The numbers in parentheses indicate the endpoints of the deletions.

Table 2.2 List of other *S. cerevisiae* strains used

Name	Genotype	Source/Reference
W303-1A	*MAT*a *leu2-3,112 ura3-1 trp1 his3-11 ade2 can1-100*	R. Rothstein, Columbia university, New York
W303-1B	*MAT*α *leu2-3,112 ura3-1 trp1 his3-11 ade2 can1-100*	R. Rothstein, Columbia university, New York
HZH686	W303-1A *MAT*a *leu2-3,112 ura3-1 trp1 his3-11 ade2 can1-100Δmdy2::KanMX4*	This work
HZH683	W303-1B *MAT*α *leu2-3,112 ura3-1 trp1 his3-11 ade2 can1-100Δmdy2::KanMX4*	This wotk
Cgx31	*MAT*α *ura3-52*	Gimeno *et al*., 1992
HZH685	Cgx31*MAT*α *ura3Δmdy2::KanMX4*	This wotk
PJ187	*MAT*a/α *gal4 gal80 his3-200 trp1-901 ade2-101 ura3-52 leu2-3,112* reporter *lacZ* (3x), *HIS3, ADE2*	Lab collection, HLS196
HZH368	MG6D *MAT*α *Δsst2-1 ura3-1 his3-11,15 ade2 trp1*	Lab collection
HZH350	BY4741 *MAT*a *Δsst1(bar1) ura3 his3-1 leu2 met15* (BY01408)	Euroscarf; Brachmann *et al*., 1998
HZH847	W303-1A *Δmdy2Δkss1::KanMX4*	This work
FY1679	*MAT*a/*MAT*α *ura3-52 trp1Δ63 leu2Δl his3Δ200 GAL2*	B. Dujon, Institute Pasteur, Paris

2.1.1.2 Media

YEPD: 1% yeast extract, 2% peptone, 2% glucose

YPRG: 1% yeast extract, 2% peptone, 3% raffinose, 1% galactose

YEPD-G418: 1% yeast extract, 2% pepton, 2% glucose, G418 (400 mg/l)

Synthetic minimal medium (SC): 0.67% yeast nitrogen base without amino acids plus 2% glucose,

100 ml amino acid-drop-out-mix (1 l medium)

SRG minimal medium: 0.67% yeast nitrogen base without amino acids, 3% raffinose, 1% galactose,

100 ml amino acid drop-out-mix (1 l medium)

Amino acid drop-out-mix: adenine, alanine, arginine, asparagine, aspartic acid, cysteine, glutamine, glutamic acid, glycine, inositol, isoleucine, lysine, methionine, phenylalanine, proline, serine, theronine, tyrosine, valine.

4 g of each of the above were used. Para-aminobenzoic acid: 0.4 g

All above ingredients were dissolved in 5 l of water. The mixture was adjusted to pH 8.0 and autoclaved.

Solid media were prepared in flasks, containing 1 l of medium and 2% agar, which is sufficient for 30-40 plates. All components were autoclaved together for 15 min at 121°C and a pressure of 15 psi (1.05 kg/cm^2). The plates were dried at room temperature for 1-2 days after pouring, and could be stored in sealed plastic bags for over 3 months.

2.1.2 *Escherichia coli* strains and media

2.1.2.1 *E. coli* strains

DH5αF′:   F′ *endA1 hsdR17*r$_k$-m$_k$+ *supE44 thi-1 recA1 gyrA relA*Δ(*lacZYA-argF*)U169 (ϕ 80Δ(*lacZ*)M15) (Gibco BRL, Gaithersburg MD, USA)

XL1 blue: *recA1 endA1 gyrA96 thi-1 hsdR17 supE44 relA1 lac* [F'*proAB lacI^{q}ZΔM15* Tn*10* (Tet^r)] (Stratagene, La Jolla, USA)

2.1.2.2 Media

LB medium: 1% tryptone peptone, 0.5% yeast extract, 0.5% NaCl

LB-ampicillin: ampicillin (50 μg/ml) was added to 1 l of medium to select the strains bearing plasmids.

2.1.3 Plasmids and oligonucleotides

2.1.3.1 Plasmids

The plasmids used in this study are listed in Table 2.3. The plasmids which were constructed in the course of this study are listed in Table 2.4.

Table 2.3 List of the plasmids used in this study

Plasmid	Composition			Source/Reference
	Description	Marker	CEN / 2μ	
pRS423	pBluescript	*HIS3*	2μ	ELS26/Christianson *et al*., 1992
pRS424	pBluescript	*TRP3*	2μ	EGX224/Christianson *et al*., 1992
pRS425	pBluescript	*LEU2*	2μ	EGX225/Christianson *et al*., 1992
pRS426	pBluescript	*URA3*	2μ	EGX226/Christianson *et al*., 1992

p413GAL	pRS413*GAL1p, CYC1* terminator	*HIS3*	*CEN*	ELS22/Mumberg *et al*., 1994
p414GAL	pRS414*GAL1p, CYC1* terminator,	*TRP1*	*CEN*	ELS23/Mumberg *et al*., 1994
p415GAL	pRS415*GAL1p, CYC1* terminator,	*LEU2*	*CEN*	ELS24/Mumberg *et al*., 1994
p416GAL	pRS416*GAL1p, CYC1* terminator	*URA3*	*CEN*	ELS25/Mumberg *et al*., 1994
pSB234	*FUS1*-promoter-*lacZ*	*URA3*	2μ	EFB12/Lab collection
pRS424METGFP	pRS424, *MET25* promoter, GFP	*TRP1*	2μ	EHB309/Mumberg *et al*., 1994
pUG36METGFP	*MET25* promoter, yEGFP3, *CYC1* terminator	*URA3*	*CEN*	Guldener *et al*., 2000
pUG6	PFAG-*KanMX4, TEF2* promoter, *TEF2* terminator	*URA3*	*CEN*	EWK10/Guldener *et al*., 1996
pSH47	*GAL1p*, Cre recombinase	*URA3*	*CEN*	EWK1/Guldener *et al*., 1996
pGREG526	pRS416 *GAL*p-13MYC	*URA3*	*CEN*	EWK75/G. Jansen, BRI, Montreal
pGREG546	pRS416 *GAL*p-GST	*URA3*	*CEN*	EWK83/G. Jansen, BRI, Montreal
pGREG576	pRS416 *GAL*p-GFP	*URA3*	*CEN*	EWK87/G. Jansen, BRI, Montreal
pGREG524	pRS414 *GAL*p-13MYC	*TRP1*	*CEN*	EWK73/G. Jansen, BRI, Montreal
pAD2-His3	Two-Hybrid *GAL4* activation domain	*LEU2*	2μ	ELS552/Lab collection
PMBD-His3	Two-Hybrid *GAL4* DNA binding domain	*TRP1*	2μ	EWK67/Lab collection
pGAD424	Two-Hybrid-*GAL4*-AD	*LEU2*	2μ	EB247/Chien *et al*., 1991
pGBT9	Two-Hybrid-*GAL4*-BD	*TRP1*	2μ	EB246/Lab collection
pSE1111	pGAD-*SNF4*	*LEU2*	2μ	EGX111/Elledge *et al*., 1993
pKB40.1	pGAD-*STE4*	*LEU2*	2μ	EGX119/Clark *et al*., 1993
pKB87.2	pGAD-*STE18*	*LEU2*	2μ	EGX122/Clark *et al*., 1993
pKB153-10	pGAD-*GPA1*	*LEU2*	2μ	EGX123/Clark *et al*., 1993
pRL22	pGAD-*STE20*	*LEU2*	2μ	EGX173/Leeuw *et al*., 1995
pSL2289	pGAD-*STE5*	*LEU2*	2μ	EGX174/Printen and Sprague, 1994
pSL2091	pGAD-*STE11*	*LEU2*	2μ	EGX202/Printen and Sprague, 1994
pSL2168	pGAD-*STE7*	*LEU2*	2μ	EGX283/Printen and Sprague, 1994
pSL2175	pGAD-*FUS3*	*LEU2*	2μ	EGX284/Printen and Sprague, 1994
pSL2122	pGAD-*KSS1*	*LEU2*	2μ	EGX285/Printen and Sprague, 1994
PSL2477	pGAD-*STE11-K444R*	*LEU2*	2μ	EGX286/Printen and Sprague, 1994
pRL1	pGAD-*CLA4N*	*LEU2*	2μ	EGX288/Lab collection
pRL61A	pGAD-*CDC24*	*LEU2*	2μ	EGX289/Lab collection
pRL58	pGAD-*CDC42Val12*	*LEU2*	2μ	EGX290/Lab collection
pRL39	pGAD-*CDC42*	*LEU2*	2μ	EGX291/Lab collection
pRL6	pGAD-*STE20-C* (498-939)	*LEU2*	2μ	EGX292/Leeuw *et al*., 1995

pRL26	pGAD-*STE20-N* (1-497)	*LEU2*	2μ	EGX293/Leeuw *et al.*, 1995
pRL22	pGAD-*STE20*	*LEU2*	2μ	EGX294/Leeuw *et al.*, 1995
pKB85.8	pGAD-*STE4*^{hpl21-1}	*LEU2*	2μ	EGX322/Clark *et al.*, 1993
pRL51	pGAD-*BEM1-C* (157-551)	*LEU2*	2μ	EGX324/Leeuw *et al.*, 1995
pRL5	pGAD-*BEM1*	*LEU2*	2μ	EGX325/Leeuw *et al.*, 1995
pSE1112	pGBD-*SNF1*	*TRP1*	2μ	EGX113/Elledge *et al.*, 1993
EGX357	pGAD-*STE50*	*LEU2*	2μ	EGX357/Lab collection

Table 2.4 List of plasmids constructed in this study

Name	Composition			Construction
	Description	Marker	CEN/2μ	
pZH79	pGREG526MYC-*MDY2*	*URA3*	*CEN*	*In vivo* homologous recombination between *MDY2-ORF* PCR product and pGREG526 vector
pZH81	pGREG546GST-*MDY2*	*URA3*	*CEN*	*In vivo* homologous recombination between *MDY2-ORF* PCR product and pGREG546 vector
pZH80	pGREG576GFP-*MDY2*	*URA3*	*CEN*	*In vivo* homologous recombination between *MDY2-ORF* PCR product and pGREG576 vector
pZH78	pAD2-*MDY2*	*LEU2*	2μ	*In vivo* homologous recombination between *MDY2-ORF* PCR product and pAD2-HIS3 vector
pZH82	pMBD-*MDY2*	*TRP1*	2μ	*In vivo* homologous recombination between *MDY2-ORF* PCR product and pMBD vector
pZH150	pRS416-*MDY2*p-MYC-*MDY2*	*URA3*	*CEN*	*GAL1* promoter was swapped with *MDY2* promoter in pGREG526MYC-*MDY2*
pZH151	pRS416-*MDY2*p-GST-*MDY2*	*URA3*	*CEN*	*GAL1* promoter was swapped with *MDY2* promoter in pGREG546GST-*MDY2*
pZH152	pRS416-*MDY2*p-GFP-*MDY2*	*URA3*	*CEN*	*GAL1* promoter was swapped with *MDY2* promoter in pGREG576GFP-*MDY2*
pZH149	pRS426-*MDY2*p -*MDY2*	*URA3*	2μ	*MDY2* fragment (990bp) inserted in the *Spe*I and *Kpn*I sites of pRS426
pZH176	pGREG526MYC-*STE5*	*URA3*	*CEN*	*In vivo* homologous recombination between *STE5-ORF* PCR product and pGREG526 vector
pZH177	pGREG546GST-*STE5*	*URA3*	*CEN*	*In vivo* homologous recombination between *STE5-ORF* PCR product and pGREG546 vector
pZH178	pGREG576GFP-*STE5*	*URA3*	*CEN*	*In vivo* homologous recombination between *STE5-ORF* PCR product and pGREG576 vector
pZH189	pGREG524MYC-*STE5*	*TRP1*	*CEN*	*In vivo* homologous recombination between *STE5-ORF* PCR product and pGREG524 vector
pZH190	pRS416-*STE5*p-GST-*STE5*	*URA3*	*CEN*	*GAL1* promoter was swapped with *STE5* promoter

					in pGREG546GST-STE5
pZH179	pGREG526MYC-*FUS3*	*URA3*	*CEN*		*In vivo* homologous recombination between *FUS3-ORF* PCR product and pGREG526 vector
pZH180	pGREG546GST-*FUS3*	*URA3*	*CEN*		*In vivo* homologous recombination between *FUS3-ORF* PCR product and pGREG546 vector
pZH181	pGREG576GFP-*FUS3*	*URA3*	*CEN*		*In vivo* homologous recombination between *FUS3-ORF* PCR product and pGREG576 vector
pZH188	pGREG524MYC-*FUS3*	*TRP1*	*CEN*		*In vivo* homologous recombination between *FUS3-ORF* PCR product and pGREG524 vector

2.1.3.2 Cognate-clone plasmids

The term 'cognate clone' refers to the vector pRS416 containing a single-gene insert, which was used to complement the yeast mutant strain in which that particular gene had been deleted. This method was used to test whether the reduced mating efficiency of the deletion strain was really caused by the deletion of that ORF.

The cognate clones used in this work were the following:

pYCG-*YNL214w*, pYCG-*YJL199c*, pYCG-*YBR041w*, pYCG-*YOL087c*, pYCG-*YOR311c*

pYCG-*YOL101c*, pYCG-*YNR018w*, pYCG-*YBL029w*, pYCG-*YOL111c*, pYCG-*YDL005c*

pYCG-*YBL059w*, pYCG-*YBR283c*, pYCG-*YGL100w*, pYCG-*YGL133w*, pYCG-*YNL097c*

pYCG-*YNL119w*, pYCG-*YLL051c*, pYCG-*YDL202w*, pYCG-*YDL201w*, pYCG-*YDL189w*

pYCG-*YJL122w*, pYCG-*YBR217w*, pYCG-*YJL134w*, pYCG-*YJL145w*, pYCG-*YDL231c*

pYCG-*YLL057c*

The plasmid name indicates the name and chromosomal location of the ORF it carries; for example,

pYCG-*YNL214w* stands for: **p**lasmid **Y**east **C**ognate **G**ene-**Y**east **N** (chromosome XIV) **L**eft arm + ORF-number

w = **W**atson strand; **c** = **C**rick strand.

2.1.3.3 Oligonucleotide primers

Primer	Size	Oligo Seq (5´- to -3´)	Site	Target or application
A50 STE5-5-800	27	CCCGAGCTCACACGATGCTTTAGCTCA	*Sac*I	*STE5* promoter
A51 STE5-3+500	21	GGGCTGCAGAGAGATCGTACT	*Pst*I	*STE5* terminator
A74 rec1-ste5	57	GAATTCGATATCAAGCTTATCGATACCGTCG ACAATGATGGAAACTCCTACAGACAA		*STE5*-ORF fusion
A75 rec2-ste5	57	GCGTGACATAACTAATTACATGACTCGAGGT CGACCTATATATAATCCATATGGAGG		*STE5*-ORF fusion
A96 yol111-280p5	29	CCCACTAGTCTAGTAAGGGTTAGATTGAG	*Spe*I	*MDY2* promoter
A97 yol111-1p3	30	CCCGGATCCGATTAATTTTGTATAAAGTTA	*Bam*HI	*MDY2* promoter

A98 yol111-60t3	28	CCGGTACCGTAAGCGCAACCGTGATAAA	*Kpn*I	*MDY2* terminator
A99 rec1-yol111	54	GAATTCGATATCAAGCTTATCGATACCGTCG ACAATGAGCACATCCGCCAGCGG		*MDY2*-ORF fusion
A100 rec2-yol111	56	GCGTGACATAACTAATTACATGACTCGAGGT CGACTTATTTGGCCAGAGACCAGCC		*MDY2*-ORF fusion
A107 yol111-500p5	29	CCCGAGCTCGCACTCGTACCACCCGGGTC	*Sac*I	*MDY2* promoter
A108 yol111-1p3	30	CCCACTAGTGATTAATTTTGTATAAAGTTA	*Spe*I	*MDY2* promoter
A111 FUS3-5D	67	CGTTTGAACTACAAGGAAATAAGGCAGAGA AAAAGAAAGGAAAATAATCAGCTGAAGCTT CGTACGC		*FUS3* gene disruption
A112 FUS3-3D	66	GTATACATTGTTCTTCGGGTTGATATTTTAAT GATAATGATGGCTAGCATAGGCCACTAGTGG ATC		*FUS3* gene disruption
A115 FUS3-1P	30	CCCACTAGT ATTATTTTCCTTTCTTTTTC	*Spe*I	*FUS3* promoter
A116 FUS3-800P	30	CCCGAGCTCGGAAAAAGAGTACGGTAGTTG	*Sac*I	*FUS3* promoter
A117 KAN3-5	25	CGCACCTGATTGCCCGACATTATCG		Deletion check
A119 rec1-FUS3	55	GAATTCGATATCAAGCTTATCGATACCGTCG ACAATGCCAAAGAGAATTGTATAC		*FUS3*-ORF fusion
A120 rec2-FUS3	55	GCGTGACATAACTAATTACATGACTCGAGGT CGACCTAACTAAATATTTCGTTCC		*FUS3*-ORF fusion
A121 Yol111c-5D	69	CGATACAGAGATAAACTAGCGAAGAATAAT AACTTTATACAAAATTAATCCAGCTGAAGCT TCGTACGC		*MDY2* gene disruption
A122 Yol111c-3D	70	AAGCGCAACTGTGTAAAATAACAAGTATGT ACGTACTAACTATACTAATCGCATAGGCCAC TAGTGGATC		*MDY2* gene disruption
A123 KAN5-3	25	CGGTTTGGTTGATGCGAGTGATTTT		Deletion check

2.2 Chemicals, enzymes and antibodies

2.2.1 Chemicals

Chemicals	**Source**
α-factor	Sigma
acrylamide	Serva
agar	Difco
agarose	Sigma
ammoniumpersulfate	Serva
dimethyl formamide	Janssen
ethanol	Riedel de Haen
NC-Filter membrane	Schleicher & Schuell
galactose	Acro organics
glass beads	Braun
glucose	Caesar & Loretz GmBH
glutathione sepharose 4B	Amersham pharmcia
glycerine	Roth
isopropanol	Fluka
ONPG	Sigma
polyethylene glycol 4000	Roth
raffinose	Serva
sorbit	Sigma
yeast nitrogen base w/o amino acid	Difco
yeast extract	Difco

Other reagents that are not mentioned above were purchased from Acro Organics (New Jersey, USA); Amersham International (Little Chalfont, Buckinghamshire, England); Amicon (Beverly, Mass., USA); BioRad (Richmond, USA); Braun (Melsungen); Caesar & Loretz GmbH (Hilden); Dianova (Hamburg), Difco-Laboratories (Detroit, Mich., USA); Fluka AG (Basel, Switzerland); Gibco (Paisley, Scotland); Janssen Chimica (Belgium); Merck (Darmstadt); Oxoid (Wesel); Pharmacia (Freiburg); Pierce (Utah, USA); Qiagen (Hilden); Riedel de Haën (Seelze); Roche (Mannheim); Roth (Karlsruhe); Serva (Heidelberg); Sigma (St. Louis, Mo., USA); Whatman (Maidstone, Kent, UK).

2.2.2 Enzymes

Enzyme	Company
restriction enzymes	New England Biolabs (Schwalbach) and Roche (Mannheim)
T4 DNA ligase	Roche (Mannheim)
calf intestinal alkaline phosphatase (CIP)	Roche (Mannheim)
DNA polymerase	Roche (Mannheim)

2.2.3 Antibodies

Antibody	Description	Company
anti-c-MYC	monoclonal mouse IgG	Oncogene
anti-GST	rabbit polyclonal IgG	Santa Cruz
anti-mouse IgG-AP	alkaline phosphatase (conjugate)	Dianova
anti-mouse IgG-HRP	peroxidase (conjugate)	Dianova
anti-rabbit IgG-AP	alkaline phosphatase (conjugate)	Dianova
anti-rabbit IgG-HRP	peroxidase (conjugate)	Dianova

2.3 Methods

2.3.1 Mating assay

2.3.1.1 Semi-quantitative mating assay

Strains of opposite mating type (*MATa* and *MATα*) were grown to log-phase in SD medium. Equal numbers of cells of each mating type were mixed and centrifuged at 20°C and 10,000 rpm for 4 min. The cell pellets were then transferred to a NC membrane on a YPD plate. The plates were incubated at 30°C for 4.5 h, and then the cells were transferred to Eppendorf tubes for serial 10-fold dilution. Dilutions were spotted (in 3.5-µl aliquots) onto an SD plate and incubated at 30°C for 2 days. The mating efficiency of a cross between wild-type strains was used as the positive control and a *STE50 × ste50* mutant or *FUS2 × fus2* cross was used as the negative control. The mating efficiencies of the crosses between mutant (*MATa mut* or *MATα mut*) and wild-type strain and the bilateral mutant cross (*MATa mut × MATα mut*) were obtained by comparison with the controls.

2.3.1.2 Quantitative mating assay

Quantitative mating assays were performed as described by Elion *et al.* (1990) in order to determine the efficiency of diploid formation. The cultures of opposite mating type (*MAT*a and *MAT*α) were grown to log-phase in SD medium. The same number of cells (3×10^6 cells) of each mating type were mixed and centrifuged at 20°C and 10,000 rpm for 4 min. The cell pellets were then transferred onto a NC membrane on a YPD plate. The plates were incubated at 30°C for 4.5 h, then the cells were transferred to the Eppendorf tubes for serial 10-fold dilution. Dilutions (100 µl) were spread on SD plates and the plates were incubated at 30°C for 2 days. The total numbers of cells (Nt) and the numbers of diploid cells (N_d) were then counted. By comparing the total number of cells with the number of diploid cells, the mating efficiency (ME, in %) could be determined. In this assay the mating efficiency of a cross between two wild-type strains was used as the control. The relative mating efficiencies (Rme) of the crosses between mutants (*MAT*a *mut* and *MAT*α *mut*) and the wild-type strain, or the bilateral mutant mating cross were obtained by calculation (the calculation formula is given below). Tests were always carried out in duplicate.

N_t -- Total number of cells (*MAT*a or *MAT*α)

N_d -- Number of diploid cells

ME (%) -- Mating efficiency (absolute)

Rme (%) -- Relative mating efficiency (as compared with wild-type strain)

ME (%) = N_d/N_t* (N_t*: is the lower total number of cells (for *MAT*a or *MAT*α)

Rme (%) = ME (%) of mutant / ME (%) of wild-type strain

2.3.1.3 Assay for zygote formation

The assay for zygote formation was performed essentially as described by Elion *et al.* (1990). The cultures of opposite mating type (*MAT*a and *MAT*α) were grown to log-phase in YPD or SD medium. The same numbers of cells (3×10^6 cells) of each mating type were mixed and centrifuged at 20°C and 10,000 rpm for 4 min. The cell pellets were transferred onto NC filters on a YPD plate. The plate was incubated at 30°C for different periods of time (1 h, 2 h, 3 h, 4 h and 5 h). The cells on the NC membrane were then washed off with 1 ml sterile water, and pelleted by centrifugation at 20°C and 10,000 rpm for 4 min. The pellets were then resuspended in 1× PBS buffer and fixed with 3.7% formaldehyde. Cells were routinely fixed overnight and washed twice with 1× PBS buffer prior to analysis under the microscope. The numbers of whole cells and zygotes were counted and the efficiency of zygote formation was calculated.

2.3.2 Isolation and characterization of plasmid DNA

2.3.2.1 Isolation of plasmid DNA from *E. coli*

Aliquots (5 ml) of LB medium containing ampicillin were inoculated with transformed *E. coli* cells, and incubated overnight at 37°C. Each culture was then transferred into a 2 ml Eppendorf tube and harvested by centrifugation at 9,000 rpm for 1 min. Then the pellet was resuspended in 300 μl of P_1 (50 mM Tris/HCl (pH 8.0) with 10 mg/ml RNase) by vortexing. Then 300 μl of P_2 (0.2 M NaOH, 1% SDS) was added to the mixture and the Eppendorf tubes were carefully inverted. After that the mixture was incubated at room temperature for 5 min. Then 300 μl of P_3 (3 M KOAc, pH 5.5) was added to the mixture and the tubes were inverted carefully. The mixture was centrifuged at 4°C and 13,000 rpm for 30 min and then the supernatant was transferred to a fresh tube. After adding 700 μl of absolute ethanol to the supernatant, the mixture was centrifuged at 13,000 rpm for 20 min. The pellet was resuspended in 1 ml of 70% ethanol and centrifuged at 13,000 rpm for 5 min. The supernatant was then removed and the pellet was dried at room temperature for 15 min. Finally the pellet was redissolved in 30 μl of Milli-Q water and stored at -20°C.

2.3.2.2 Agarose gel electrophoresis of plasmid DNA

Agarose gel electrophoresis of plasmid DNA was performed according to standard protocols (Sambrook *et al*., 1989). Gels were prepared by adding 50 ml electrophoresis buffer TBE (45 mM Tris-borate, 1 mM EDTA) to 0.35 g of agarose. The slurry was heated in a microwave oven until the agarose dissolved to give a final concentration of 0.7%. The solution was cooled to 60°C and ethidium bromide was added to a final concentration of 0.5 μg/ml. The warm agarose solution was then poured into the mould. Gels were between 3 mm and 5 mm thick. After the gel had set completely, the comb was removed carefully. Enough electrophoresis buffer was added to cover the gel to a depth about 1 mm. The samples of DNA were mixed with the desired gel loading buffer and slowly loaded into the slots of the submerged gel using a disposable micropipette. The marker λ DNA digest was loaded into slots on the left or right side of the gel. A voltage of 1-5 V/cm was applied and electrophoresis continued until the bromophenol blue and xylene cyanol FF had migrated the appropriate distances through the gel. The electric current was then turned off and the agarose gel was photographed.

2.3.2.3 Plasmid isolation from yeast cells

A 10 ml culture was grown to log phase and transferred to a sterile 15 ml centrifuge tube. The cells were harvested by centrifugation at 3000 rpm for 5 min. The pellet was washed with deionized water and was centrifuged again. Then the pellet was resuspended in 1 ml of P_1 (50 mM Tris/HCl (pH 8.0) containing 10 mg/ml RNase). Then 1 ml of P_2 (0.2 M NaOH, 1% SDS) was added and mixed well. A

2/3 volume of glass beads was added and the mixture was vortexed at 4°C for 3 min. The mixture was centrifuged at 3,000 rpm for 2 min and 1 ml of supernatant was transferred to a fresh Eppendorf tube. Then 0.5 ml of P_3 (3 M KOAc, pH 5.5) was added to the tubes and the mixture was incubated in ice for 15 min.   The mixture was transferred to two Eppendorf tubes (750 μl per tube) and centrifuged at 10,000 rpm for 15 min. Then 750 μl isopropanol was added to the supernatant and centrifuged at 13,000 rpm for 30 min. The pellet was washed with 1 ml of 70% ethanol and centrifuged at 13,000 rpm for 5 min. Finally the pellet was allowed to dry at room temperature and resuspended in 10 μl of Milli-Q water.

2.3.3 Transformation of *S. cerevisiae*

2.3.3.1 A simple procedure for transformation of *S. cerevisiae*

A 200-μl aliquot of PEG_{4000}/LiAc was added to the well of a microtiter plate. Fresh yeast cells were picked from a single colony with a pipette tip and resuspended in the PEG_{4000}/LiAc solution. Then 1 μg of plasmid DNA was mixed into the solution, followed by 10 μl of carrier DNA and 10 μl of DTT. The microtiter plate was then incubated at 30°C for more than 6 h. The culture was heat-shocked in a 42°C water bath for 10 min, spread on the SD plates and incubated at 30°C for 2 days.

2.3.3.2 High efficiency LiAc-transformation

High efficiency LiAc transformation was performed according to the method described by Ito *et al.* (1983). A 5-ml overnight culture was inoculated into 50 ml medium. The culture was then grown to log phase at 30°C (5×10^6-1×10^7 cells/ml; OD_{600} 0.2-0.6). The cells were harvested in a sterile 50-ml centrifuge tube. The supernatant was discarded and the pellet was resuspended in 25 ml of sterile water. After centrifugation, the pellet was resuspended in 1.0 ml of 100 mM LiAc. The suspension was transferred to a 1.5-ml microfuge tube. Samples were then pipetted into Eppendorf tubes. Cells were collected by centrifugation and the supernatant was removed. The following ingredients were added to the pellet in the order given: 240 μl of PEG_{3350} (50% w/v), 36 μl of 1.0 M LiAc, 10 μl of SS-DNA (10 mg/ml), X μl of plasmid DNA (0.1-10 μg, fragment:vector = 3:1 for *in vivo* recombination); (74 - X) μl of H_2O; to give a total volume of 360 μl.

The tubes were vortexed until the pellet was completely dispersed. The tubes were incubated at 30°C for 30 min, and then heat-shocked in a water bath at 42°C for 20 min. After heat shock the mixture was centrifuged for 15 sec and the supernatant was removed. Then 200 μl of sterile water was pipetted into each Eppendorf tube, and the pellet was resuspended by pipetting it up and down. Samples were spread onto SD plates. The plates were then incubated at 30°C for 2 days.

Solutions:

(1) 1.0 M lithium acetate stock solution

(2)   PEG$_{3350}$ 50% w/v

35 ml of H$_2$O was added to 50 g of PEG$_{3350}$ (Sigma P3690) and dissolved for 30 min, then H$_2$O was added to the mixture to give a final volume of 100 ml and the mixture was autoclaved.

2.3.4 Transformation in *E. coli*

2.3.4.1 Simple transformation

Simple transformations were performed according to the method described by Hanahan (1983). Competent cells were thawed on ice, and 100 µl of competent cells was mixed with plasmid DNA. The mixture was incubated on ice for 30 min. Then the mixture was heat-shocked at 42°C for 45 sec, 1 ml of LB medium without ampicillin was added to the mixture and incubated at 37°C for 1 h. Then the sample was centrifuged at 20°C and 9,000 rpm for 2 min and the supernatant was discarded. The pellet was resuspended in the rest of the medium and spread onto LB-ampicillin plates. Plates were incubated at 37°C until colonies formed.

2.3.4.2 Electro-transformation

A 1-l volume of LB medium was inoculated with 100 µl of an overnight culture (5 ml LB medium) which had been inoculated with *E.coli* cells and grown to OD$_{600}$ = 0.5-0.8. The culture was placed in ice for 30 min and then centrifuged at 3,000 rpm and 4°C for 15 min. The pellet was washed with 0.5 l of cold H$_2$O and centrifuged at 3,000 rpm and 4°C for 15 min. Then the pellet was washed with 0.25 l of cold H$_2$O and centrifuged at 3,000 rpm 4°C for 15 min. The pellet was resuspended in 20 ml of 10% glycerol, and cells were collected by centrifugation at 3,000 rpm and 4°C for 10 min. Then the pellet was resuspended in the 2-3 ml of 10% glycerol. The cells were transferred to an Eppendorf tube (100 µl aliquot) and were stored at -70°C immediately.

Competent cells were thawed on ice, and 50 µl of diluted plasmid DNA (5 µl DNA + 45 µl H$_2$O) was mixed with 50 µl of competent cells. The mixture was transferred to a 1-mm cuvette. The transformation parameters were: 200 Ω, 1.6 KV, 25 µF. Then 1 ml LB medium was added to wash the cuvette, and transferred to an Eppendorf tube. The mixture was incubated at 37°C for 1 hr. Cells were harvested by centrifugation at 8,000 rpm for 1 min. The pellet was resuspended in the rest of the medium and spread on LB-ampicillin plates. Plates were incubated at 37°C for 1-2 days.

2.3.5   Manipulation of DNA

2.3.5.1 Restriction analysis of DNA

Reaction mixtures were designed to include 1-10 units of restriction enzyme (Roche, Mannheim or New England Biolabs, Schwalbach), 0.1 mg/ml BSA, 1× optimal reaction buffer, 1 µg of the appropriate DNA and double-distilled water in a 20-µl (or 50-µl) reaction volume. Reactions were

incubated at the temperature appropriate for the restriction enzyme for 2 h. The restriction fragments were checked by gel electrophoresis in TBE buffer.

2.3.5.2 Dephosphorylation of DNA fragments

Reaction mixtures, including 1× dephosphorylation buffer (Roche, Mannheim), calf intestinal alkaline phosphatase (CIP), DNA fragments and double-distilled water, were incubated at 37°C for 45 min. The enzyme was then inactivated at 60°C for 10 min.

2.3.5.3 Ligation of DNA fragments

Reaction mixtures, including 1× ligation buffer (Roche, Mannheim), 1 μg of DNA fragments (vector : fragment = 1:3) and 1-10 units ligase, were incubated at 16°C for more than 4 h. The ligation products were then used for transformation of *E.coli*.

2.3.6   Polymerase Chain Reaction (PCR)
2.3.6.1   PCR of plasmids

Template DNA was diluted from plasmid DNA to an optimal concentration. The components of the reaction were mixed and PCR was performed according to the following scheme. An Expand high fidelity PCR system (Roche, Mannheim) was used for these experiments. PCR products were checked by electrophoresis on in TBE-agarose gels.

Reaction system		**Reaction plan**
template DNA	1 μl	94 ºC-------5'
PCR buffer 2	10 μl	94 ºC------ 1' ⌉
primer	1 μl x 2	55 ºC------ 1' ⎪ 20 cycles
dNTP mix	16 μl	68 ºC------ 1' ⌋
polymerase	1 μl	68 ºC------ 10'
H₂O	70 μl	4 ºC
Total	100 μl	

2.3.6.2   PCR on whole cells

Fresh yeast cells were picked up with a pipette tip, resuspended in 40 μl of 0.02 M NaOH solution in an Eppendorf tube, and mixed well. Then the tube was heated in a microwave oven for 90 sec. After that samples were incubated at room temperature for 30 min. Samples were then stored at -20ºC for 1 h. The following components were mixed well in PCR reaction tubes and PCR was performed

according to the following reaction scheme, using the Expand high-fidelity PCR system (Roche, Mannheim). The PCR products were checked by gel electrophoresis in TBE.

Reaction system		Reaction plan
dNTP'S	10 µl	94 ºC-------5'
buffer 3 (w/o MgCl$_2$)	6 µl	94 ºC------ 1' ⎤
primer	1 µl x 2	55 ºC------ 1' | 35 cycles
polymerase	1 µl	68 ºC------ 1' ⎦
H$_2$O	33 µl	68 ºC------ 10'
buffer 4 (MgCl$_2$)	6 µl	4 ºC
cell	2 µl	
Total	60 µl	

2.3.7   Determination of pheromone production (halo assay)

2.3.7.1   a-Factor production

The halo assay for **a**-factor production was performed as described by Elion *et al*. (1990). Cultures of mutant (*MAT***a** *mut*) and wild-type strains were grown to log phase (OD$_{600}$ 0.4-0.5). Approximately 1x10^5 lawn cells (Δ*sst2-1*) which is supersensitive to **a**-factor were mixed with 5 ml of top agar (0.6%, pH 4.5) at 45°C, and poured onto YPD plates. The mutant (*MAT***a**) and wild-type cells were harvested and 4×10^6 cells were spotted onto the top agar. A wild-type *MAT***a** strain was used as the positive control and a wild-type *MAT*α strain as the negative control. Plates were incubated at 30°C for 48 h and then photographed.

2.3.7.2 α-Factor production

The halo assay for α-factor production was performed exactly as described above, except that *MAT*α *mut* and lawn cells (Δ*sst1*) were used, and a wild-type *MAT*α strain was used as the positive control whereas a wild-type *MAT***a** strain was used as the negative control.

2.3.8   Pheromone response assay (halo assay)

To determine the sensitivity of mutant strains to pheromone-induced cell cycle arrest, an α-factor halo assay was performed. Cultures of mutants and wild-type strain (*MAT***a**) strains were grown to log phase (OD$_{600}$ 0.4-0.5). Approximately 10^5 cells were mixed with 5 ml of 45°C top agar (0.6%, pH 4.5) and poured onto a YPD plate. Filter discs (Whatman paper) soaked with 4 different concentrations of α-factor (0.5 µg, 1 µg, 2 µg, 5µg) were placed on the top agar. The wild-type strain was used as the positive control, while *ste11* and *ste50* mutants were used as the negative controls. Plates were incubated at 30°C for 48 h and then photographed.

2.3.9   Determination of β-galactosidase activity on plates (X-gal overlay assay)

Cultures of mutant (*MAT*a *mut*) and wild-type (*MAT*a) strains harbouring the plasmid pSB234 (*FUS1-lacZ* reporter) were grown to log phase (OD_{600} 0.2-0.4). Samples containing 3×10^7 cells were harvested and the pellet was resuspended in SD medium to give a final volume of 500 µl. The cells were the treated with 5 µM α-factor (final concentration) and incubated at 30°C for 1.5-2 h. The cells were then inspected under the microscope for the formation of shmoos, harvested and concentrated to a final volume of 12 µl. A 3.5-µl of these cells was then spotted onto an SD plate and the plate was dried in a sterile cabinet for 0.5 h. To make the overlay, 5 ml of 10 mg/ml melted agarose was mixed with 4.8 ml of 1.0 M sodium phosphate buffer (pH 7.0) and 100 µl of 10% SDS in a test tube. Then 100 µl of 10 mg X-gal/ml was added to the test tube and mixed thoroughly. The mixture was carefully poured onto the SD plate, which was then incubated at 30°C and photographed every 6 or12 h.

Stock solutions:

- 1.0 M Sodium phosphate buffer, pH 7.0 (57.7 ml Na_2HPO_4 (1.0 M) and 42.3 ml NaH_2PO_4 (1.0 M))
- 10% SDS
- 10 mg X-gal/ml (dimethyl formamide)

2.3.10   Determination of β-galactosidase activity in liquid phase

Pheromone induction and measurement of β-galactosidase activity were performed as described by Trueheart and Fink (1987). Cultures of mutant (*MAT*a *mut*) and wild-type (*MAT*a) strains harbouring plasmid pSB234 were grown to log phase (OD_{600} 0.2-0.4). α-Factor was added to 28-ml cultures to a final concentration of 5 µM. Samples (1 ml) samples were taken after the cells had been induced with α-factor for 0, 30, 60, 90, 120, 180, 240 and 300 min. At each time point 77 µl of culture was also fixed with 3.5% formaldehyde for the investigation of shmoo formation. The 1 ml samples were centrifuged at 13,000 rpm 4°C for 5 min. The pellet was quickly resuspended in 100 µl of lysis buffer and stored at -70°C overnight. Then 700 µl of ONPG solution (1 mg/ml ONPG in Z-buffer) was added and the reaction was allowed to proceed at 30°C for from 0 to 2 h [control: 100 µl lysis buffer plus 700 µl of ONPG solution (1 mg/ml ONPG in Z-buffer)]. The reaction was stopped with 0.5 ml of 1 M Na_2CO_3 until the development of a yellow color. The reaction mixture was centrifuged at 13,000 rpm for 10 min. The $A_{420\,nm}$ values of the supernatants were measured, using the formula:

$$\text{Miller units} = \frac{A_{420\,nm} \times 1000}{A_{600\,nm} \times \text{Time (min)} \times \text{Volume (ml)}}$$

<u>Z-buffer</u>

$Na_2HPO_4 \cdot 2H_2O$ 10.6 g; $NaH_2PO_4 \cdot H_2O$ 5.5 g; KCl 0.75 g; $MgSO_4 \cdot 7H_2O$ 0.25 g; pH 7.0

ONPG solution: 1 mg/ml ONPG in Z-buffer

Lysis buffer (200ml): 20 ml 1.0 M Tris-HCl (pH 7.0) + 100 μl Triton X-100 + 179.90 ml H_2O

2.3.11 Determination of the shmoo and budding indexes

Cultures of mutant (*MAT*a *mut*) and wild-type (*MAT*a) strains were grown to log-phase (OD_{600} 0.2-0.4). α-Factor was added to the cultures to a final concentration of 5 μM. Samples were taken after incubation with α-factor for 0, 30, 60, 90, 120, 180, 240 and 300 min and fixed immediately with 3.7% formaldehyde. Cells were washed twice with 1× PBS buffer before microscopy. At least 300 cells per sample were counted and the numbers of shmoos and unbudded cells were recorded. The shmoo index was defined as the percentage of shmoos relative to the toal number of cells. The budding index was defined as the percentage of unbudded cells.

2.3.12 Microscopy
2.3.12.1 Investigation of GFP (green fluorescent protein) localization in zygotes

Cultures of opposite mating type (*MAT*a and *MAT*α) harbouring a plasmid which carries the GFP gene under the control of the *MET25* promoter were grown to log phase. Equal numbers ($3×10^6$) of cells of each mating type were mixed and harvested by centrifugation. The cells were transferred to a NC membrane on a YPD plate. The plates were incubated at 30°C for 2 h, 3 h and 4 h, and then the cells were washed from the membrane with 1 ml of sterile water. The cells were harvested by centrifugation. Pellets were sonicated briefly to break up clumps. The localization of GFP in zygote was investigated by immunofluorescence microscopy.

2.3.12.2 Simultaneous detection of DAPI and GFP

Cultures of strains harbouring a plasmid carrying the GFP gene under the control of the *GAL1* promoter were grown to log-phase in SRG medium. Cells were harvested and washed with 1× PBS buffer (pH 7.4) in Eppendorf tubes. The cells were sonicated briefly and fixed with 70% ethanol for 12 min. Then the cells were washed again with 1× PBS buffer, stained with DAPI (4', 6-diamidino-Z-phenylindole, 1μg/ml DAPI) at room temperature for 12 min, and washed again with 1× PBS buffer. The localization of GFP-fusion protein and nuclei stained with DAPI was investigated by immunofluorescence microscopy.

2.3.13   Gene disruption and verification of disruption by PCR

2.3.13.1 Gene disruption

Gene disruption in *S.cerevisiae* was performed according to the method described by Guldener *et al.* (1996). The fragment carrying the *LoxP-kanMX-LoxP* disruption cassette was amplified by PCR. PCR products were precipitated by adding 96% ethanol (2-2.5 times the volume of the PCR mixture) and 3 M NaAc (1/10 the volume of the PCR mixture), followed by incubation at -20°C for 20 min. Then the mixture was centrifuged at 13,000 rpm for 10 min and 100 µl of 70% ethanol was added to the pellet. After the pellet was allowed to dry at room temperature, 10 µl of water was added. Yeast cells were transformed with the *LoxP-kanMX-LoxP* disruption cassette by the high efficiency LiAc transformation method (see above). Single colonies were isolated from YPD plates containing G418 and prepared for further analysis.

2.3.13.2 Verfication of gene disruption by PCR

A well separated colony growing on a YPD plate containing G418 was picked with a pipette tip and resuspended in 40 µl of 0.02 M NaOH solution in an Eppendorf tube. The tube was heated in a microwave for 90 sec, then the tube incubated at room temperature for 30 min. The sample was stored at -20ºC for 1 h. A PCR was then performed to check the length of the fragments.

2.3.13.3 Marker rescue by induction of *cre* expression

Marker rescue by induction of *cre* expression was performed according to the method described by Gueldener *et al.* (1996). The *cre* expression vector pSH47 was transformed into the disruption strain (*YFG* = your favorite gene) *yfg::loxp-kanMX-loxP*) to select for uracil prototrophy on an SD plate. The plate was incubated at 30°C for 3 days. Two transformants were picked and resuspended in 2 ml of YPG medium. The cultures were incubated at 30°C for 2 h. Then approximately 200 cells were spread onto a YPD plate. After incubation of the plate at 30°C for 2 days, the colonies were replicated onto a YPD plate containing G418 (400 mg/l G418). About 80 to 90% of the colonies had lost the kan[r] marker and carried one single *yfg::loxp* in the chromosomal locus. Colonies that could not grow on YPD plus G418 were checked and the loss of the kan[r] marker was confirmed by diagnostic PCR analysis. The *cre* expression vector pSH47 was removed from the strain by streaking the strain on plates containing 5-fluoro-orotic acid to select for the loss of the plasmid.

2.3.14 Two-hybrid assay

In order to test for protein-protein interactions in a *GAL4* two hybrid system, the plasmids pGAD-X and pMBD-Y were constructed and co-transformed into the diploid strain PJ187. The culture of strain PJ187 harbouring two plasmids was grown overnight in SD-trp[-] leu[-] medium. A rapid replica was

made onto SD-trp⁻ leu⁻his⁻ plates, followed by incubation at 30°C overnight. Then 5 ml of melted

agarose (10 mg/ml) was mixed with 4.8 ml of 1.0 M sodium phosphate buffer (pH 7.0), and 100 µl of

10% SDS in a test tube. Then 100 µl of 10 mg X-gal/ml DMF was added to the test tube and mixed

thoroughly, and the mixture was carefully poured onto the SD plate. The plate was incubated at 30°C

for 2 days and then photographed.

2.3.15 SDS-Polyacrylamide Gel Electrophoresis of proteins

2.3.15.1   Preparation of protein extracts

A 25-ml volume of SRG medium was inoculated from a 5-ml overnight culture of cells in SRG

medium and grown to an OD_{600} value of 0.4-0.8. Four OD_{600} units of cells were harvested by

centrifugation at 3,000 rpm for 5 min. The pellet was washed with 1 ml of E-buffer in an Eppendorf

tube. Cells were collected by centrifugation at 13,000 rpm for 3 min. The pellet was resuspended in

150 µl of E-buffer* and a 2/3 volume of glass beads was added. The mixture was vortexed at 4°C for

3 min. 100 µl E-buffer* was added to the Eppendorf tube and mixed well. Then the mixture was

centrifuged at 13,000 rpm and 4°C for 3 min. The supernatant was transferred to a fresh Eppendorf

tube. A 10-µl aliquot of the supernatant was mixed with 10 µl of 2x sample buffer containing 10 mM

DTT. The mixture was then heated at 85°C in a water bath for 10 min and loaded onto an SDS

polyacrylamide gel.

<u>E-buffer (500 ml)</u>

Tris/HCl (pH 7.4) 25 mM		(12.5ml from 1 M Tris/HCl pH 7.4)
EDTA	5 mM	(5 ml from 500 mM EDTA)
Triton X-100	0.1 %	(0.5 ml from 100% Triton X-100 or 5 ml 10% Triton X-100)
Glycerol	10 %	(50 ml from 100% glycerol)
NaCl	150 mM	(15 ml from 5 M NaCl)

<u>E-buffer* 1ml (for 3 samples)</u>

The following materials were added to E-buffer:

1 mM DTT (10 µl from 1 M DTT)

1 mM PMSF (2 µl from 500 mM stock or 10 µl from 100 mM stock)

0.1 mM protease inhibitor mixture (4 µl protease inhibitor mixture: pepstatin (1 mg/ml); aprotinin (1 mg/ml);

leupeptin (5 mg/ml); antipain 5 mg/ml)

0.1 mg/ml soybean, trypsin inhibitor (10 µl 10 mg/ml stock)

2.3.15.2 Gel preparation

SDS polyacrylamide gels were prepared according to the standard protocol (Sambrook *et al*., 1989).

Glass plates were washed with ethanol and H_2O. The glass plates were inserted into the gel frame and

sealed with 1% agarose on both sides. The compositions of resolving gel, stacking gel and gel loading buffer were as follows:

Resolving gel (7.5%)	Stacking gel	Gel-loading buffer
5 ml 30% acrylamide	1.7 ml 30% acrylamide	30.2 g Tris
5 ml 1.5M Tris/HCl (pH 8.8)	1.25 ml 1M Tris/HCl (pH 6.8)	144 g glycin
10 ml H_2O	7 ml H_2O	1% SDS
200 µl 10% SDS	100 µl 10% SDS	1 l water
40 µl Temed	25 µl Temed	
50 µl 10% APS	25 µl 10% APS	

2.3.15.3 Electrophoresis

A 10-15 µl aliquot of protein ladder marker and 20 µl samples were loaded into the slots of the SDS-polyacrylamide gel. A current of 13 mA was applied to the gel overnight until the tracking dye reached the end of the gel.

2.3.15.4 Transfer of proteins from SDS-polyacrylamide gels to filters (Western blotting)

Electrophoretic transfer of proteins from the polyacrylamide gels to a filter membrane was performed according to the standard protocol (Sambrook *et al.*, 1989). The protein was transferred from the SDS-polyacrylamide gel to an NC membrane at 4°C and 200 mA for 3-4 h. The membrane was allowed to dry at room temperature for 30 min and stained with Ponceau S to check equal loading and transfer efficiency.

Buffer
15 g Tris, 72 g glycin, 1 liter methanol (20%). Add water to 5 liter.

2.3.16 Immunolabelling of protein blots

The blot was blocked in Tris-buffered saline (1× PBS) containing 0.1% Tween 20 and 5% bovine serum albumin (BSA) and incubated with primary and secondary antibody according to standard protocols (Sambrook *et al.*, 1989). The following antibodies and dilutions were used:

Antibody	Description	Dilution	Company
anti-c-Myc	monoclonal mouse IgG	1:1000	Oncogene
anti-GST	rabbit polyclonal IgG	1:1000	Santa Cruz
anti-mouse IgG-AP	alkaline phosphatase (conjugate)	1:5000	Dianova
anti-mouse IgG-HRP	peroxidase (conjugate)	1:50000	Dianova
anti-rabbit IgG-AP	alkaline phosphatase (conjugate)	1:5000	Dianova
anti-rabbit IgG-HRP	peroxidase (conjugate)	1:50000	Dianova

The protein bands were detected by one of two separate methods.

(1) Alkaline phosphatase detection system. Immunoblots probed with anti-c-Myc monoclonal antibody or anti-GST polyclonal antibody were developed with alkaline phosphatase conjugated anti-mouse or anti-rabbit secondary antibody. Colorimetric detection of bound antibody was carried out in 25 ml of substrate buffer containing 0.1 mg/ml BCIP and 1 mg/ml NBT.

(2) Chemiluminescent detection system. Immunoblots probed with anti-c-Myc monoclonal antibody or anti-GST polyclonal antibody were treated with peroxidase conjugated anti-mouse or anti-rabbit secondary antibody. In this case, visualization of bound antibody was done by incubation of the immunoblots with Lumi light Western blotting substrate and luminescent bands were detected using Fuji film LAS-1000 combined with the image reader LAS-1000 V1 program.

20 x PBS			Substrates		
200 μM $NaH_2PO_4.H_2O$	27.6 g		0.1 M Tris/HCl	pH 8.8	(66.67 ml 1.5 M Tris/HCl, pH8.8)
3 M NaCl	175.32 g		0.1 M NaCl		(20 ml 5 M NaCl)
water	1 l		2 mM $MgCl_2$		(2 ml 1.0 M $MgCl_2$)
pH 7.2			in 1 l water		

2.3.17 Protein interaction analysis

2.3.17.1 Pull down assay

Protein extracts (extracts 1 and 2) for pull-down assays were prepared as described in Section 2.3.15.1. Approximately 180 μl of extract 1 was added to 40 μl of 50% glutathione-Sepharose (glutathione-Sepharose was washed twice with E-buffer before use). The mixture was incubated at room temperature for 1 h, then centrifuged at 5,000 rpm and 4°C for 1 min and the supernatant was removed using a glass capillary pipet. The pellet was washed 4 times (once every 10 min) with 1 ml of E-buffer** at 4°C and then centrifuged at 5,000 rpm and 4°C for 1 min. The supernatant was discarded following the last washing step. Then about 180 μl of extract 2 was added and the mixture was incubated at 4°C for 3 h. The glutathione-Sepharose beads were pelleted by centrifugation at 5,000 rpm and 4°C for 1 min. Then the pellet was washed twice with E-buffer** and once with fresh E-buffer. After the last wash, 40 μl of 2× sample buffer containing 20 mM DTT was added to the tube to elute the bound proteins from the glutathione-Sepharose beads. The inner surface of the Eppendorf tube was dried with Whatman filter, and the proteins were analyzed by SDS-polyacrylamide gel and detected by Western analysis (refer to section 2.3.16).

E-buffer (500 ml)

Tris/HCl (pH 7.4) 25 mM   (12.5ml from 1.0 M Tris/HCl, pH 7.4)

EDTA   5 mM   (5 ml from 500 mM EDTA)

Triton X-100   0.1 %   (0.5 ml from 100% Triton X-100 or 5 ml 10% Triton X-100)

glycerol   10 %   (50 ml from 100% glycerol)

NaCl   150 mM   (15 ml from 5 M NaCl)

E-buffer*

The following materials were added to E-buffer:

1 mM DTT (10 µl from 1.0 M DTT)

1 mM PMSF (2 µl from 500 mM stock or 10 µl from 100 mM stock)

0.1 mM protease inhibitor mixture (4 µl protease inhibitor mixture: pepstatin (1 mg/ml); aprotinin (1 mg/ml); leupeptin (5 mg/ml); antipain 5 mg/ml)

0.1 mg/ml soybean, trypsin inhibitor (10 µl 10 mg/ml stock)

E-buffer**

The following materials were added to E-buffer:

0.05% DOC	5 µl -10% stock
1 mM PMSF	10 µl -100 mM stock
1 µg/ml aprotinin	1 µl -1 mg/ml stock (10 mg in 10 ml ethanol)
1 mM DTT	1 µl -1.0 M stock

2.3.18 Galactose depletion assay

The galactose depletion assay was performed according to the protocol described by Esch *et al.* (2002). Cultures were grown to early log phase in the appropriate selective medium containing 3% raffinose and 1% galactose for the expression of *GAL-MYC-FUS3, GAL-MYC-STE5* or *GAL-GST-STE5*. Cells were then harvested, washed, and transferred to medium containing 2% glucose to inhibit further transcription of the fusion gene. After the removal of a sample for protein extract preparation, incubation of the cultures was continued without or with pheromone (final concentration of 5 µM α-factor) to activate the mating pheromone response pathway. Whole cell extracts were prepared for immunoblot analysis as described above.

2.3.19 Invasive growth assay

The plate-washing assay was performed essentially as described previously (Cullen and Sprague, 2002). Equal concentrations of mutant and wild-type cells were spotted on YPD plates; invasion was allowed to proceed for 3 days at 30°C and the plates were photographed, and then washed vigorously with water and rubbed with a wet finger to remove cells that had not invaded the agar. The plates were then photographed again.

2.3.20 Analysis of sensitivity to hyperosmolarity

Analysis of sensitivity to hyperosmolarity was performed as described by Jansen *et al*. (2001). Cells of mutant and wild-type strains were grown in YPD medium to an OD_{600} value of 0.8, and serial 10-fold dilutions (over a 10,000-fold range) were spotted on solid medium containing 1.5 M sorbitol and 1.0 M NaCl. Plates were incubated for 2 days at 30°C and then photographed.

2.3.21 Bio-informatics

Genes related to defined ORFs, gene function and related information including cellular role, biochemical function, location, mutant phenotype, domains, motifs, physical interaction, functional genomics and drug effects, etc. were obtained from Proteome (http://www.proteome.com/databases/YPD/YPDsearch-long.html), MIPS (http://www.mips.biochem.mpg.de/cgi-bin/proj/eurofan/eurofan_2/n99/search.pl), NCBI (http://www.ncbi.nlm.nih.gov) and SGD (http://genome-www.stanford.edu/cgi-bin/SGD/search).

3. Results

3.1 Functional analysis to specify the reduced mating efficiency of single gene deletion mutants of *S. cerevisiae*

In the course of a large-scale screen performed in the context of the EU program EUROFAN, a project directed towards the functional analysis of single-gene deletion strains of the yeast *S. cerevisiae*, 55 strains were identified that displayed reduced mating efficiency. These 55 mutants and 9 other strains were the starting point for this study. The major goal was to characterize in detail novel genes required for the mating of *S. cerevisiae* (Table 2.1).

3.1.1   Assessment of the mating efficiency of the 64 single-gene deletion mutants

3.1.1.1 Semi-quantitative mating analysis

The 64 single-gene deletion mutants were first analyzed for mating efficiency using a semi-quantitative assay. Each deletion mutant (and the corresponding wild-type gene) was available in both mating types, and these strains were crossed *inter se*. Hence, in each case, the *MAT***a** and *MAT*α mutants were crossed with the wild-type (WT) strain of opposite mating type, and with each other. The cross WT *MAT***a** × WT *MAT*α was used as the positive control, and a *ste50* × WT cross was used as the negative control. The tests were performed on SD-agar plates. The production of viable diploids was measured by using complementary auxotrophic markers, thus ensuring that only diploid cells could grow (see Methods for details). An example of the semi-quantitative mating assay is illustrated in Fig 3.1. The mating results for the mutant x WT crosses and *MAT***a** *mut* × *MAT*α *mut* cross were compared with those the positive and the negative controls. The detailed results are shown in Table 3.1. In this semi-quantitative mating assay, only 38 of the 64 single-gene deletion mutants tested showed a significant reduction in mating efficiency.
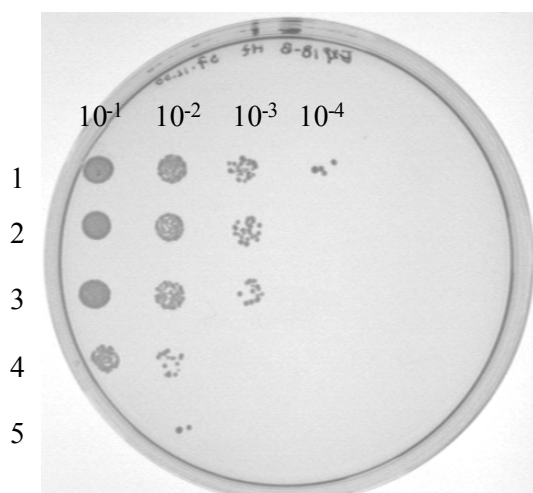

Fig 3.1. Semi-quantitative mating assay. (1) The cross WT *MAT***a** x WT *MAT*α (positive control). (2) the mutant (*MAT***a**) was crossed with wild-type strain (*MAT*α). (3) the mutant (*MAT*α) was crossed with wild-type strain (*MAT***a**). (4) the cross mutant (*MAT***a**) x mutant (*MAT*α). (5) the cross *ste50* x WT (negative control).

Table 3.1. Results of semi-quantitative mating assay and complementation test

Strain number	ORF	Mating defect	**MATa** mutant x wild-type (mating efficiency)	**MATα** mutant x wild-type (mating efficiency)	**Bilateral** homozygous deletants cross (mating efficiency)	Complemen -tation by cognate clone	Gene name (previously identified as)
10001	*YOL088c*	-	++++	++++	++++	-	*MPD2*
10002	*YOL087c*	+	+++	+++	+++	yes	-
10003	*YOR311c*	+	++++	++++	++	no	-
10009	*YBR041w*	+	++++	++++	+++	no	*FAT1*
10016	*YNL058c*	-	++++	n.d	n.d	-	
10018	*YNL054w*	-	++++	++++	++++	-	*VAC7*
10023	*YNL214w*	+	++++	++++	++	yes	*PEX17*
10032	*YJL199c*	+	++++	+++	+++	yes	
10035	*YOL101c*	+	++++	++++	++	no	-
10039	*YNL196c*	+	+++	+++	+++	yes	*SLZ1*
10058	*YBR016w*	-	++++	++++	++++	-	-
10068	*YJL047c*	+	++++	++	+	-	*RTT101*
10070	*YJL058c*	-	++++	++++	++++	-	-
10115	*YBL042c*	+	+++	++++	+	-	*FUI1*
10121	*YNL164c*	-	++++	++++	++++	-	-
10141	*YLR077w*	-	++++	++++	++++	-	-
10143	*YNR018w*	+	++++	++++	+	no	-
10145	*YNR021w*	-	++++	++++	++++	-	-
10165	*YOL111c*	+	+++	+++	++	yes	-
10166	*YOL072w*	-	++++	n.d	n.d	-	-
10171	*YDL005c*	-	++++	n.d	n.d	-	*MED2*
10185	*YBL036c*	-	++++	++++	++++	-	-
10188	*YBL029w*	+	++++	++++	+++	no	-
10190	*YBL025w*	-	++++	n.d	n.d	-	*RRN10*
10250	*YGL100w*	+	+++	++++	++	yes	*SEH1*
10303	*YGL133w*	+	++++	+++	++	-	*ITC1*
10312	*YNL107w*	+	+++	++++	++	-	*YAF9*
10319	*YLR104w*	+	++++	0	+	-	-
10349	*YBR078w*	+	+++	+++	+	partly	*ECM33*
10359	*YNL097c*	+	+++	++++	++	yes	*PHO23*
10372	*YBL048w*	-	+++	++++	++++	-	
10373	*YNL059c*	+	++++	+++	+	yes	*ARP5*
10380	*YBR283c*	+	++++	+++	++	partly	*SSH1*
10419	*YDR063w*	+	+++	+++	++	-	-
10423	*YJL134w*	+	++	++++	++	-	-

Strain number	ORF	Mating defect	*MATa* mutant x wild-type (mating efficiency)	*MATα* mutant x wild-type (mating efficiency)	**Bilateral** homozygous deletants cross (mating efficiency)	Complemen-tation by cognate clone	Gene name (previously identified as)
10424	*YJL134w*	+	++++	++++	+++	yes	*LCB3*
10425	*YJL145w*	+	++++	++++	+++	no	*SFH5*
10426	*YJL146w*	-	++++	++++	++++	-	*IDS2*
10427	*YJL147c*	-	++++	++++	++++	-	-
10428	*YJL148w*	-	++++	++++	++++	-	*RPA34*
10429	*YJL149w*	-	n.d	++++	n.d	-	-
10430	*YDL202w*	+	+++	++++	+	no	*MRPL11*
10431	YDL201w	+	+++	++++	+++	yes	-
10434	*YDL189w*	+	+	+++	+	yes	
10438	*YJL122w*	+	0	++++	0	no	-
10446	*YDL018c*	-	++++	++++	++++	-	
10454	*YOR09w*	-	++++	++++	++++	-	
10458	*YNL100w*	-	n.d	++++	n.d	-	-
10459	*YNL099c*	-	++++	++++	++++	-	
10470	YBR217w	+	++++	+	+	partly	*APG12*
10475	*YDL158c*	+	0	+	0	-	-
10489	*YDL048c*	-	++++	++++	++++	-	*STP4*
10495	*YOL151w*	-	++++	++++	++++	-	*GRE2*
10496	*YOL124c*	-	++++	++++	++++	-	-
10505	*YNL119w*	+	0	++++	0	yes	
10565	*YNL331c*	-	++++	++++	++++	-	
10566	YOL057c	+	++++	+	+	yes	
10614	*YDL231c*	+	+++	+++	++	no	-
10615	*YLL051c*	+	++	++++	++	yes	
10623	*YGL085w*	-	++++	++++	++++	-	-
10624	*YGR016w*	+	+	++++	++	-	-
10659	*YNL080c*	+	++	++++	+	-	-
10674	*YJR074w*	+	++	+++	++	-	*MOG1*
10740	*YNL323w*	+	++++	++++	+++	-	-

Mating defect (+); no defect (-). Mating efficiency: wild-type (++++); 50-90% (+++); 10-50% (++); < 10% (+); n.d (not done).   Complementation test: can be complemented (yes); can be partly complemented (partly); can't be complemented (no); n.d (not done); no cognate clone (-). In the following, the final digits of each strain number are used to refer to that strain (e.g. mutant 39 corresponds to strain number 10039).

The 38 mutants that showed a significant reduction in mating efficiency could be classified into four groups:

(I) Nine mutants (2, 39, 165, 349, 419, 434, 475, 614, 674) displayed reduced mating efficiency in all three mating tests (*MAT***a** *mut* × WT, *MAT*α *mut* × WT, and *MAT***a** *mut* × *MAT*α *mut*).

(II) Eight mutants (32, 68, 303, 319, 373, 380, 470, 566) displayed reduced mating efficiency in the *MAT*α *mut* × *MAT***a** WT cross and in the bilateral mutant cross (*MAT***a** *mut* × *MAT*α *mut*).

(III) 12 mutants (115, 250, 312, 359, 423, 430, 431, 438, 505, 615, 624, 659) displayed a mating defect in the *MAT***a** *mut* × *MAT*α WT cross and in the bilateral mutant cross.

(IV) The remaining 9 mutants (3, 9, 23, 35, 143, 188, 424, 425, 740) displayed a mating defect only in the cross between the two deletion strains; i.e. only when both mating partners carried the same mutation.

3.1.1.2. Complementation of the mating defects

Due to the possibility that the mating defect in any of the deletion strains might have been caused indirectly during strain construction, it was necessary to demonstrate that the deletion mutation itself was responsible for the phenotype. This was done by carrying out complementation tests. Each of the deletion mutants was transformed with the cognate wild-type clone. The control strains, including the wild-type strain, were transformed with the empty pRS416 vector. Unfortunately, no cognate clones were available for 12 of the mutants. The other twenty-six mutants (2, 3, 9, 23, 32, 35, 39, 143, 165, 188, 250, 349, 359, 373, 380, 424, 425, 430, 431, 434, 438, 470, 505, 566, 614, 615) were transformed with cognate clones and the mating assay was performed. The results of these tests are shown in Table 3.1.

In 14 mutants (2, 23, 32, 39, 165, 250, 359, 373, 424, 431, 434, 505, 566, 615) the mating defect could be complemented by the respective cognate clone. In three cases (349, 380, 470), the defect could only be partially complemented by the cognate clone. The mating defect observed in the cross between *MAT*α *mut566* and *MAT***a** WT and in the bilateral mutant cross (*MAT***a** *mut566* × *MAT*α *mut566*) could also only be partly complemented by the respective WT clone.

3.1.1.3 Data analysis and selection of candidates for further study

In order to select candidates from these 38 mutants for further studies, the information available in the published literature and in the databases (YPD, SGD, MIPS etc.) was analysed in detail. Of the 38 ORFs, 22 ORFs have a designated gene name; the other 16 ORFs represented ORFs of unknown function (Table 3.1). Mutant 250 was previously reported to exhibit no apparent defect in the bilateral mutant cross, but in my experiments the mutant 250 showed significantly reduced mating efficiency. The mating defect in deletion mutant 303 was previously reported (Victoria and Mazon, 2000). In another study the bilateral mating defect of deletion mutant 165 was reported (Iwanejko *et al*., 1999).

However, I found that deletion mutant 165 showed a significant reduction in mating efficiency in all three tests.

The criteria used to select novel mutants were as follows. (1) The mutant should show the defect in three mating tests. (2) Transformation with the cognate clone should complement the mating defect. (3) Where available, the information in the databases and the literature should suggest a direct relationship between gene product and/or phenotype and the mating defect of the mutant. Based on these criteria, the following 15 mutants were selected for further study.

(I) *YOL087c* (deletion mutant 2) showed reduced mating efficiency in all three mating tests. This mating defect could be complemented by the cognate clone. The protein encoded by *YOL087c* has one WD (WD-40) domain. The null mutant exhibits reduced growth in YPG and SD medium (EUROFAN-project; Mips.gsf.de).

(II) *YNL196c* (deletion mutant 39; gene *SLZ1*) showed reduced mating efficiency in all three mating tests. The mating defect could be complemented by the cognate clone. It has been observed that Slz1 is a sporulation-specific protein which has a leuzine zipper domain. Moreover, Slz1 exhibits interaction with Crm1 (the exportin beta-karyopherin, which functions in the export of certain proteins from the nucleus). *MAT***a** and *MAT*α strains bearing the deletion differed in their mating efficiencies (EUROFAN-project; Mips.gsf.de).

(III) *YOL111c* (deletion mutant 165) exhibited reduced mating efficiency in all three mating tests. The mating defect could be complemented by the cognate clone. The protein encoded by *YOL111c* shows similarity to the human ubiquitin-like protein GdX. A null mutant appears to be relatively insensitive to gamma rays or UV irradiation (Iwanejko *et al*., 1999), and displays reduced growth in YPD, YPG and SD media (Iwanejko *et al*., 1999).

(IV) *YGL100w* (deletion mutant 250; gene *SEH1*) showed significantly reduced mating efficiency in the bilateral mating test and in the cross with the *MAT***a** WT. The mating defect could be complemented by the cognate clone. Seh1 is found in a complex with a nuclear pore protein which is a member of the WD (WD-40) repeat family. Seh1 localizes symmetrically on both sides of the nuclear pore and the peripheral membrane, and is a nuclear import/export protein (Lillo *et al*., 2000).

(V) *YGL133w* (deletion mutant 303; gene *ITC1*) showed reduced mating efficiency in the bilateral mating test and in the cross with the *MAT***a** WT strain. Because no cognate clone was available, the corresponding complementation test has not been carried out. Itc1 is a subunit of the Isw2 chromatin remodelling complex and is located in the nucleus. The *MAT*α mutant shows an abnormal morphology (Victoria and Mazon, 2000).

(VI) *YBR078w* (deletion mutant 349; gene *ECM33*) exhibited reduced mating efficiency in all three mating tests. The mating defect could be complemented by the cognate clone. Ecm33 is a protein with a predicted GPI-anchor signal and is involved in the structure or biosynthesis of the cell wall. Ecm33 associates with the plasma membrane (Tohe *et al*., 1999; Terashima *et al*., 2003).

(VII) *YNL059c* (deletion mutant 373; gene *ARP5*) showed reduced mating efficiency in the bilateral mating test and in the cross with *MAT**a*** WT. The mating defect could be complemented by the cognate clone. The Arp5 (Actin-related protein) is related to the Ino80 complex, is located in the nucleus, and is associated with the actin cytoskeleton. The null mutant shows reduced growth in YPD and SD media, and displays a distorted cell shape (with an elongated bud and a large neck) and an increased cell size. In addition, the null mutant also exhibits phenotypic differences in *MAT**a*** and *MATα* backgrounds and is temperature sensitive for growth (Grava *et al.*, 2000; Shen *et al.*, 2003).

(VIII) *YBR283c* (deletion mutant 380; gene *SSH1*) showed reduced mating efficiency in the bilateral mating test and in the cross with *MAT**a*** WT. The mating defect could be partly complemented by the cognate clone. Ssh1 has 10 predicted transmembrane segments, is a component of the Ssh1-Sss1-Sbh2 complex, and is involved in protein translocation into the endoplasmic reticulum (South *et al.*, 2001).

(VIIII) *YJL145w* (deletion mutant 425; gene *SFH5*) showed reduced mating efficiency in the bilateral mating test. This mating defect could be complemented partly by the cognate clone. Sfh5, encoded by *YJL145w*, is annotated as a putative phosphatidylinositol transfer protein (Schnabl *et al.*, 2003).

(X) *YDL201w* (deletion mutant 431) displayed reduced mating efficiency in the bilateral mating test and in the cross with *MATα* WT. The mating defect could be complemented by the cognate clone. Moreover, the protein encoded by *YDL201w* is a putative methyltransferase, and is highly conserved among eukaryotes. The null mutant has a normal growth rate in YPD medium, but shows reduced growth in YPG (Bahr *et al.*, 1999).

(XI) *YBR217w* (deletion mutant 470; gene *APG12*) showed reduced mating efficiency in the bilateral mating test and the cross with *MAT**a*** WT. The mating defect could be complemented partly by the cognate clone. Apg12 is a ubiquitin-like modifier and plays an essential role in the formation of the autophagosome membrane during autophagy (Rodriguez-Navarro *et al.*, 1999).

(XII) *YNL119w* (deletion mutant 505) displayed reduced mating efficiency in the bilateral mating test and the cross with *MATα* WT. The protein encoded by *YNL119w* is possibly involved in cytoplasmic ribosome function. Null mutants show temperature sensitivity on non-fermentable carbon sources and a slow-growth phenotype at reduced temperature (Capozzo *et al.*, 2000).

(XIII) *YLL057c* (deletion mutant 566) exhibited reduced mating efficiency in the bilateral mating test and in the cross with *MAT**a*** WT. The mating defect in the *MATα mut566* × *MAT**a*** WT cross and in the bilateral muting cross between the mutant haploid strains could only be partly complemented by the respective cognate clone. The protein encoded by *YLL057c* shows similarity to the C-terminal half of a dioxygenase enzyme from *E. coli* (Zhang *et al.*, 2001).

(XIV) *YLL051c* (deletion mutant 615; gene *FRE5*) exhibited reduced mating efficiency in the bilateral mating test and in the cross with *MATα* WT. The mating defect can be complemented by the cognate clone. Fre5, encoded by *YLL051c*, shows similarity to the ferric reductase Fre2 and is subject to regulation by iron. Fre5 is located in the plasma membrane and has six transmembrane segments.

The *FRE5* gene is probably subject to regulation by Aft1 (a transcription factor that regulates genes involved in iron uptake and the control of cell size), since binding elements for this transcription factor are present in its promoter region (Georgatsou and Alexandraki., 1999).

(XV) *YGL106w* (deletion mutant 624; gene *KAP122*) showed reduced mating efficiency in the bilateral mating test and in the cross with *MAT*α WT. *YGL106w* encodes the nuclear transport factor Kap122. Kap122 is a member of the karyopherin-beta family, is found in the nucleoplasm, nuclear pores and the cytoplasm, and in the peripheral membrane, and functions in the import of the Toa1-Toa2 complex into the nucleus (Titov *et al.*, 1999).

These 15 mutants, 10 of which had already been specifically named on the basis of previous phenotypic tests, were selected for more extensive tests aimed at identifying the site of the defect in the mating process. To do this, these mutants were subjected to a quantitative mating assay (see below), and tested for mating pheromone production, pheromone response, polarized morphogenesis, cell fusion and nuclear fusion.

3.1.1.4 Quantitative mating analysis of 15 mutants

The quantitative mating analysis was performed as described under Methods (2.3.1.2). The results for the 15 mutants are shown in Table 3.2. All 15 mutants showed significantly reduced mating efficiency and could be classified into three groups.

(I) Four mutants (250, 431, 505, 615) displayed significantly reduced mating efficiency in mating tests involving the *MAT*a *mut* strain (i.e. in the crosses *MAT*a *mut* × *MAT*α WT and *MAT*a *mut* × *MAT*α *mut*).

(II) Five mutants (303, 373, 380, 470, 566) showed significantly reduced mating efficiency in the *MAT*α *mut* × *MAT*a WT cross and in the bilateral cross between the two mutant mating partners.

(III) Six mutants (2, 39, 165, 349, 425, 624) exhibited reduced mating efficiency in all mating tests.

Table 3.2A. Mutants showing significant reduced mating efficiency in *MAT*a and bilateral mating

Strain number	ORF name	Mating defect	*MAT*a mutant x WT cross (%)	*MAT*α mutant x WT cross (%)	Bilateral cross of homozygous deletants (%)	Gene name
250	*YGL100w*	+	18.2	75.3	3.47	*SEH1*
431	*YDL201w*	+	14.8	98.4	22.9	-
505	*YNL119w*	+	0	94.2	0	-
615	*YLL051c*	+	6.34	93.7	11.9	*FRE6*

Table 3.2B. Mutants showing significantly reduced mating efficiency in *MATα* and bilateral mating

Strain number	ORF name	Mating defect	*MAT***a** mutant x WT cross (%)	*MAT*α mutant x WT cross (%)	Bilateral cross of homozygous deletants (%)	Gene name
303	*YGL133w*	+	72.2	6.93	7.27	*ITC1*
373	*YNL059c*	+	94.8	17.6	23.7	*ARP5*
380	*YBR283c*	+	97.4	19.7	19.2	*SSH1*
470	*YBR217w*	+	62.6	1.10	0.50	*APG12*
566	*YOL057c*	+	51.2	0.765	0.221	-

Table 3.2C. Mutants showing reduced mating efficiency in *MAT***a**, *MAT*α and the bilateral mating

Strain number	ORF name	Mating defect	*MAT***a** mutant x WT cross (%)	*MAT*α mutant x WT cross (%)	Bilateral cross of homozygous deletants (%)	Gene name
2	*YOL087c*	+	31.0	53.8	10.4	-
39	*YNL196c*	+	75.8	74.3	58.9	*SLZ1*
165	*YOL111c*	+	79.6	25.8	5.30	-
349	*YBR078w*	+	32.3	2.52	1.31	*ECM33*
425	*YJL145w*	+	75.0	87.9	54.3	*SFH5*
624	*YGL016w*	+	43.5	77.6	30.3	*KAP122*

3.1.2   Pheromone production by the 15 mutants

Haploid cells stimulate each other by secreting peptide pheromones. *MAT***a** cells secrete the **a** mating pheromone (**a**-factor) whereas *MAT*α cells secrete α mating pheromone (α-factor). Studies on pheromone production in the single deletion mutants were carried out to determine whether the mating defect was caused by a disturbance in pheromone production.

3.1.2.1 α-Factor production by the 15 mutants

Production of α-factor by *MAT*α cells of each of the 15 mutants was tested in a halo assay. The halo

assay is based on the fact that secretion of α-factor arrests the growth of *MAT***a** cells by inhibiting cell cycle progression in the G$_1$ phase. The level of α-factor produced by the mutants is reflected in the

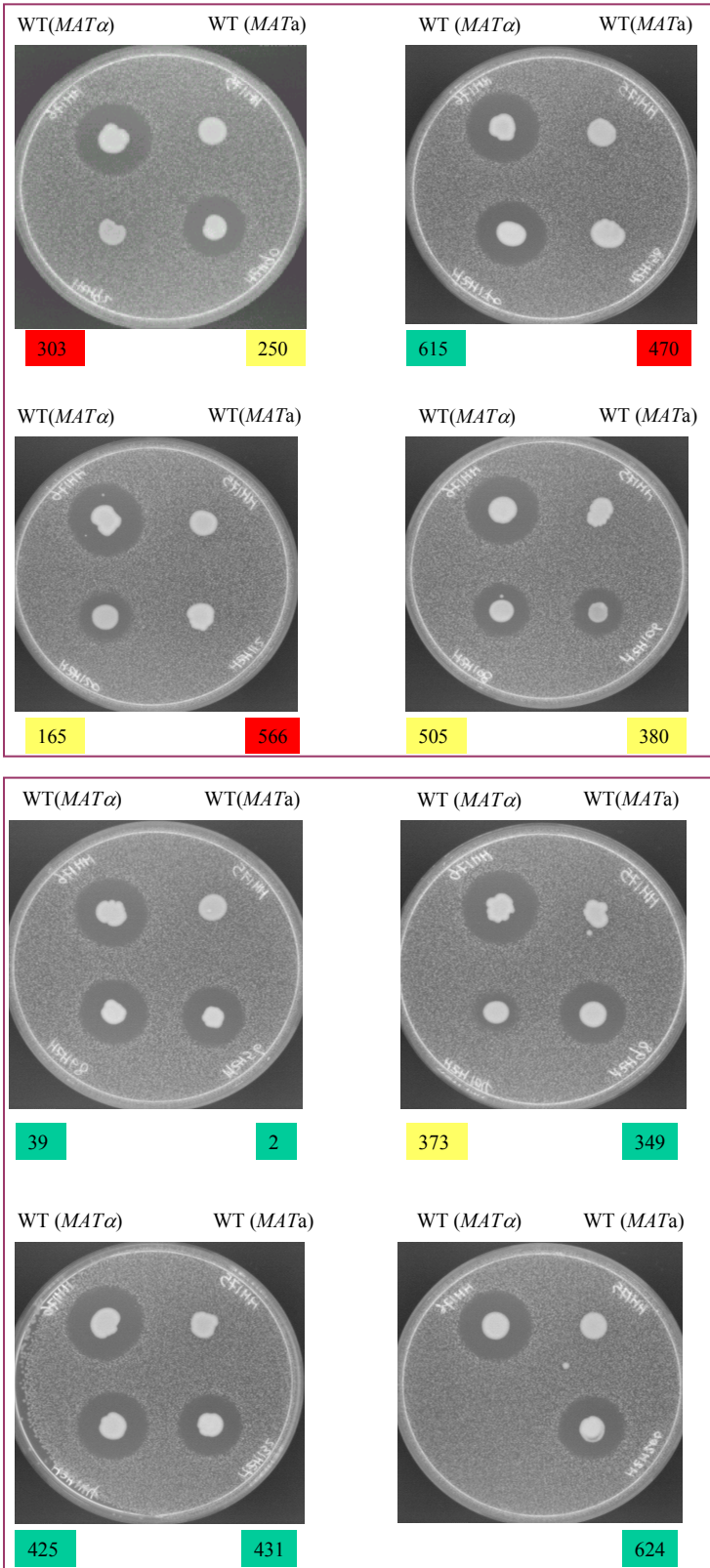Fig. 3.2 α-factor production of 15 mutants (halo assay) as described under methods (2.3.7.2). The size of the halo induced by each of the mutants was compared with that produced by the wild-type strain. Lawn cell is *MAT*a *sst1* mutant which is supersensitive to α-factor. Red indicates a total defect in pheromone production, yellow a partial defect in pheromone production; and green indicates no defect in pheromone production.

size of the halo. Results are shown in Fig 3.2. Three mutants (303, 470, 566) did not induce the formation of any halo. This strongly suggests that they are almost totally defective in the production of α-factor and implies that they might be perturbed in mating-type regulation (see below). Four mutants (165, 250, 380, 505) produced a smaller halo than the wild-type strain, suggesting that they are partially defective in α-factor production. Seven mutants (2, 39, 349, 425, 431, 615, 624) showed no defect in α-factor production.

The three mutants (303, 470, 566) that failed to produce detectable levels of α-factor were also examined for the ability to synthesize **a**-factor, in order to check for possible mating type switching. However, none of the mutants formed a halo when grown on a lawn of the *sst2* mutant (Fig 3.3). These results suggest that the defect in α-factor production in these mutants does not result from mating type switching. It is however possible that they exhibit a defect in mating type gene regulation.
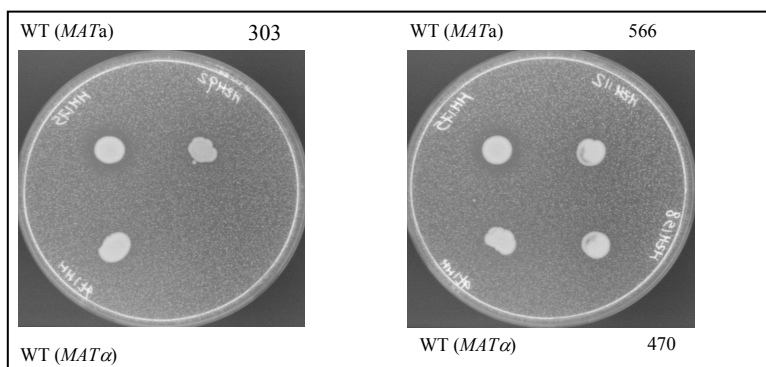

Fig 3.3. Examination for mating type switching (halo assay). Wild-type strain and mutant cells were grown to log-phase. 0.6% top agar was mixed with 10^5 lawn cells (*sst2* mutant). Approximately 4×10^6 wild-type cells and mutant cells were dropped on the top agar. Wild-type strain (*MAT*a) was used as the positive control and wild-type strain (*MAT*α) represented the negative control. The plates were incubated at 30°C for 2 days and photographed.

3.1.2.2 a-Factor production by the 15 mutants

In this experiment the 15 *MAT***a** mutants were tested in a halo assay on a lawn of *MAT*α cells, and the production of **a**-factor was evaluated by measuring the size of the halo. The results showed that the sizes of the halos induced by these 15 mutants were similar to that produced by the wild-type strain (data not shown). These findings suggest that none of the 15 mutants are defective in **a**-factor production.

3.1.3 Analysis of the pheromone response in the 15 mutants

In response to pheromone, *MAT***a** and *MAT*α cells undergo many physiological changes that allow mating to occur efficiently. In essence, the role of the pheromones is to induce a transient developmental transformation of growing cells into cells that possess the characteristics of gametes. The suite of changes elicited in haploid cells by exposure to pheromone includes (1) increased transcription of genes whose products facilitate mating -- either directly by promoting cell and nuclear

fusion or indirectly by contributing to the alterations in cellular physiology necessary to accommodate these processes; (2) arrest of the mitotic cell division cycle in the G_1 phase; (3) preparation of the cell surface and the nucleus for fusion with the cognate organelles of the mating partner; and (4) alterations in cell polarity and morphology that both dictate and reflect the localization of the mating partner (Sprague and Thorner, 1992).

To study whether the mutant haploid cells of either mating type undergo mitotic arrest in the G_1 phase upon exposure to the opposite mating factor, I again used the halo assay. The response of *MAT*a cells of the 15 mutants to α-factor was first analyzed. *MAT*a wild-type strains with the same genetic background were used as the positive control and *MAT*a cells carrying *ste11* or *ste50* mutations were used as negative controls. Different concentrations of α-factor were pipetted onto Whatman filter discs placed on lawns of the mutant tester cells. After the plates had been incubated at 30°C for 48 h, halos were formed. The results are shown in Fig 3.4. The halo size formed on lawns of mutants 2, 380 and 505 was larger than that seen with the wild-type strain. This suggests that these three mutants are supersensitive to α-factor as compared with the wild-type strain.
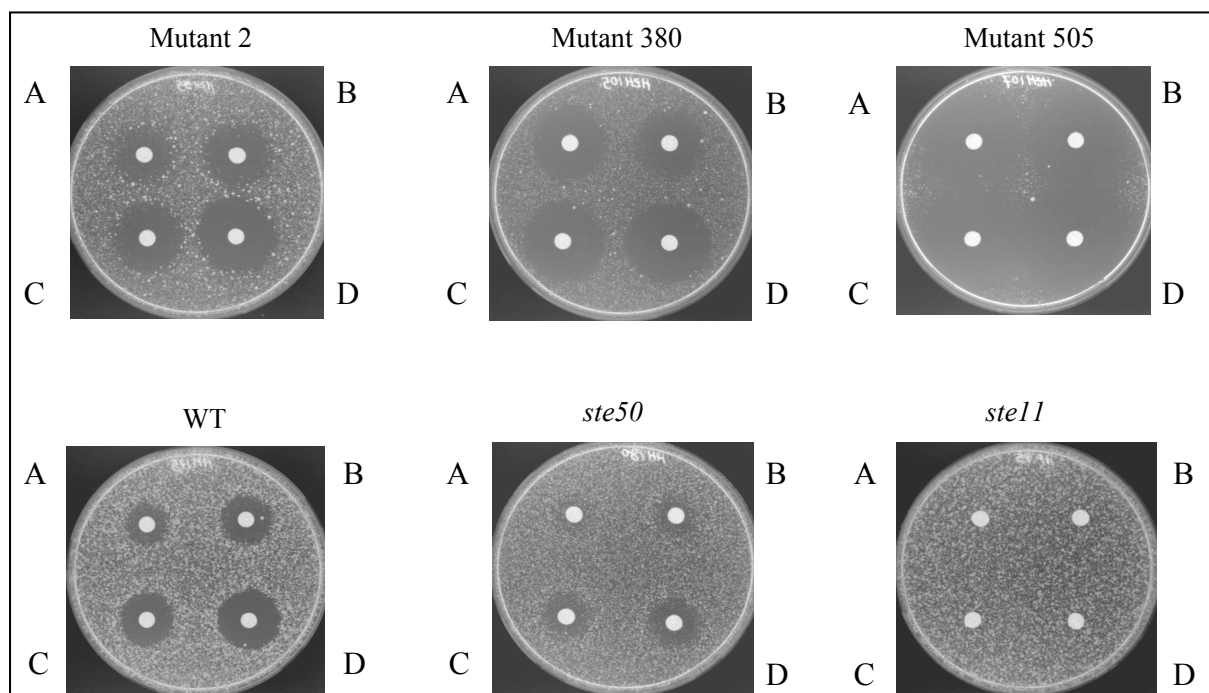
Fig 3.4. Pheromone response assay (halo assay). Cultures of wild-type and mutant strains were grown to log-phase and then approximately 10^5 cells of each strain were mixed with melted 0.6% top agar. Whatman filter discs soaked with different concentration of α-factor were placed on the top agar. The concentration of α-factor were as follows: A, 0.5 μg; B, 1 μg; C, 2 μg; D, 5 μg. The plates were incubated at 30°C for 48 h and photographed. In this test, wild-type strain was used as positive control, *ste11* and *ste50* were used as negative controls. The halo sizes of mutants were compared with the controls.

3.2 Characterization of the mating-defective mutants with respect to morphogenesis, cell fusion and nuclear fusion

In contrast to our knowledge of the components of the mating pheromone signal transduction pathway and their interactions, relatively few proteins are known to be specifically involved in the various downstream events in the mating process (Sprague and Thorner, 1992; Erdman *et al.*, 1998). For example, it is likely that some mating-specific components that link general polarity proteins to specified sites of cell growth during mating remain undescribed. Some of these components would be expected to help direct the growth and form of the mating projection (shmoo). Understanding the downstream events in the mating process, including polarized morphogenesis, cell fusion, and nuclear fusion, is therefore of general importance for the elucidation of the whole process.

3.2.1 Analysis of mutants for the ability to activate the pheromone response pathway

The mating pheromone response pathway is initated by the activation of a receptor-coupled signal transduction cascade. The **a**- and α-factor pheromones are bound by the *STE2* and *STE3* gene products, respectively, which are seven-transmembrane-segment (TMS) receptors and are coupled to a heterorimeric G protein complex. Transduction of the signal by the MAPK cascade leads to activation of the transcription factor Ste12, which, in turn, promotes the transcription of a set of genes (e.g. *FUS1*, *AGA1*) involved in mating-specific functions. These functions include cell cycle arrest in G_1, polarized morphogenesis (shmoo formation), cell agglutination, cell fusion, nuclear fusion, and adaptation to the pheromone signal (Sprague and Thorner, 1992).

3.2.1.1 Activation of the reporter gene *FUS1::lacZ*

A standard test for the induction of mating-specific functions involves measurement of the level of induction of *FUS1*, a gene that is highly induced in the presence of pheromone (Trueheart and Fink, 1987). By using a Fus1-β-galactosidase fusion protein, which is under the control of the *FUS1* promoter and is encoded by *FUS1-lacZ*, as a reporter, the level of *FUS1* expression induced by the exposure of the 15 mutants and the wild-type cells to α-pheromone can be determined by measuring the β-galactosidase activity.

3.2.1.1.1 The X-gal overlay assay

In the semi-quantitative X-gal overlay assay the pheromone sensitivity of each of the 15 mutants harbouring the *FUS1-lacZ* reporter gene (pSB234) was tested. A *ste11* mutant and a *ste50* mutant were used as negative controls, and the wild-type strain was used as the positive control. The plates were incubated at 30°C and photographed after 1 h, 12 h, 24 h and 48 h (Fig 3.5).
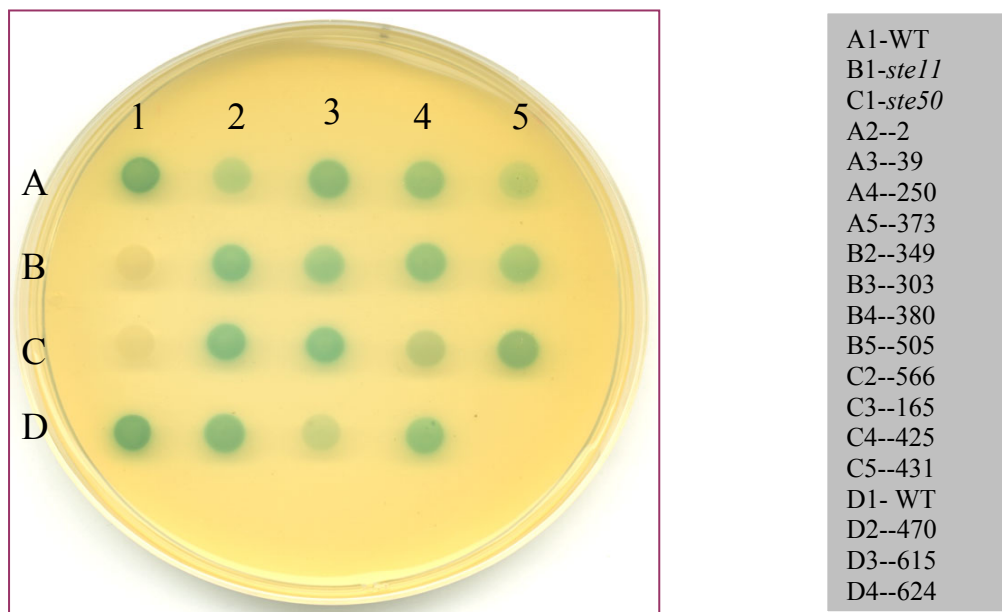
Fig 3.5 X-gal overlay assay as described under methods (2.3.9). Cultures of log-phase yeast strains which harbour pSB234 plasmid were induced with 5 µM α-factor and harvested. Approximately the same amount of cells (1×10^6) of each strain were dropped on the SD plate. 10 ml of 10 mg/ml melted agarose was mixed with 10 mg X-gal/ml DMF and two other ingredients (sodium phosphate buffer and SDS) and the mixture was put on the top of an SD plate. The plate was incubated at 30°C and photographed every 12 h. In this assay a wild-type strain was used as the positive control, whereas *ste11* and *ste50* mutants were used as negative controls. The above photo was taken after incubation at 30°C for 12 h.

It is clear that after 1 h of incubation the wild-type strain and many mutants have already developed a blue colour, whereas the s*te11* and s*te50* mutants remain white. After 12 h incubation the blue colour of the wild-type strain has become much stronger, and the negative controls are still white (see Fig 3.5). Four mutants show a signal intensity that is intermediate between the wild-type strain and the negative controls. These findings suggested that these four mutants (2, 373, 425, 615) have a reduced ability to induce *FUS1-lacZ* expression in response to α-factor. The four mutants were therefore further tested using a quantitative reporter gene assay.

3.2.1.1.2   β-Galactosidase activity

The four mutants (2, 373, 425, 615) which showed reduced *FUS1-lacZ* expression in the X-gal overlay assay were re-examined for β-galactosidase activity using a quantitative enzyme assay. The wild-type strain was used as a positive control, and the s*te11* and s*te50* mutants were used as the negative controls. The four mutants showed significantly reduced β-galactosidase activities as compared with the wild-type strain, but exhibited slightly higher β-galactosidase acitivities than those of the s*te11* and s*te50* (Fig 3.6).
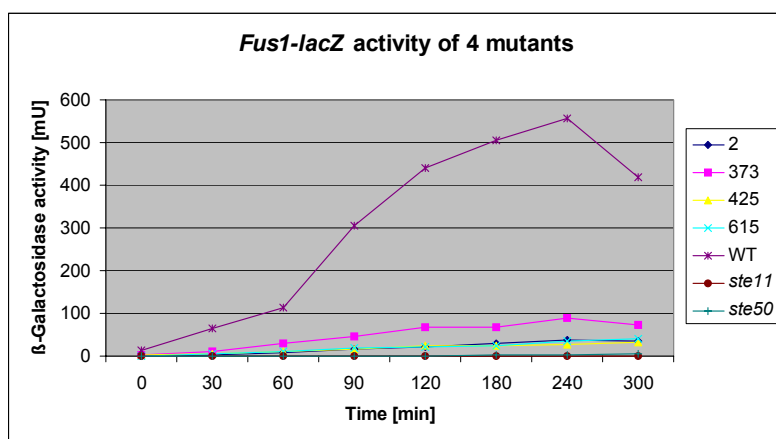
Fig 3.6 Time course of *FUS1-lacZ* induction (β-galactosidase activity) of 4 mutants. Cultures were grown to log-phase and treated with 5 µM α-factor for the induction of *FUS1-lacZ*. Samples were harvested at the indicated times for the measurement of β-galactosidase activity as described in Methods. The cell morphology was also monitored under the microscope.

The wild-type strain showed a maximum of 560 mU of β-galactosidase activity after induction with 5 µM α-factor for 240 min, and none of the wild-type cells had budded after incubation for 90 min in the presence of 5 µM α-factor. In contrast, the s*te11* mutant showed only 0.12 mU of β-galactosidase activity after incubation with 5 µM α-factor for 300 min, and almost 30% of the cells had budded after 90 min of incubation. The s*te50* mutant showed 4.9 mU of β-galactosidase activity after incubation with 5 µM α-factor for 300 min, and again almost 30% of these cells had formed buds after a 90-min incubation.

Table 3.3. The level of unbudded cells after 90 min treatment with α-factor

Strain	Unbudded cells (%)
Wild-type	100
Mutant 2	95.7
Mutant 373	98.6
Mutant 425	96.6
Mutant 615	98.7
Ste11	70.1
Ste50	70.5

The four mutants all expressed less than 100 mU of galactosidase activity (range ~30-to ~90), and over 90% of the cells remained unbudded after 90 min treatment with α-factor (Table 3.3). These results demonstrate that the four mutants (2, 373, 425 and 615) show a markedly reduced capacity to

induce the *FUS1-lacZ* reporter, and a slight reduction in the ability to arrest the cell cycle upon exposure to α-factor (Table 3.3).

3.2.1.2 Shmoo index

Determination of the shmoo index is used to evaluate the rate of polarized morphogenesis in the mating pheromone response pathway. In this test *MAT***a** cells of the 15 mutants were grown to log phase and then treated with 5 µM α-factor for 90 min. Samples were harvested and at least 200 cells were counted in every sample. The shmoo index of each of the 15 mutants is shown in Fig 3.7. One mutant (373) showed a higher percentage of shmoo formation than the wild-type strain, while three other mutants (349, 566, 624) exhibited a much lower level of shmoo formation than the wild-type strain.
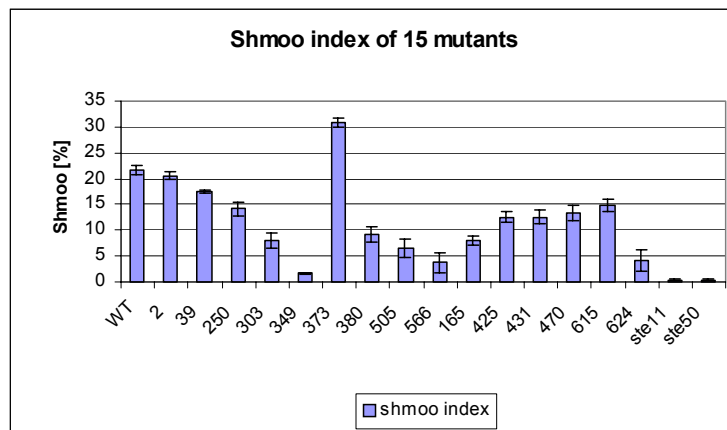

Fig 3.7. Shmoo index of 15 mutants. Cultures of wild-type and mutant strains were grown to log-phase and treated with 5 µM α-factor (final concentration). Samples were taken after 90 min incubation and the number of shmoos were counted in at least 300 cells per samples. Wild-type strain was used as the positive control and *ste11* and *ste50* were used as negative controls. Values represent the average of three independent experiments.

3.2.1.3   The kinetics of zygote formation

The kinetics of zygote formation was measured in an effort to detect possible defects in this process (Fig 3.8). Cultures of both mating types (*MAT*a and *MAT*α) of each of the 15 mutants were grown to log phase, and equal numbers of cells of both mating types ($3x10^6$ cells) were mixed. The cell pellets were then transferred onto a NC filter placed on a YPD plate. The plates were incubated at 30°C for varying lengths of time (1 h, 2 h, 3 h, 4 h, and 5 h). Samples were harvested after the indicated times and photographed under the microscope. The wild-type strain formed zygotes within 1 h and the zygote frequency had reached its maximum after 2 h of incubation. In four of the mutants (380, 425, 431 and 624) zygote formation reached its maximum after 3 h of incubation (Fig 3.8 A). In four other

4 cases (165, 250, 349, 615) zygote formation attained a maximum only after 4 h incubation (Fig 3.8B). Three mutants (2, 39, 373) continued to form zygotes for 5 h (Fig 3.8C), and four mutants (303, 470, 505, 566) showed almost no zygote formation (Fig 3.8D). These results suggest that most of the mating-defective mutants show a delay in zygote formation, but four of them exhibit a complete block in this process.
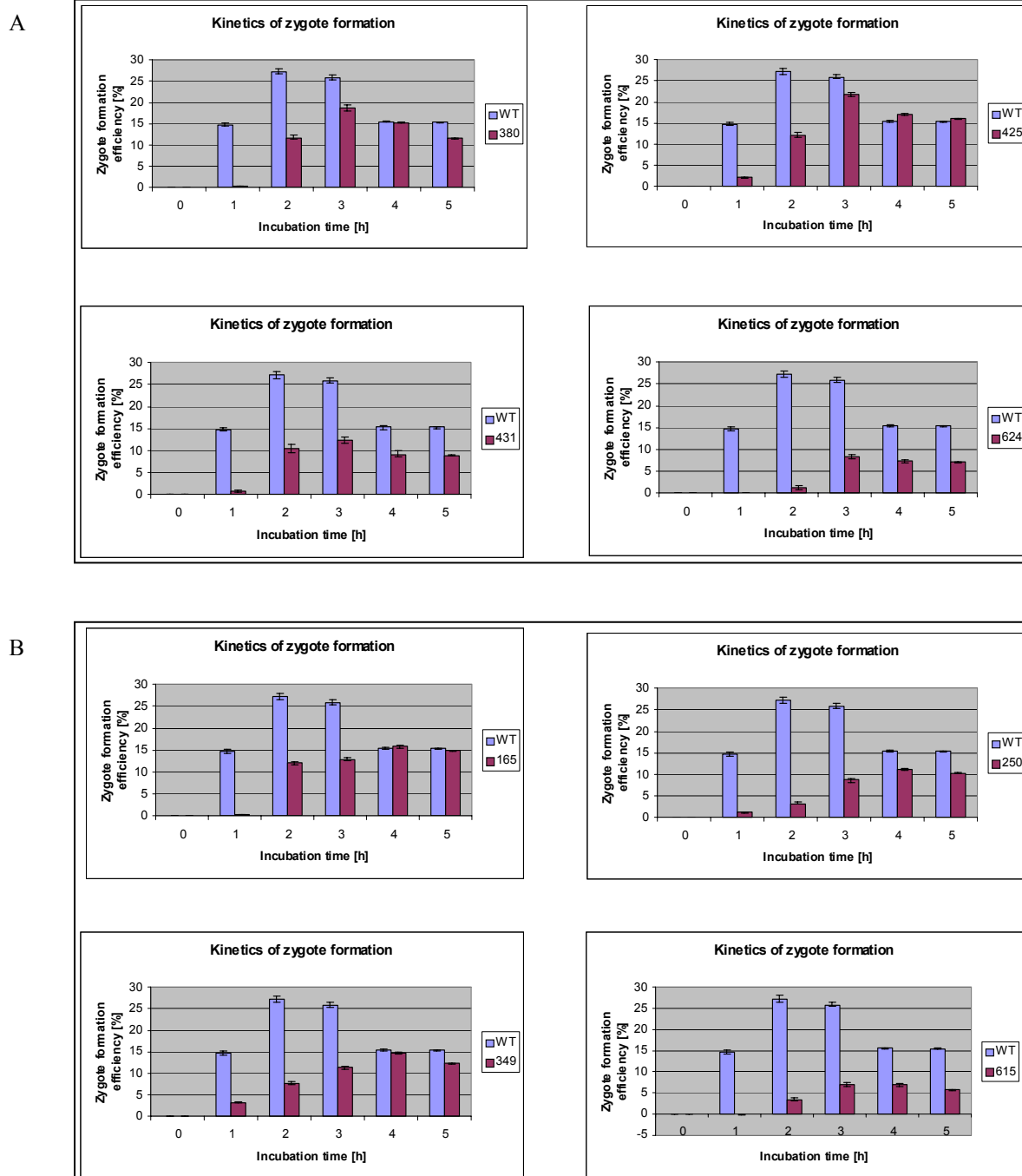
Fig 3.8 Kinetics of zygote formation. Cultures of wild-type strain and mutants were grown to log phase and the same numbers of opposite mating type cells were mixed and incubated on the NC-filter on the YPD plate. Samples were harvested after different hours of incubation. The cell morphology was investigated in the light microscope and the number of zygotes and whole cells were counted. Values represent the average of three independent experiments. (A) 4 mutants with reduced rate of zygote formation exhibited maximum rate of zygote formation after 3 h incubation. (B) 4 mutants with reduced rate of zygote formation exhibited maximum rate of zygote formation after 4 h incubation. (C) 3 mutants with reduced rate of zygote formation exhibited maximum rate of zygote formation after 5 h incubation. (D) 4 mutants showed very low percentage of zygote formation.

C
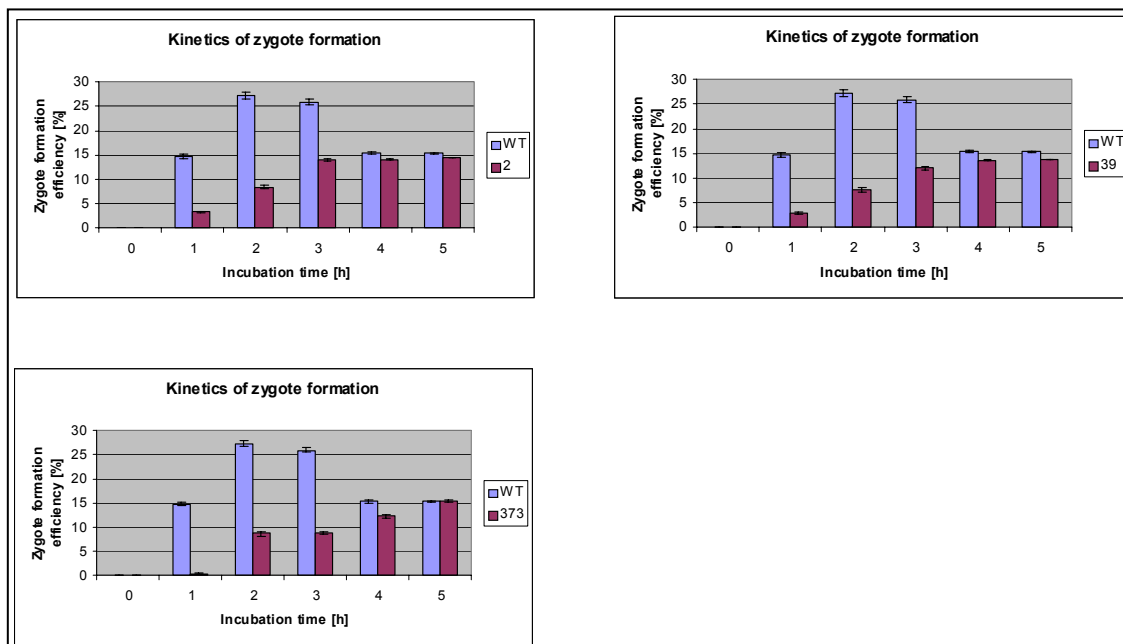
D
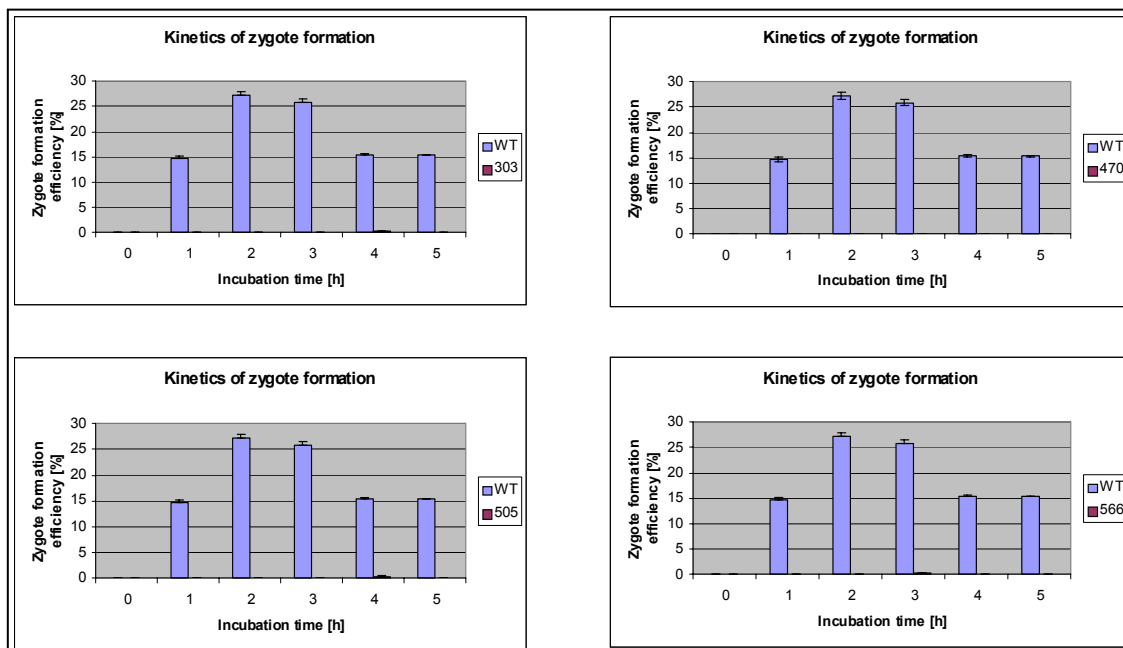
3.2.2 Analysis of the 15 mutants by fluorescence microscopy for defects in cell fusion and nuclear fusion

To allow detailed microscopic observation for possible defects in cell fusion and nuclear fusion, mutant *MAT***a** or *MAT*α cells were transformed with a GFP-encoding plasmid (green fluorescent protein) which expresses a form of GFP that is distributed throughout the whole cell. This allowed us to readily distinguish fused zygotes from unfused mating pairs by scoring whether GFP had spread to both cells (indicating successful cell fusion) or remained restricted to one mating partner (indicating a

defect in fusion). Using this assay, we observed unambiguously that mating between partners produced a mixture of fused zygotes and unfused mating pairs. In this assay the wild-type strain was used as the positive control, and zygote formation by each of the 15 mutants was tested in the bilateral mating cross between the haploid deletants. Among the 15 mutants no obvious defects in cell fusion were observed. Simultaneous detection of GFP and nuclei staining with DAPI revealed that only one mutant (the *ssh1* deletion mutant 380) exhibited an obvious defect in nuclear fusion (Fig 3.9). It cannot be excluded that some mutants that were defective in nuclear membrane fusion were overlooked, since cells that have completed nuclear membrane fusion cannot always be clearly distinguished from those that merely display nuclear membrane contact without successful fusion by this method.

Wild-type strain   ***ssh1* deletion mutant 380**
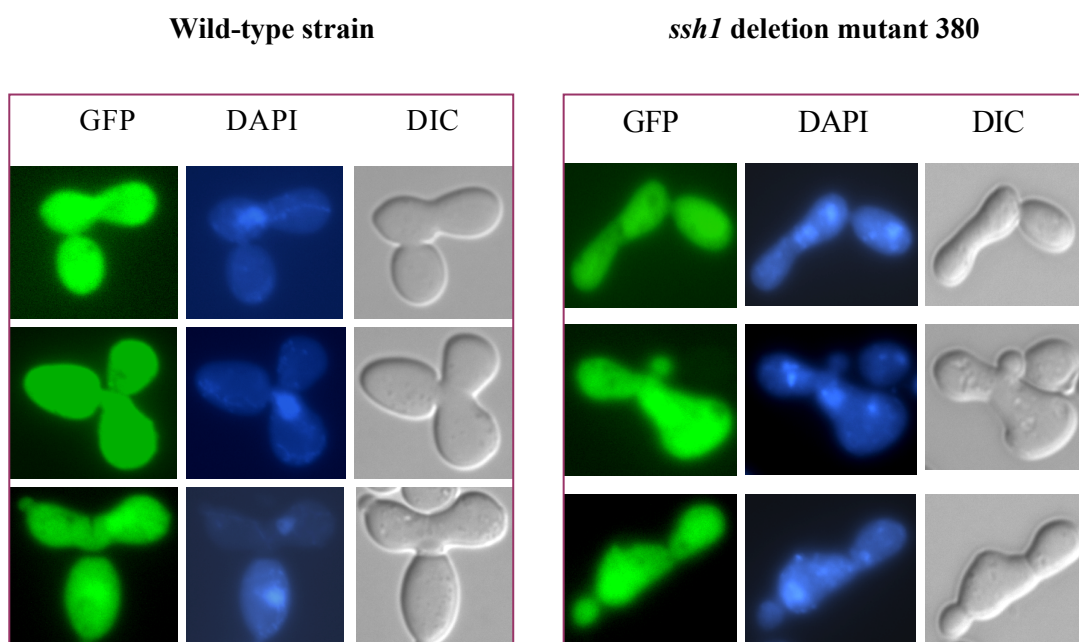
Fig 3.9. Simultaneous detection of GFP and nuclei staining with DAPI during zygote formation. Left: zygote formation of wild-type strain; right: zygote formation of *ssh1* deletion mutant 380. The wild-type and mutant 380 strains were transformed with plasmid pRS424METGFP or pUG36METGFP and grown to log-phase. The same number of *MAT*a and *MAT*α cells were mixed and incubated on the NC-filter on the YPD plate. Samples were taken after different incubation times. The localization of GFP and nuclei staining with DAPI in zygotes was investigated by immunofluorescence microscopy.

3.3 Functional analysis of the role of *MDY2* in mating of *S. cerevisiae*

In the second part of this work, I focus on one of the 15 genes discussed in the preceding sections, *YOL111c*. This gene, which is located on chromosome XV, will be referred to as *MDY2* in the following. *MDY2* is required for the mating of *S. cerevisiae*. The *MDY2* ORF encodes a 212-residue protein, which contains an ubiquitin-like domain (the *UBL* domain). The closest homologue of *MDY2* is the 157-amino acid human protein GdX. Residues 74-208 of *MDY2* share 34% identity with the N-terminal 123 residues of GdX. *GdX* is a single-copy gene, spans about 3.5 kb of genomic DNA and is located 40 kb downstream from the *G6PD* gene at *Xq28*. *GdX* is conserved in evolution and is a "housekeeping" gene that encodes a protein similar to ubiquitin (Toniolo *et al*., 1988). In order to analyse the function of *MDY2* in the mating of haploid *S. cerevisiae* cells, I investigated the phenotypes of the *mdy2* deletion mutant and an *MDY2*-overexpressing strain, the subcellular localization of Mdy2, its interaction partners of Mdy2 and its possible role in modification of other proteins involved in the mating process.

3.3.1 Disruption of *MDY2* and phenotypic analysis of the *mdy2* deletant

The first step in the functional analysis of *MDY2* was the complete deletion of the gene using an efficient gene disruption cassette which was developed by Guldener *et al.* (1996). The phenotypic analysis of the *mdy2* deletion mutant included the use of the quantitative mating assay, determination of the shmoo and budding indexes, and measurements of pheromone production, pheromone response, and pheromone-induced *FUS1-lacZ* expression.

3.3.1.1 Disruption of *MDY2* in *S. cerevisiae* strain W303

A schematic representation of the disruption of *MDY2* in *S. cerevisiae* W303 by the *LoxP-KanMX-LoxP* cassette through homologous recombination is shown in Fig 3.10. *MDY2* was disrupted in both *MAT***a** and *MAT*α cells. G418-resistant transformants of haploid cells were checked for disruption of the gene by PCR. The PCRs were done using combinations of primers complementary to sequences within the cassette (3 *KAN* and 5 *KAN*) and to sequences flanking the target sequence (A96-*MDY2* and A98-*MDY2*). The expected size of the 5'-terminal PCR product obtained from the correct deletant is 1080 bp and the 3'-terminal PCR product is 733 bp. The expected size of the entire PCR product obtained from the correct deletant is 2172 bp.

The PCR products obtained from the transformants were subjected to agarose gel electrophoresis. The results (Fig 3.11) showed that the PCR products obtained from the putatively deleted transformants exhibited the cassette-specific sizes predicted for correct integration. The PCR analysis therefore

suggests that the gene disruption cassette has been correctly integrated at the *MDY2* locus in the haploid cells of both mating types (*MAT***a** and *MAT*α) in *S. cerevisiae* W303 (Fig 3.11).
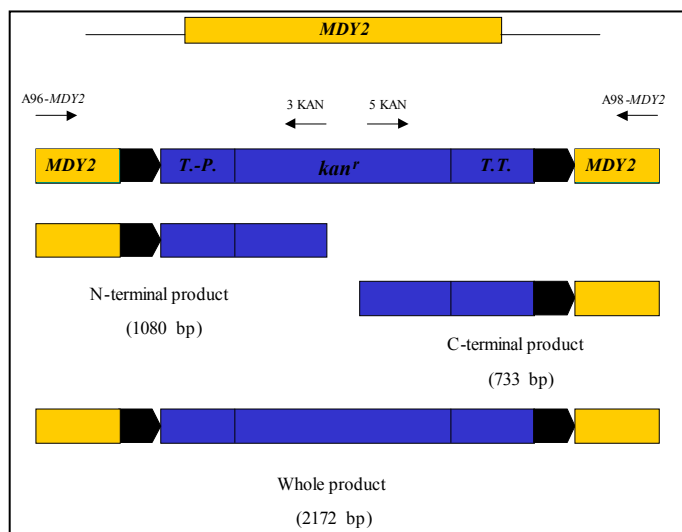

Fig 3.10. Diagram of the disruption of *MDY2* in *S. cerevisiae* W303. Plasmid pUG6 was used as PCR template to generate the disruption cassette (*LoxP-KanMX-LoxP* cassette). The verification PCRs were done using combinations of primers complementary to sequences within the cassette (3 *KAN* and 5 *KAN*) and to sequences flanking the target sequence (A96-*MDY2* and A98-*MDY2*).
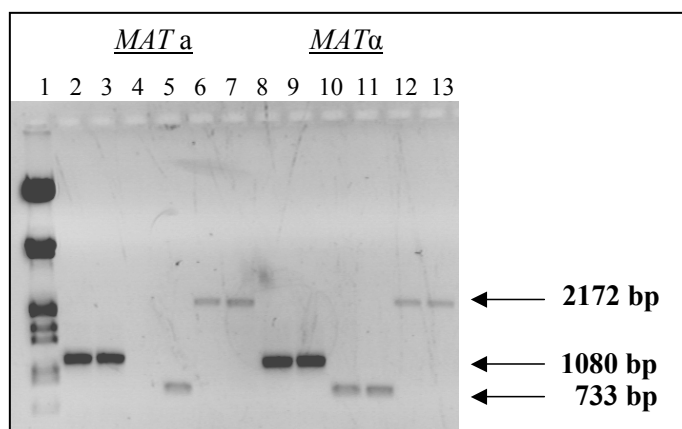
Fig 3.11. Disruption of *MDY2* in *S. cerevisiae* W303. PCR analysis of G418 resistant transformants. The PCR fragments are indicated with arrows. In this experiment *MAT***a** and *MAT*α haploid cells were disrupted respectively. Slots 1: λ-DNA digested with *Eco*RI and *Hind*III. Slots 2-3: N-terminal PCR product of *MAT*a transformants (HZH686); Slots 5: C-terminal PCR product of *MAT*a transformants; Slots 6-7: The whole PCR product of *MAT*a transformants. Slots 8-9: N-terminal PCR product of *MAT*α transformants (HZH683); Slots 10-11: C-terminal PCR product of *MAT*α transformants; Slots 12-13: The whole PCR product of *MAT*α transformants.

3.3.1.2   Deletion of *MDY2* results in reduced mating efficiency

The *mdy2* deletion mutant constructed using the *LoxP-KanMX-LoxP* cassette was analyzed for mating efficiency using the quantitative mating assay (see Methods). The results are shown in Fig 3.12. The efficiency of diploid formation in the *MAT***a** *mdy2* × *MAT*α *MDY2* cross was 4.10 (±0.4)%. The value

for the reciprocal cross (*MAT*α *mdy2* × *MAT*a *MDY2*) was 6.10 (±1.3)%; and the corresponding value for the bilateral mutant cross was 2.89 (±0.93)%. Compared to the wild-type strain (mating efficiency 18.9% ± 2.9), the *mdy2* deletion mutant thus exhibits a significant reduction in mating efficiency. The effect of the *mdy2* deletion on the mating efficiency of *MAT*a cells is slightly greater than that on the mating ability of *MAT*α cells.
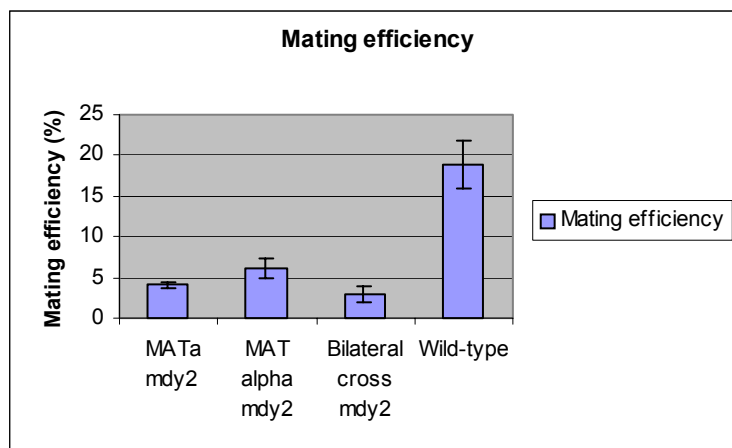
Fig. 3.12. Quantitative mating assay of different *mdy2* deletants. Bars represent the average deviation of the percentage of diploid formation in two independent experiments. Values are an average of two independent experiments.

3.3.1.3. Analysis of the shmoo and budding indexes of *mdy2* deletion mutants

Mating pheromones block the *S. cerevisiae* cell cycle in G_1 at START, and thus allow the cells to enter the mating pathway. G_1-arrested cells become large and pear-shaped (forming shmoos) and are able to aggregate, fuse and undergo karyogamy (Cross *et al.*, 1988; Andrews and Herskowitz, 1990). The proportion of unbudded cells reflects the extent of G_1 arrest induced by pheromone treatment. Wild-type strains showed no budded cells after 2 h of pheromone treatment and these cells had adapted to pheromone after 4 h of incubation. In contrast, the *mdy2* mutant exhibited a low percentage (5%) of unbudded cells after α-factor treatment. Hence, induction of G_1 arrest is slightly delayed in the *mdy2* mutant (Fig 3.13).
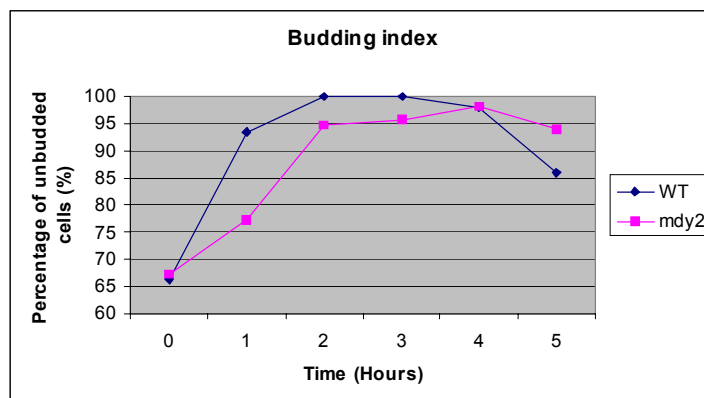
Fig. 3.13. Budding index. Cultures of *mdy2* mutant (HZH686) and wild-type strains (W303-1A) were grown to log phase and treated with 5 μM α-factor (final concentration). Samples were taken after different incubation time and the number of unbudded cells was counted in samples of at least

The rate of shmoo formation in *MAT***a** *mdy2* cells is different from that in wild-type cells (Fig 3.14). Wild-type strains showed a maximum of 80% shmoos after 2 h of exposure to α-factor, whereas only about 40% of *mdy2* mutant cells were converted into shmoos after 2 h of treatment with α-factor. The mutant thus shows an approximately 50% reduction in the efficiency of shmoo formation in comparison to a wild-type strain.
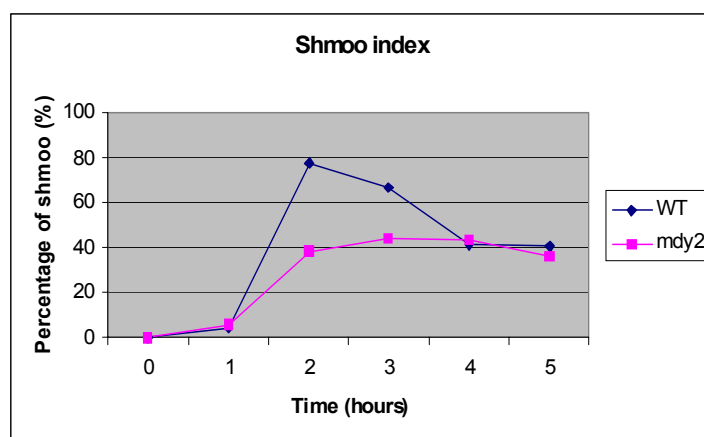
Fig. 3.14. Shmoo index. Cultures of *mdy2* mutant (HZH686) and wild-type strains (W303-1A) were grown to log phase and treated with 5 μM α-factor (final concentration). Samples were taken after different incubation time and the number of shmoos were counted in samples of at least 300 cells .

3.3.1.4 α-Pheromone production is reduced in *MAT*α *mdy2* deletion strains

*MAT*α cells of the *mdy2* mutant were also tested for the ability to produce and secrete α-factor in a plate halo assay by spotting the cells on top agar overlain on a *MAT***a** lawn. The level of α-factor was

evaluated by measuring the size of the halo (Fig 3.15). We observed that the halo formed by the *mdy2* mutant was smaller than that induced by wild-type strain after 48 h of incubation at 30°C. This observation is consistent with the results obtained with a *mdy2* deletion in the S288C background (see section 3.1.2.3). These results thus suggest that the *MAT*α *mdy2* mutant is partially defective in the production or secretion of α-factor.

WT
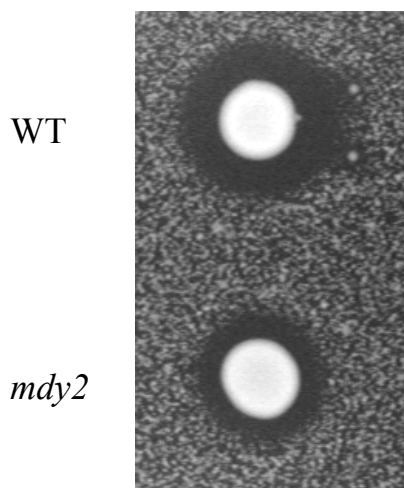
mdy2

Fig 3.15. Halo asssay of α-factor production. 0.6% top agar was mixed with 10^5 lawn cells (*MAT*a *sst1* mutant). Approximately 4×10^6 wild-type cells (W303-1B) or *mdy2* mutant cells (HZH683) were dropped directly on the top agar. The plate was incubated at 30°C for 2 days and photographed. Two independent experiments were carried out in this assay.

3.3.1.5 Impaired growth arrest upon exposure of *mdy2* mutant cells to α-factor

In this assay *MAT*a *mdy2* cells were tested and *MAT*a *MDY2* cells were used as the positive control. α-Factor was added to NC filter discs placed on top of a lawn of the *MAT*a tester cells, and the plates were incubated at 30°C for 72 h. At the end of this period, the plates were examined. The response of the *mdy2* mutant to α-factor differed little, if at all, from that of the wild-type cells (Fig 3.16).

WT   *mdy2*
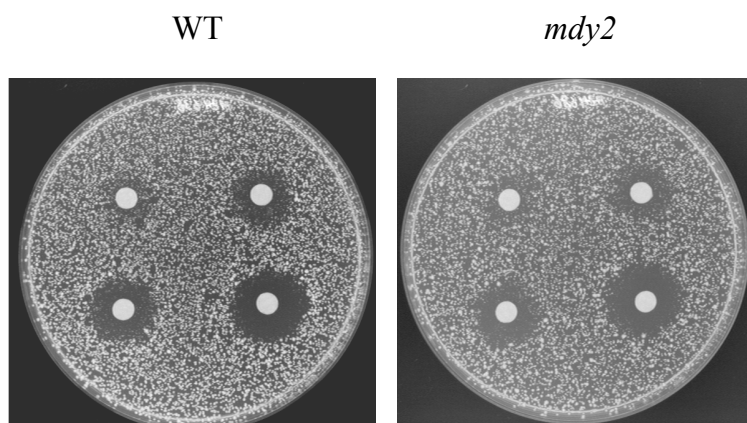
Fig 3.16. Growth arrest upon exposure to α-factor (halo assay). Wild-type strain (W303-1A) and *mdy2* mutant cells (HZH686) were mixed with 0.6% top agar and spread on the plates, and filter discs with 0.5 μg, 1.0 μg, 2.0 μg and 5.0 μg α-factor were placed on each plate (clockwise from upper left). Pictures were taken after 72 h incubation at 30°C. The formation of a halo around the disc indicates growth arrest.

3.3.1.6 Analysis of pheromone induced *Fus1-lacZ* reporter activity in *mdy2* cells

The *mdy2* mutant and wild-type strains which had been transformed with a reporter *FUS1-lacZ* plasmid (pSB234) were tested for α-factor induced *FUS1-lacZ* expression. Cultures were grown to log-phase and α-factor was added to a final concentration of 5 μM. Samples were taken at different times and β-galactosidase activity was measured (Fig 3.17). The activity maxima observed in the two strains were the same, and the kinetics of induction differed only slightly between the wild-type strain and the *mdy2* mutant.
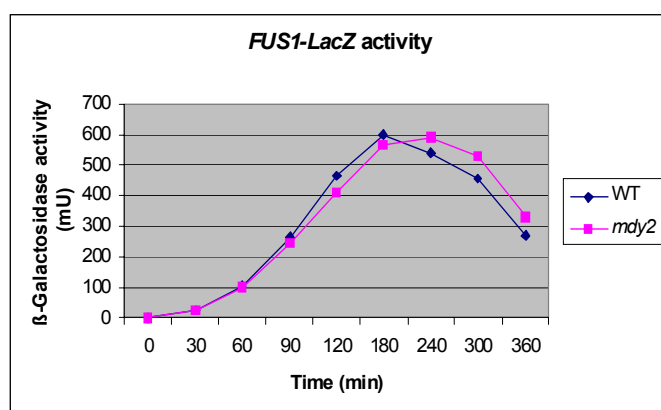

Fig 3.17. Time course of *FUS1-lacZ* induction after addition of α-factor to haploid strains. Cultures of log-phase of wild-type strain (W303-1A) and *mdy2* mutant (HZH686) harbouring plasmid pSB234 were shifted to a fresh medium and treated with 5 μM α-factor for induction of *FUS1-lacZ.* Samples were harvested at indicated times for the measurement of β-galactosidase activity.

3.3.2   Analysis of the effects of *MDY2* overexpression

3.3.2.1   Overexpression of *MDY2* increases mating efficiency

In this test, *mdy2* mutants of both mating types were transformed with 2μ *MDY2* plasmids. Wild-type cells, transformed with the 2μ vector, were used as control. The *MAT*a *mdy2* mutant bearing 2μ *MDY2* plasmids was crossed to the *MAT*α *mdy2* mutant bearing 2μ *MDY2* plasmids; this cross resulted in a diploid formation efficiency of 23 (±0.7)%. The *MAT*a *MDY2* × *MAT*α *MDY2* cross gave a value of 15.6 (±2.7%). Thus the overexpression of *MDY2* in the *mdy2* deletant causes a slight increase in mating efficiency as compared with the wild-type strain (Fig 3.18).
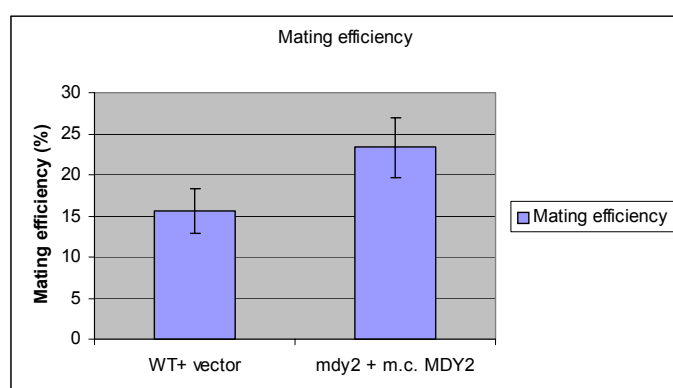
Fig 3.18.   Mating efficiency of overexpression of *MDY2*. Wild-type strains (W303-1A) were transformed with 2μ vector (pRS426), *mdy2* mutant (HZH686) were transformed with 2μ *MDY2* plasmids (pRS426-*MDY2*). Quantitative mating assay was conducted as described in Materials and Methods. An average of two independent assays is shown as the percentage of diploid cells divided by the total number of cells. Bars represent the average deviation of the percentage of diploid formation in two independent experiments.

3.3.2.2 Increased dosage of *MDY2* in the *mdy2* mutant restores the wild-type rate of shmoo formation

In order to investigate if overexpression of *MDY2* affects the shmoo index and the budding index, *MAT***a** *mdy2* cells were transformed with 2μ *MDY2* plasmids and wild-type strains were transformed with the empty 2μ vector as control. The cells were stimulated with 5 μM α-factor. Samples were taken at different times, and the numbers of shmoos and unbudded cells were counted. The results showed that overexpression of *MDY2* leads to a slight increase in the formation of shmoos as compared with wild-type strains (Fig 3.19).
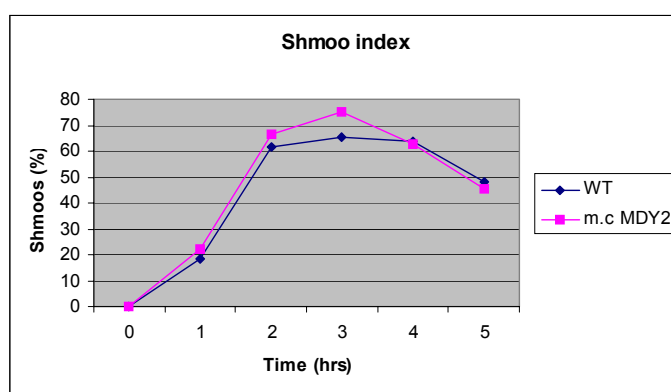
Fig 3.19   Shmoo index. Wild-type strain W303-1A was transformed with a 2μ vector (pRS426) and *mdy2* mutant (HZH686) was transformed with the 2μ *MDY2* plasmids (pRS426-*MDY2*). The cultures were grown in SD medium to log phase and treated with 5 μM α-factor. The samples were taken after different incubation times and the number of shmoos was counted from at least 300 cells per sample.

The budding indexes for these two strains are shown in Fig 3.20.   The results suggest that overexpression of *MDY2* promotes G_1 arrest upon exposure to α-factor.
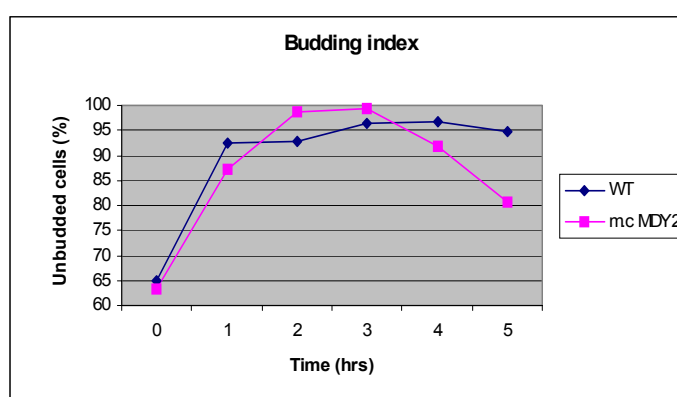
Fig 3.20. Budding index. Wild-type strain W303-1A was transformed with the 2μ vector pRS426 and *mdy2* (HZH686) was transformed with the 2μ *MDY2* plasmids (pRS426-*MDY2*). The cultures were grown in SD medium to log-phase and treated with 5 μM α-factor. The samples were taken after different incubation times and the number of budded and unbudded cells was counted from at least 300 cells per sample. The percentage of the unbudded cells is shown.

3.3.2.3 Overexpression of *MDY2* corrects the defect in α-pheromone production observed in the *mdy2* mutant

*MAT*α *mdy2* cells harbouring 2μ *MDY2* plasmids were tested in this assay for complementation of the defect in α-factor production observed in *mdy2* deletants. A wild-type strain was transformed with the 2μ vector as a control. The production of α-factor was determined by measuring halo sizes. *mdy2* mutants harbouring 2μ *MDY2* plasmids formed nearly the same size of halo as the wild-type strain after 48 h of incubation at 30°C (Fig 3.21).
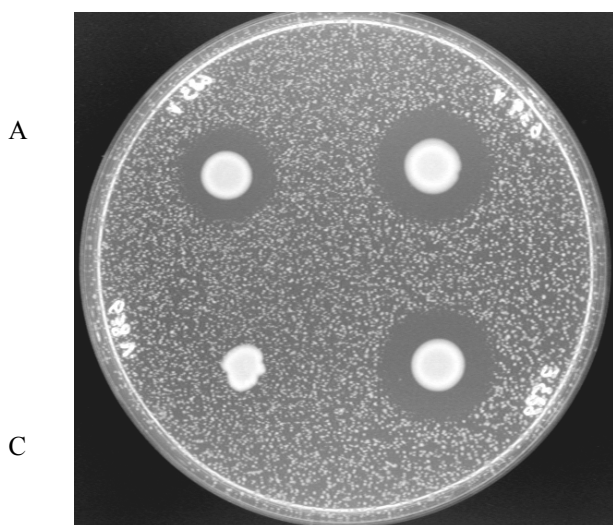
Fig 3.21.   α-factor production. (A) *mdy2* (HZH683) transformed with the 2μ vector pRS426.   (B) Wild-type W303-1B transformed with 2μ vector pRS426.   (C) Wild-type W303-1A transformed with 2μ vector pRS426. (D) *mdy2* (HZH683) transformed with 2μ *MDY2* plasmids (pRS426-*MDY2*). Lawn cells were *MAT*a *sst1* mutants. Approximately 4x10^6 cells of each strain were dropped on the top agar. The plate was incubated at 30°C for 2 days and then photographed.

3.3.2.4 *MDY2* in high copy enhances pheromone induced G$_1$ arrest of the *mdy2* mutant

In this assay *MAT*a *mdy2* cells bearing 2μ plasmids were tested for pheromone induced G$_1$ arrest. *MAT*a WT cells which had been transformed with the empty vector were used as controls. α-Factor was added to NC filter discs placed on lawns of the tester cells.

WT + vector   *mdy2* + vector   *mdy2* + m.c. *MDY2*
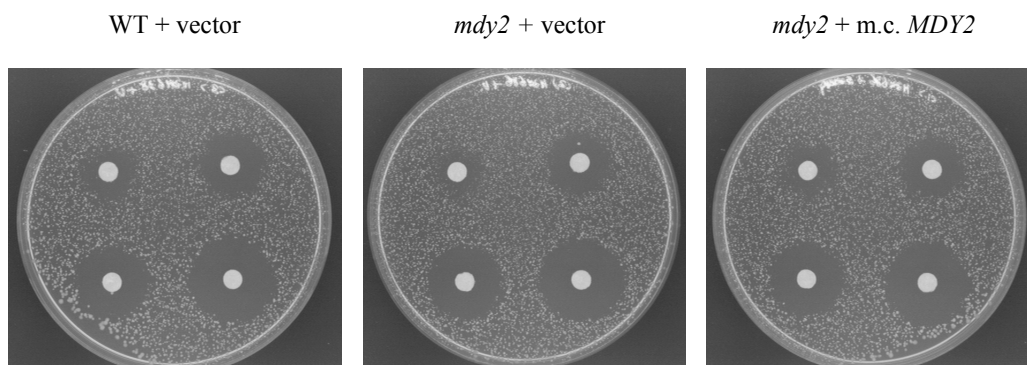
Fig 3.22.   α-pheromone induced growth arrest in plate halo assay. Approximately 10^5 *MAT*a cells of each of the following strains: wild-type strain W303-1A and *mdy2* mutant (HZH686) bearing control vector pRS426 and *mdy2* mutant harbouring 2μ *MDY2* respectively, were mixed with melted soft top agar respectively and plated on the YPD agar plates. 0.5 μg, 1.0 μg, 2.0 μg and 5.0 μg α-factor was spotted on the Whatman filter discs (clockwise from upper left). Photos were taken after 2 days incubation at 30°C.

After 48 h of incubation halos had formed. The results shown in Fig 3.22 depict the effect of α-factor on different strains. The *mdy2* mutant harbouring the high-copy-number *MDY2* plasmid showed a similar halo size to the wild-type strain, whereas the *mdy2* mutant bearing the empty vector showed a slight reduction in the ability to induce G_1 arrest.

3.3.2.5 Overexpression of *MDY2* leads to an increase in pheromone-induced *Fus1-lacZ* expression

In this assay, *mdy2* mutants which had been transformed with the reporter *FUS1-lacZ* and a plasmid bearing *MDY2* under the control of the *GAL1* promoter were tested for pheromone induced *FUS1-lacZ* expression. Wild-type and *mdy2* mutant strains harbouring the vector were used as controls. The cultures were grown to log-phase and the cells were treated with different concentrations of *α*-factor. After 90 min of incubation, samples were taken and the β-galactosidase acitivity was measured. The results are shown in Fig 3.23.
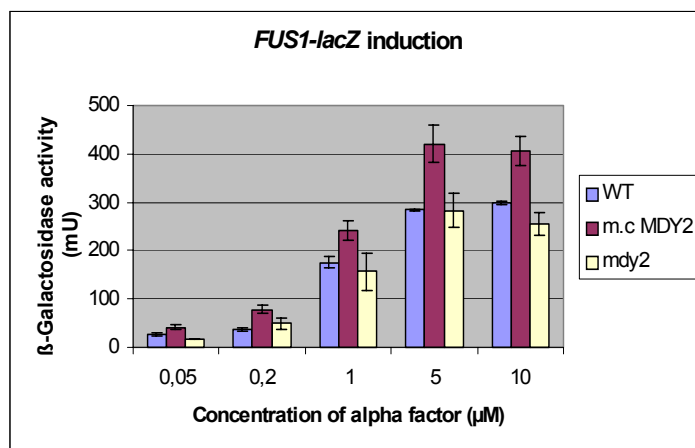
Fig 3.23. Pheromone induced *FUS1-lacZ* expression. Wild-type W303-1A and *mdy2* (HZH686) carrying empty vector pRS416 and *mdy2* mutant harbouring pRS416-GAL-*MDY2* were grown to log phase in SRG medium and then induced with different concentration of *α*-factor (0.05, 0.2, 1, 5 and 10 μM) for 90 min respectively. The β-galactosidase activity was measured. The data represents average of three independent assays.

The *mdy2* mutant harbouring pRS416-*GAL1-MDY2* showed a 1.5-fold increase in β-galactosidase activity relative to that of the wild-type strain or the *mdy2* mutant. The *mdy2* mutant and the wild-type strain showed nearly the same β-galactosidase activity (see also 3.3.1.6).

3.3.3 Identification of Mdy2 interaction partners

3.3.3.1 Two-hybrid analysis

To further explore the function of *MDY2*, possible protein-protein interactions between its product Mdy2 and proteins involved in the mating pheromone response pathway were investigated. The two-hybrid system was used to determine whether Mdy2 interacts *in vivo* with known components of the mating pheromone response pathway. To this end *MDY2* was fused to a sequence encoding the DNA-binding domain (BD) of *GAL4*, which binds to the upstream activation site (UAS) of the *GAL1* promoter. The test strain PJ187 carried the reporter genes *lacZ* and *HIS3*, which are under the control

of the *GAL1* UAS (Janssen *et al*., 2001). PJ187 diploid cells were co-transformed with two-hybrid AD- and BD- plasmids (listed in Table 3.5). If the two hybrid protein interact, they reconstitute a functional transcription factor that activates one or more reporter genes that contain binding sites for the DNA binding domain. Transformants were tested for their ability to grow on medium lacking histidine, and were assayed for β-galactosidase expression. Growth on medium lacking histidine indicates two-hybrid formation between the *MDY2*-BD and Gene-X-BD. Furthermore, such interactions are indicated by the appearance of a blue colour in the X-gal overlay assay. The results are presented in Table 3.5 and Fig 3.24.

Table3.5. Two-hybrid interactions between Mdy2 and proteins involved in mating pheromone response pathway

No.	AD fusion	BD fusion	Color	Growth (his⁻trp⁻leu⁻)
528	*SNF4*	*SNF1*	(Blue) +	+
529	*MDY2*	vector	(white) -	-
530	vector	*MDY2*	-	-
531	vector	vector	-	-
532	*SNF4*	*MDY2*	-	-
533	*STE4*	*MDY2*	-	-
534	*STE18*	*MDY2*	-	-
535	*GPA1*	*MDY2*	-	-
536	*STE20*	*MDY2*	-	-
537	*STE5*	*MDY2*	+++	++
538	*STE11*	*MDY2*	-	-
539	*STE7*	*MDY2*	++	++
540	*FUS3*	*MDY2*	++++	++
541	*KSS1*	*MDY2*	++	++
542	*STE11-k444r*	*MDY2*	-	-
543	*CLA4N*	*MDY2*	-	-
544	*CDC24*	*MDY2*	+	+
546	*CDC42*	*MDY2*	-	-
547	*STE20C(498-939)*	*MDY2*	-	-
548	*STE20N(1-497)*	*MDY2*	-	-
550	*STE4* [hpl121-1]	*MDY2*	-	-
552	*BEM1*	*MDY2*	-	-
553	*STE50*	*MDY2*	-	-

Co-expression of BD-*MDY2* with AD plasmids bearing *FUS3*, *STE5*, *STE7*, *KSS1* and *CDC24* led to the induction of *lacZ* and growth on medium lacking histidine. The interaction of Snf1 and Snf4 was used as the positive control. Based on the relative intensity of the colour reaction, the interaction

between Fus3 and Mdy2 appeared to be stronger than that between Ste5 and Mdy2. The interaction between these two was much stronger than that between Snf1 and Snf4 (control). The interactions of Mdy2 with Ste7, Kss1 and Cdc24, on the other hand, were relatively weak.
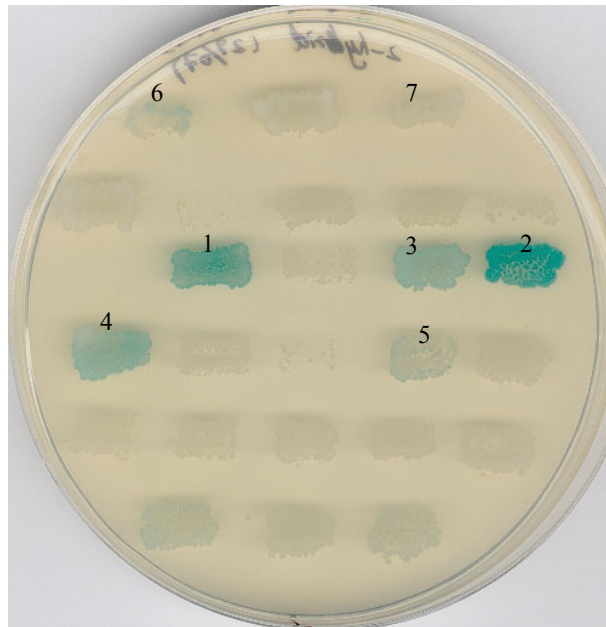
Fig 3.24. Protein-protein interaction between Mdy2 and Fus3, Ste5, Ste7, Kss1 and Cdc24 in the two hybrid X-gal overlay assay. Two-hybrid analysis was performed in PJ187 strain. Transformants grew well in SD-trp⁻leu⁻ medium. 10 ml of 10 mg/ml melted agarose mixed with 10 mg X-gal/ml DMF and 2 other ingredients (sodium phosphate buffer and SDS) were poured on the top of SD plate. The plate was incubated at 30°C and photographed after 48 h. The numbers indicated in the plate refered to following transformants:

1. pAD-*STE5* + pMBD-*MDY2*
2. pAD-*FUS3* + pMBD-*MDY2*
3. pAD-*STE7* + pMBD-*MDY2*
4. pAD-*KSS1* + pMBD-*MDY2*
5. pAD-*CDC24* + pMBD-*MDY2*
6. pAD-*SNF1* + pMBD-*SNF4* (positive control)
7. Vector + pMBD-*MDY2* (Negative control)

3.3.3.2 Pull down analysis

In order to further investigate the interaction between Fus3 and Mdy2 a pull-down assay was performed. A functional Myc epitope-tagged *FUS3* and a functional GST epitope-tagged *MDY2* were
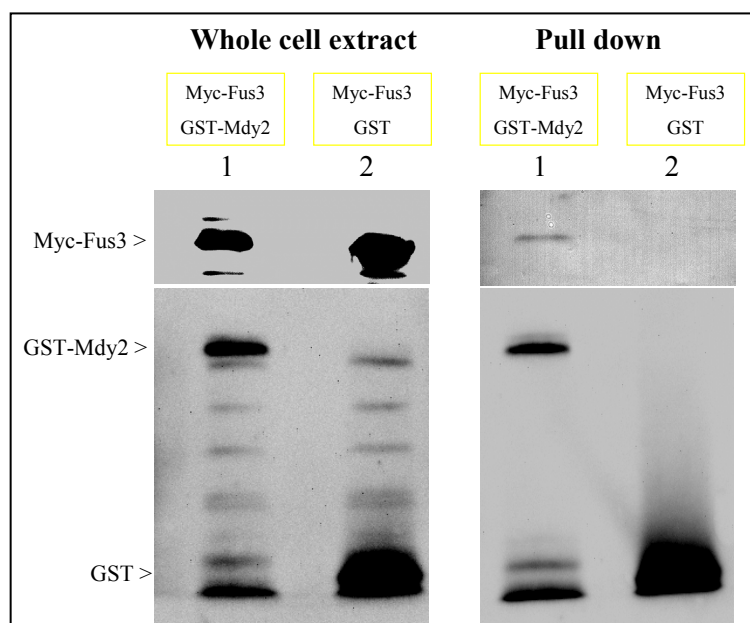
Fig 3.25. Pull down assay. *Left panels* levels of Myc-Fus3, GST-Mdy2 and GST in whole cell extracts. Samples of whole cell extracts were fractionated by SDS-PAGE and analysed on western blots using anti-Myc (*upper panel*) and anti-GST (*lower panel*) antibodies. Myc-Fus3 + GST-Mdy2 (lane 1); Myc-Fus3 + GST (lane 2). *Right panel* Co-purification of Myc-Fus3 and GST-Mdy2. immunodetection of associated Myc fusion protein (*upper lane*) and chemical luminscence detection of GST fusion protein (*lower panel*).

expressed in yeast cells respectively. The GST fusion protein and any associated proteins were purified from the total cellular extract using glutathione-Sepharose beads, and subsequently analyzed by immunoblotting using an anti-Myc antibody. Myc-Fus3 was found to co-purify with the GST-Mdy2 fusion protein (Fig. 3.25). In contrast, no Myc-Fus3 was associated with GST itself. The differences in binding affinity were unlikely to be due to lack of expression of GST because proteins are readily detected in either lysates or eluates (Fig. 3.25).

Based on the results of the two hybrid assay and the pull down assay, it can be confidently concluded that Mdy2 interacts specifically with Fus3. In the following experiments I looked for possible changes in the modification of the MAPK Fus3 during pheromone induction in the presence or absence of *MDY2*.

3.3.4 Mdy2 and the dynamics of MAPK Fus3 modification

Activated Fus3, like other MAP kinases from stimulated eukaryotic cells, is highly phosphorylated on the tyrosine and threonine residues that are conserved among all members of this protein kinase family (Gartner *et al*., 1992; Errede *et al*., 1993; review Nishida and Gotoh, 1993). The activation of Fus3 can be viewed as a two-step process. Autophosphorylation results in the formation of a low level of constitutively tyrosine-phosphorylated Fus3. In response to mating pheromone, Ste7 phosphorylates both the unphosphorylated and the tyrosine-phosphorylated Fus3 on threonine and tyrosine. As autophosphorylation of Fus3 occurs only on tyrosine, Ste7-dependent phosphorylation of the threonine residue is absolutely necessary for Fus3 activation and for subsequent efficient phosphorylation of its target substrates, including Ste12 and Far1 (Elion *et al*., 1993).

To determine whether Mdy2 plays a role in the modification of Fus3, the p*GAL*-Myc-*FUS3* plasmid was constructed. The modification of the functional Myc-Fus3 fusion protein in wild-type and *mdy2* mutant strains was investigated in a galactose depletion assay. Cultures of wild-type and *mdy2* cells harbouring plasmid p*GAL*-Myc-*FUS3* were grown to log-phase, induced by transfer to galactose medium for 4 h, and then shifted into glucose medium containing 5 μM α-factor (final concentration). Samples were taken at various time points and monitored for Fus3 modification. In the wild type, the phosphorylated form of Fus3 appeared rapidly in response to α-factor, and two pheromone-induced Myc-Fus3 bands were observed (Fig 3.26), which is in agreement with the data reported by Cherkasova and Elion (2001). The *mdy2* mutant, in contrast, showed only one weak pheromone-induced band of Myc-Fus3 after induction with 5 μM α-factor. *mdy2* cells which carried both the p*GAL*-Myc-*FUS3* plasmid and the pRS426-*MDY2* plasmid showed two pheromone-induced bands of Myc-Fus3 after induction with 5 μM α-factor, just like the *MDY2* wild-type strain. These results strongly suggest that Mdy2 plays a role in the pheromone-induced phosphorylation of Fus3.
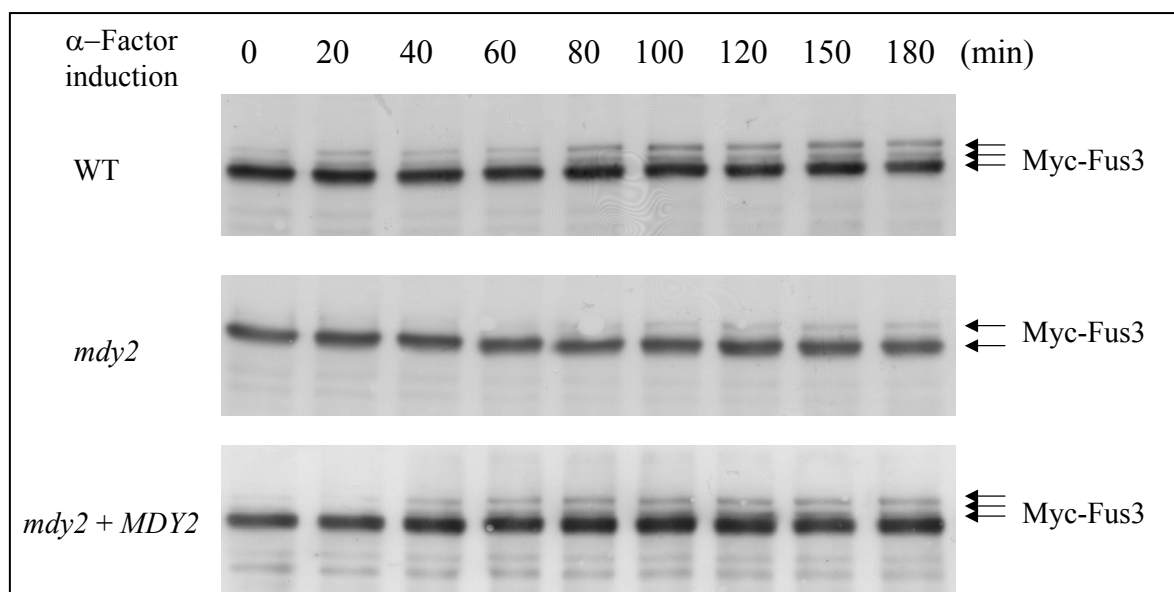
Fig 3.26. Mdy2 and pheromone induced phosphorylation of Myc-Fus3. Cultures of wild-type strain (W303-1A) (*upper panel*) and *mdy2* mutant (HZH686) harbouring pGAL-Myc-*FUS3* (*middle panel*) and *mdy2* mutant harbouring both pGAL-Myc-*FUS3* and 2μ *MDY2* plasmids (*lower panel*) were grown to log-phase and induced in 3% raffinose and 1% galactose medium for 4 hr, and then shifted to 2% glucose medium and treated with 5 μM α-factor for different times as indicated. The cell lysates prepared from aliquots of cultures at indicated times after shift (from galactose to glucose) were separated by SDS-PAGE and immunblotted with anti-Myc antibody. The arrow indicates the position of phospho-Fus3 and total Fus3.

3.3.5 Double deletion of *MDY2* and *KSS1* affects pheromone induced G₁ arrest

As observed in the two-hybrid assay, Mdy2 may also interact with Kss1. In the pheromone-induced G₁ arrest assay the *mdy2* mutant formed a smaller halo than the *MDY2* strain. In order to determine if deletion of *KSS1* affects pheromone-induced growth arrest in the *mdy2* mutant, the two single mutants and the *mdy2 kss1* double mutant were tested using the halo assay. After induction with α-factor for 48 h, as shown in Fig 3.27, the halo size formed on a lawn of the *mdy2 kss1* double deletion mutant was found to be slightly smaller than that formed by either single mutant.
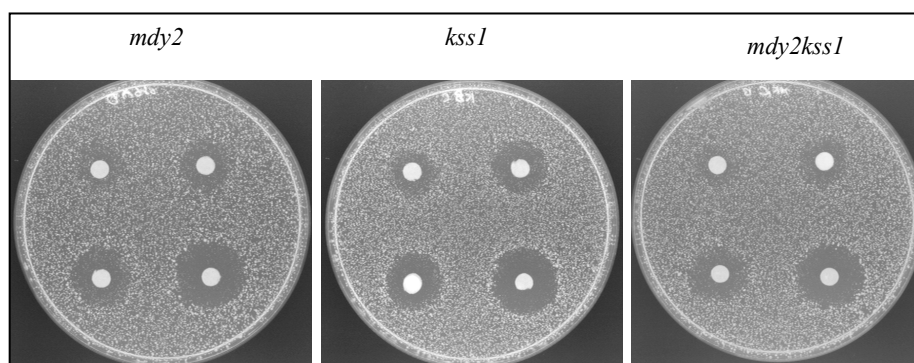
Fig 3.27. Halo assay. Cultures of Δ*mdy2* (HZH686), Δ*kss1* (HZH846), Δ*mdy2kss1* mutant (HZH847) cells were mixed with melted top agar. 0.5 μg, 1.0 μg, 2.0 μg and 5 μg α-factor were added to filter discs respectively (clockwise from upper left) and incubated at 30°C for 3 days, and the plates were photographed.

3.3.6   The effect of Mdy2 on the level of the scaffold protein Ste5

Ste5 is an essential component of the mating pheromone response pathway in *S. cerevisiae* (Blinder *et al*., 1989; Leberer *et al*., 1993; Hasson *et al*., 1993). The protein is thought to function as a scaffold upon which the protein kinases Ste11, Ste7, Fus3 and Kss1 can assemble and be efficiently activated (Choi *et al*., 1994; Kranz *et al*., 1994). In the two-hybrid assay, Mdy2 was also shown to interact with Ste5 (see Section 3.3.3.1). In the following tests, Myc-Ste5 or GST-Ste5 levels were determined in the wild-type strain and the *mdy2* mutant using the galactose depletion assay (see Methods), in order to examine the possible effect of Mdy2 on Ste5.

3.3.6.1   The levels of Myc-Ste5 in wild-type and *mdy2* mutant strains after pheromone induction, as revealed by the galactose depletion assay

To study the possible influence of Mdy2 on the level of Ste5, a plasmid encoding a Myc-tagged version of Ste5 under the control of the *GAL1* promoter was constructed. A yeast strain bearing this allele was grown to early log phase in SRG medium (3% raffinose and 1% galactose), which permits transcription of Myc-*STE5*. The cells were then transferred to a glucose medium that blocks further transcription of Myc-*STE5*. Whole cell extracts were prepared from aliquots of the culture at the indicated time points after the shift, and Myc-Ste5 was detected using immunoblot analysis with anti-Myc antibodies. As shown in Fig 3.28, after galactose depletion there was no significant difference of level of Myc-Ste5 between the wild-type strain and mutant *mdy2* strains.

Fig 3.28 Myc-Ste5 in wild-type strain (W303-1A) and *mdy2* mutant (HZH686). Cultures of wild-type and *mdy2* mutant harbouring pGAL-Myc-*STE5* were grown to log phase and induced in 3% raffinose and 1% galactose medium for 4 hr, and then shifted to 2% glucose medium and treated with 5 μM α-factor for varying length of time as indicated. The cell lysates were fractionated by SDS-PAGE and immunoblotted with anti-Myc antibody.

3.3.6.2 The levels of GST-Ste5 in wild-type and *mdy2* mutant strains after pheromone induction, as revealed by the galactose depletion assay

In order to test whether Mdy2 affects the level of Ste5, a plasmid that expresses a GST-tagged version of Ste5 under the control of the *GAL1* promoter was constructed. A yeast strain bearing this allele was grown to early log-phase in SRG medium (3% raffinose and 1% galactose), which allows transcription of the fusion gene. Then the culture was switched to medium (glucose medium) that blocked further transcription of the fusion gene, and contained 5 µM α-factor (final concentration). Whole cell extracts were prepared from aliquots of cultures at the indicated times after the shift, and the level of GST-Ste5 that remained in the samples was detected by immunoblot analysis using anti-GST antibodies.

Fig 3.29 shows that after galactose depletion the level of GST-Ste5 in mutant *mdy2* is higher than in wild-type after α-factor induction. This suggests that Mdy2 affects the stability of GST-Ste5 in the galactose depletion assay after pheromone induction.
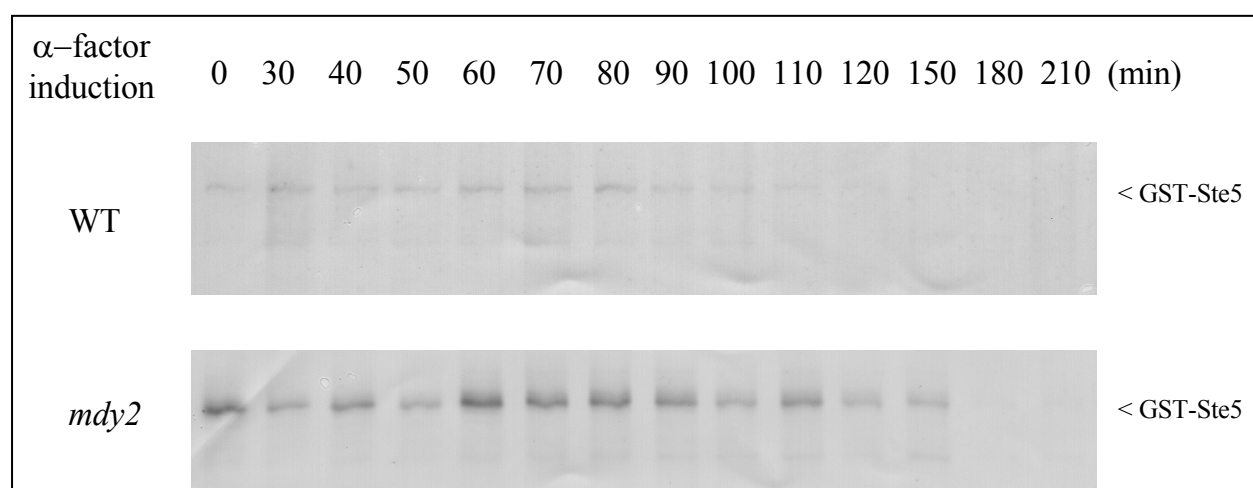
Fig 3.29. The level of GST-Ste5 in wild-type strain W303-1A and *mdy2* mutant (HZH686) in a galactose depletion assay during pheromone induction. Cultures of wild-type strain and *mdy2* mutant harbouring pGAL-GST-*STE5* were grown to log-phase and induced in 3% raffinose and 1% galactose medium for 4 hr, and then shifted to 2% glucose medium and treated with 5 µM α-factor for different times as indicated. The cell lysates were fractionated by SDS-PAGE and immunoblotted with anti-GST antibody.

3.3.6.3 The level of GST-Ste5 in wild-type and *mdy2* mutant strains in galactose depletion assay during vegetative growth, as monitored by the galactose depletion assay

To elucidate the possible role of Mdy2 in modulating the level of Ste5 in vegetatively growing cells, we used a plasmid that carries a GST-tagged version of *STE5* under the control of the *GAL1* promoter.

A yeast strain with this allele was grown to early log phase in SRG medium (3% raffinose and 1% galactose) to allow expression of GST-Ste5. The culture was then shifted to glucose medium, which blocks further transcription of GST-Ste5. Whole cell extracts were prepared from aliquots of cultures at indicated times after the shift, and the level of GST-Ste5 that persisted in the samples was detected by immunoblot analysis using anti-GST antibodies.

Results in Fig 3.30 show that after galactose depletion the level of GST-Ste5 in *mdy2* mutant is higher than in wild-type strain during vegetative growth. This suggests that Mdy2 affects the level of Ste5, at least when the latter is fused to GST (see Discussion).
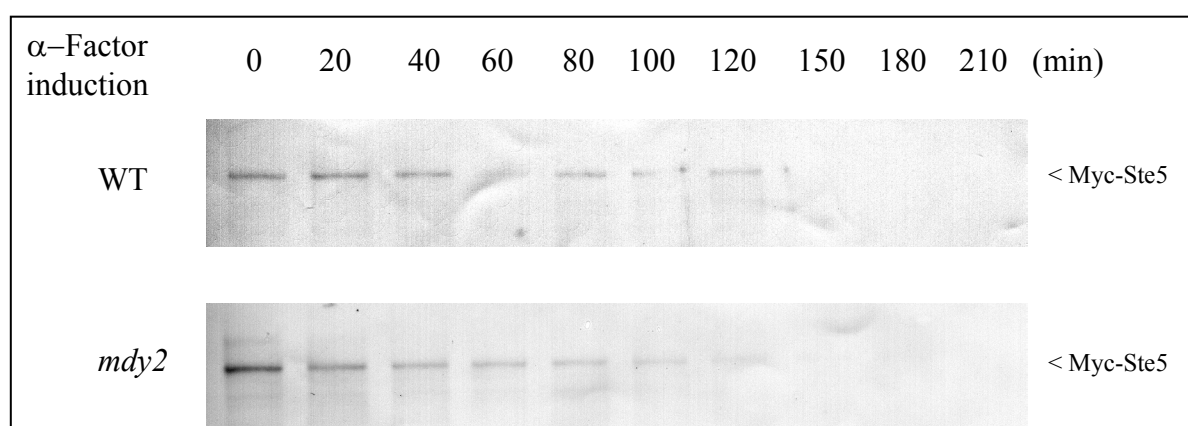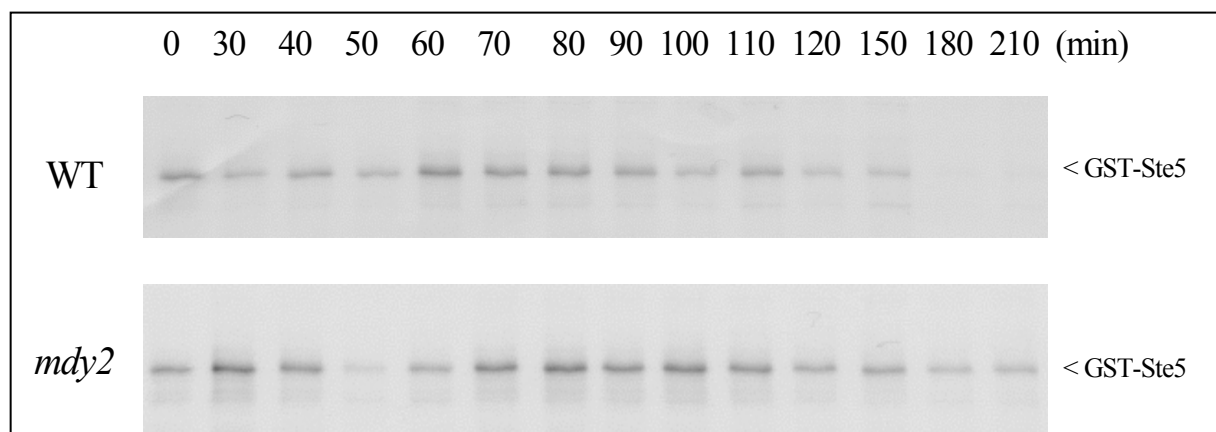

Fig 3.30. The level of GST-Ste5 in wild-type strain (W303-1A) and *mdy2* mutant (HZH686). Cultures of wild-type strain and *mdy2* mutant harbouring pGAL-GST-*STE5* were grown to log-phase and induced in 3% raffinose and 1% galactose medium for 4 hr, and then shifted to 2% glucose medium. Samples were harvested after galactose depletion for different times as indicated. The cell lysates were fractionated by SDS-PAGE and immunoblotted with anti-GST antibody.

3.3.7   Subcellular localization of Mdy2

3.3.7.1   Overexpression of GFP-*MDY2*

To study the subcellular localization of Mdy2, a plasmid carrying a fusion of *MDY2* to the gene for the green fluorescent protein (GFP) was constructed. In a mating assay the GFP-Mdy2 fusion protein was functional and could complement the reduced mating efficiency of the *mdy2* mutant. In vegetatively growing cells, GFP-Mdy2 is localized in the nucleus (Fig 3.31). In cells treated with α-factor, GFP-Mdy2 was also found to be predominantly nuclear, whereas a very small fraction was dispersed in the mating projections (Fig 3.31).
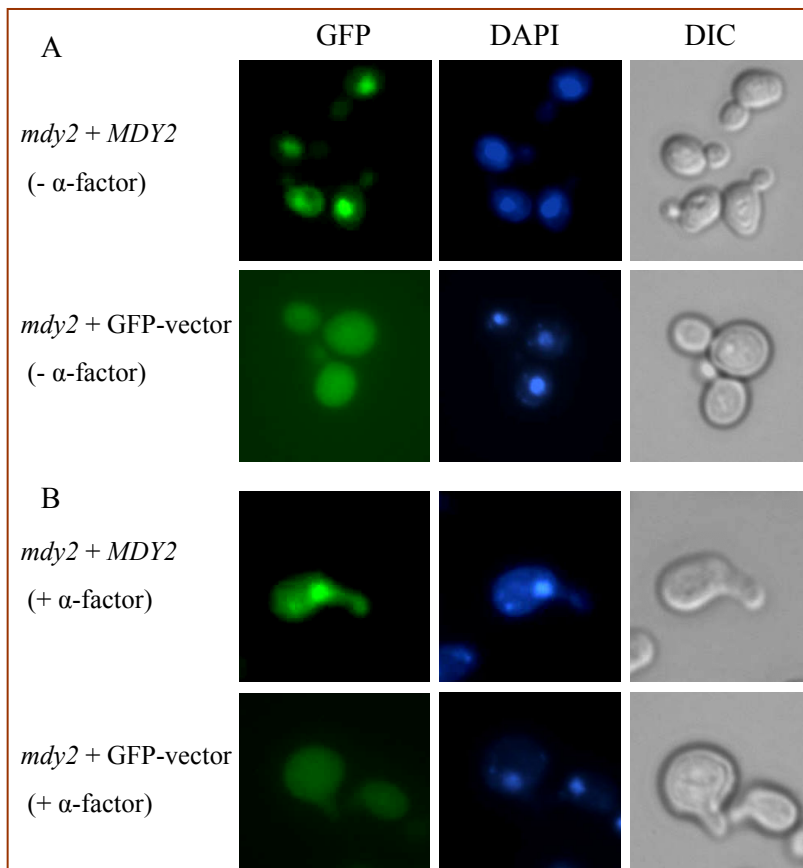
Fig 3.31. Subcellular localization of Mdy2. (A) Cells in vegetative growth. Mutant *mdy2* (HZH686) was transformed with plasmids expressing a functional GFP-Mdy2 fusion protein and transformed with the vector as a control. Cells were induced in 3% raffinose and 1% galactose, and analysed by fluorescence and phase-contrast microscope. (B) Induction with pheromone. *mdy2* mutant cells were transformed with plasmids expressing a functional GFP-Mdy2 fusion protein and transformed with the vector as a control. Cells were induced in 3% raffinose and 1% galactose, then cells were treated with 5 μM α-factor for 2 h, and analysed by fluorescence and phase-contrast microscope.

3.3.7.2 Expression of GFP-*MDY2* under its own promoter

Since overexpression may influence the cellular localization of a protein of interest, the subcellular localization of Mdy2 was also studied by expressing GFP-*MDY2* under the control of its own promoter. We constructed a plasmid that synthesized a GFP-*MDY2* fusion protein under the control of the *MDY2* promoter. During vegetative growth, GFP-Mdy2 is localized in the nucleus (Fig 3.32). After treatment with α-factor, GFP-Mdy2 was also found to be predominantly nuclear (Fig 3.32).
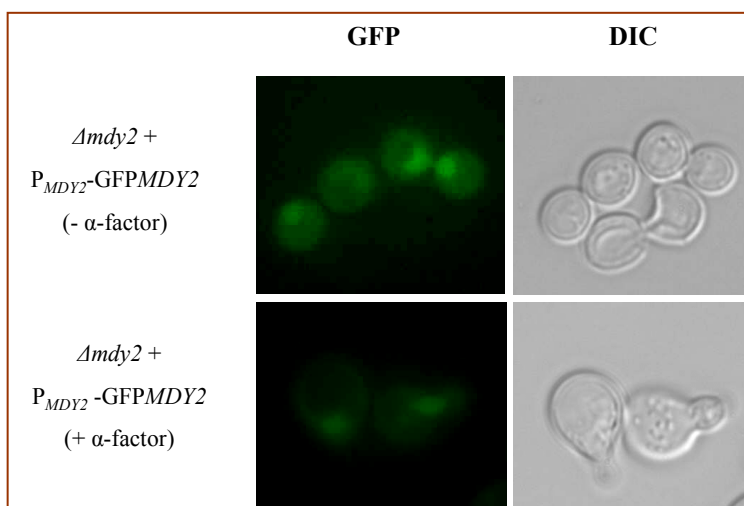
Fig 3.32. Localization of GFP-Mdy2 under the control of its own promoter. Cultures of *mdy2* mutant (HZH686) harbouring *MDY2*p-GFP-*MDY2* plasmid were grown to log phase. Half of cultures was harvested and the localization of GFP-Mdy2 fusion protein was investigated. Another half of cultures was treated with 5 μM α-factor for 2 h, and the fusion protein localization was investigated in the microscope. Since fixation of cells will destory GFP, the nucleus stained with DAPI was not investigated.

3.3.8 The effect of *MDY2* on the invasive growth pathway and the HOG pathway

3.3.8.1 Invasive growth test

Cells of *S. cerevisiae* Cgx31 undergo a developmental switch from a yeast form of growth to a filamentous form of growth (Gimeno and Fink, 1994). In haploid cells, one of the triggers for the switch to the filamentous form is nitrogen starvation. During vegetative growth, the cells are round, and bud in an axial manner (buds are formed adjacent to the site of the previous bud). When nutrients are limiting, the haploid cells become elongated, bud primarily from one pole, and acquire the ability to invade the agar substratum. The *MDY2* gene was deleted in haploid cells of the Cgx31α strain and cells were tested for invasive growth as described by Cullen and Sprague (2002). The results are shown in Fig 3.33. As compared with the wild-type strain, the *mdy2* mutant seems to show only a slight defect in invasive growth. *ste11* and *ste50* mutants are shown as controls.
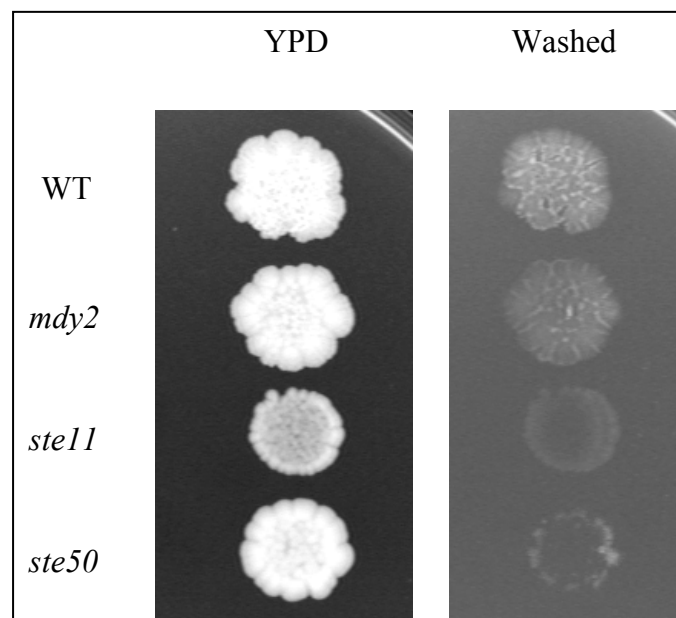
Fig 3.33 Plate washing assay. Equal concentrations of cells were spotted onto YPD medium, invasion was allowed to proceed for 3 days at 30°C. The plates were photographed (left), washed, and photographed again (right). Following strains were used: Wild-type strain (cgx31α), *mdy2* (HZH685), *ste11*(Gy130) and *ste50* (Gy128). Two independent experiments were done in this assay.

3.3.8.2 Osmosensitivity assay

Two MAPK cascades are used to activate an adaptation response to high extracellular osmolarity. To test whether Mdy2 also plays a role in the HOG pathway, the *mdy2* mutant was treated with 1.5 M sorbitol and 0.7 M NaCl. The results shown in Fig 3.34 indicate that mutant *mdy2* is not defective in

the ability to respond to high osmolarity. This suggests that *MDY2* also does not play a role in the HOG pathway.
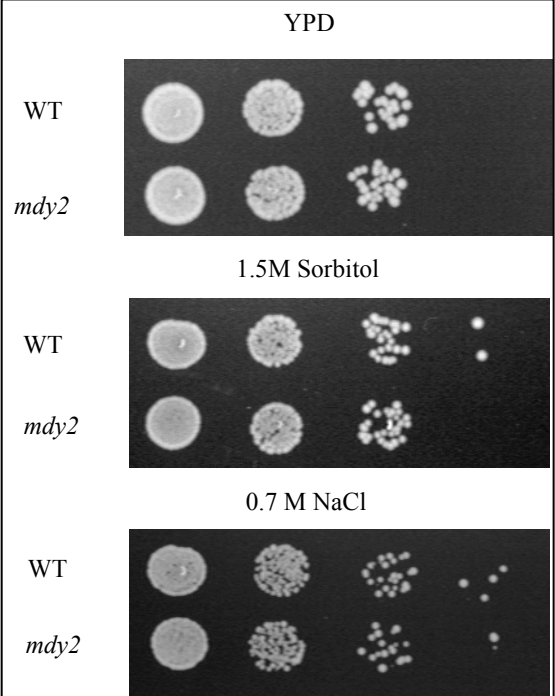
Fig 3.34. Osmosensitivity test of *mdy2*. Cultures of wild-type W303-1A and *mdy2* (HZH686) cells were grown to log phase. The same numbers of cells were harvested and serial 10-fold dilution of cells were dropped on the YPD, YPD + 1.5 M Sorbitol and YPD + 0.7 M NaCl plates. The plates were incubated at 30°C for 2 days and photographed.

4. Discussion

4.1 Identification of novel genes required for mating of *S. cerevisiae*

The two different haploid cell types (**a** cells and α cells) of *S. cerevisiae* are able to conjugate to form diploids (**a**/α cells). The mating process has provided an experimental system with which to explore the genetic control of cell-type specification and development in eukaryotic cells. The mating process has also allowed detailed investigation of the biochemical basis of intercellular signaling and intracellular signal transduction, because conjugation is triggered by the mutual exchange of diffusible peptide pheromones that act through cell-surface G protein-coupled receptors. Furthermore, study of the mating process has permitted in-depth analysis of the hormonal regulation of both gene transcription and cell cycle progression, leading to cellular differentiation (Sprague and Thorner, 1992).

The mating type itself is programmed by an intrachromosomal recombination process, which involves the transposition of genetic information from one or other of two loci, *HML* and *HMR,* into the mating locus, *MAT*. The sequence present at the *MAT* locus is expressed, and determines whether the cell is of the **a** or α mating type. This system also allows any given cell to switch mating type by replacing the information at the *MAT* locus by transposition from the appropriate *HM* locus.

A number of genes required for the mating process in *S. cerevisiae* were first identified through the isolation of a collection of mating-defective ("sterile" or *ste*) mutants that did not map at the *MAT* locus. Following the advent of recombinant DNA methodology and reproducible methods for DNA-mediated transformation of yeast, the normal genes corresponding to each of the *ste* mutations could be isolated by complementation using a library of genomic yeast DNA cloned in a suitable vector. Then a variety of selection schemes and screens were applied to identify further genes required for the mating process, and a set of genes that are directly involved in pheromone production, pheromone response, cell-cell adhesion, cell cycle control, morphogenesis, adaption and recovery were identified (review Sprague and Thorner, 1992). Subsequently, genes required for nuclear fusion were isolated and characterized (review Rose, 1996). A large-scale transposon-tagging screen was later carried out to identify genes whose expression is regulated by mating pheromone, and a set of pheromone regulated genes required for yeast mating differentiation were characterized (Erdman *et al.*, 1998).

In this present study a strategy was devised to identify mating-specific genes using a reverse genetic method that depends on examining the phenotypes of single-gene deletion mutants. To minimize the chance of overlooking genes that produce a weak phenotype, mating efficiency was tested in crosses between deletion mutants in each mating type (*MAT*a and *MAT*α) and the wild-type strain of the opposite mating type and in a bilateral mating cross between the haploid deletants. One advantage of this approach is that it allows the identification of novel genes required for different stages in the mating process, including pheromone production, G protein-initiated signal transduction, cell cycle

arrest, polarized morphogenesis, cell fusion and nuclear fusion, which have not been found by the genetic methods employed in previous studies.

In the first part of this study, 64 single-gene deletions selected in the systematic reverse genetic screen for reduced mating efficiency carried out during the EUROFAN project were investigated. In this present study, 38 of these were found to show a significant mating defect in a semi-quantitative mating assay. The 38 mutants could be classified into four groups: (I) nine displayed clearly reduced mating efficiency in all three mating tests (*MAT**a** mut × MATα* WT, *MATα mut × MAT*a WT, and *MAT*a *mut × MATα mut*); (II) eight showed reduced mating efficiency only when present in *MATα* cells; (III) 12 displayed an obvious mating defect only in the converse situation, when present in *MAT**a*** cells; and (IV) nine deletions displayed a phenotype only in both partners in the mating cross. The mutations in class I all showed a relatively slight reduction in mating efficiency when crossed to the WT strain, but displayed a significantly reduced mating efficiency in the bilateral mutant cross. This suggests that expression of these genes in either mating type is sufficient to ensure efficient mating. The mutations in the classes II, III and IV are inferred to interfere directly with the mating pheromone response pathway and influence mating efficiency in both *MAT**a*** and *MATα* cells. Mutants belonging to the classes II and III influence mating efficiency indirectly, and behave like mutants that interfere with transcriptional silencing (Lustig, 1998). These classes of mutants may cause haploid **a** or α cells to behave like **a**/α diploids (which are pheromone insensitive) by allowing them to activate the normally silent copy of the α gene (*HML*α) which is present in **a** cells, or **a** genes (*HMR*a) that are present in α cells. Gene names had already been assigned to 22 of the 38 ORFs, on the basis of earlier investigations, but these studies had not examined them for possible roles in the mating process. The remaining 16 mutations corresponded to ORFs whose functions were unknown.

Candidates were selected for further analysis on the basis of the following features: (1) the mutant should show a strong mating defect, and (2) transformation with the respective cognate clone should complement the mating defect of the mutant. A total of 15 mutants fulfilled these conditions, and were selected as good candidates for further studies. These are listed in the following Table.

Strain number	ORF	Gene name and related information
2	*YOL087c*	Deletion mutant showed reduced mating efficiency in all three mating tests. The mating defect could be complemented by the respective cognate clone. The protein encoded by *YOL087c* has one WD (WD-40) domain. (EUROFAN-project; Mips.gsf.de).
39	*YNL196c*	**SLZ1**; *slz1* deletion mutant showed reduced mating efficiency in all three mating tests. The mating defect could be complemented by the respective cognate clone. Slz1 is a sporulation-specific protein and has a leuzine zipper pattern. Moreover, Slz1 exhibits interaction with Crm1 (the exportin, β-karyopherin). (EUROFAN-project; Mips.gsf.de).
165	*YOL111c*	Deletion mutant exhibited reduced mating efficiency in all three mating tests. The mating defect could be complemented by the respective cognate clone. The protein encoded by *YOL111c* shows similarity to the human ubiquitin-like protein *GdX*. (Iwanejko *et al.*, 1999).

Strain number	ORF	Gene name and related information
250	*YGL100w*	**SEH1**; *seh1* deletion mutant showed reduced mating efficiency in the bilateral mating test and in the cross with *MATα* WT. The mating defect could be complemented by the respective cognate clone. Seh1 is found in a complex with nuclear pore protein, a member of the WD (WD-40) repeat family; Seh1 localizes symmetrically at both sides of the nuclear pore and the peripheral membrane, and is a nuclear import/export protein (Lillo *et al.*, 2000).
303	*YGL133w*	**ITC1**; *itc1* deletion mutant showed reduced mating efficiency in the bilateral mating test and in the cross with *MATa* WT. Itc1 is a subunit of the Isw2 chromatin remodelling complex and is located in the nucleus. The *MATα* mutant presents an abnormal morphology (Victoria and Mazon, 2000).
349	*YBR087w*	**ECM33**; *ecm33* deletion mutant exhibited reduced mating efficiency in all three mating tests. The mating defect could be complemented by the respective cognate clone. Ecm33 is a protein with a predicted GPI-anchor and involved in cell wall structure or biosynthesis. Ecm33 associates with the plasma membrane (Tohe and Oguchi, 1999; Terashima *et al.*, 2003).
373	*YNL059c*	**ARP5**; *arp5* deletion mutant showed reduced mating efficiency in the bilateral mating test and in the cross with *MATa* WT. The mating defect could be complemented by the respective cognate clone. The Arp5 (Actin-related protein) is related to the Ino80 complex and located in the nucleus and associated with actin-cytoskeleton. The null mutant displays a distorted cell shape and an increased cell size. (Grava *et al.*, 2000; Shen *et al.*, 2003).
380	*YBR283c*	**SSH1**; *ssh1* deletion mutant showed reduced mating efficiency in the bilateral mating test and in the cross with *MATa* WT. The mating defect could be complemented partly by the cognate clone. Ssh1 has ten predicted transmembrane segments, is a component of the Ssh1-Sss1-Sbh2 complex, and is involved in protein translocation into the endoplasmic reticulum (South *et al.*, 2001).
425	*YJL145w*	**SFH5**; *sfh5* deletion mutant showed apparently reduced bilateral mating efficiency. The mating defect could be complemented partly by the cognate clone. Sfh5 is a putative phosphatidylinositol transfer protein (Schnabl *et al.*, 2003).
431	*YDL201w*	Deletion mutant displayed reduced mating efficiency in the bilateral mating test and in the cross with *MATα* WT. The mating defect could be complemented by the cognate clone. The protein encoded by *YDL201w* is a putative methyltransferase and is highly conserved among eukaryotes. (Bahr *et al.*, 1999).
470	*YBR217w*	**APG12**; *apg12* deletion mutant showed reduced mating efficiency in the bilateral mating test and in the cross with *MATa* WT. The mating defect could be complemented partly by the respective cognate clone. Apg12 is a ubiquitin-like modifier and plays an essential role in the dynamic membrane formation of the autophagesome during autophagy (Rodriguez-Navarro *et al.*, 1999).
505	*YNL119w*	Deletion mutant displayed reduced mating efficiency in the bilateral mating test and in the cross with *MATα* WT. The protein encoded by *YNL119w* is possibly involved in cytoplasmic ribosome function. (Capozzo *et al.*, 2000).
566	*YLL057c*	Deletion mutant exhibited reduced mating efficiency in the bilateral mating test and in the cross with *MATa* WT. The mating defect of *MATa* mutant cross wild-type strain could be complemented by the respective cognate clone. The protein encoded by *YLL057c* shows similarity to the C-terminal half of *E.coli* dioxygenase (Zhang *et al.*, 2001).

615	*YLL051c*	**FRE5**; *fre5* deletion mutant exhibited reduced mating efficiency in the bilateral mating test and in the cross with *MATα* WT. The mating defect can be complemented by the respective cognate clone. Fre5 shows similarity to the ferric reductase Fre2 and is subject to regulation by iron. Fre5 is located in the plasma membrane and has six transmembrane segments. (Georgatsou and Alexandraki, 1999).
624	*YGL106w*	**KAP122**; *kap122* deletion mutant showed reduced mating efficiency in the bilateral mating test and in the cross with *MATα* WT. *YGL106w* encodes the nuclear transport factor Kap122. Kap122 is a member of the karyopherin-beta family and is located in nuclear, cytoplasmic, nucleus pore, and peripheral membrane and functions in the import of the Toa1-Toa2 complex to the nucleus (Titov *et al*., 1999).

4.2 Characterization of 15 deletion mutants with reduced mating efficiency

Haploid cells stimulate each other by secreting peptide pheromones. *MAT***a** cells secrete **a** mating pheromone (**a**-factor) whereas *MAT*α cells secrete α mating pheromone (α-factor). The binding of pheromone to its cognate receptor stimulates several cellular responses, including a global change in transcription, arrest of the cell cycle in G_1 phase and polarized morphogenesis. Polarized morphogenesis leads to the formation of a mating projection, which is directed toward the pheromone source. Polarized mating cells signal to one another through the projection, and thereby direct growth to the future site of cell contact and fusion. Cell fusion usually occurs at the tips of the projections, forming a conjugation tube or bridge. Nuclear congression and fusion then take place within this conjugation bridge.

The analysis of the 15 deletion mutants revealed various defects in pheromone production, pheromone response, polarized morphogenesis, cell fusion and nuclear fusion. In the α-factor production assay, the *itc1* deletion mutant (No. 303), the *apg12* mutant (470) and the *YLL057c* mutant (566) were found to be nearly totally defective in α-factor production. These three mutants showed significantly reduced mating efficiency in the *MAT*α *mut* × *MAT***a** WT cross and in the bilateral mutant mating cross. The genetic findings are thus compatible with the idea that the mating defects of these three mutants result from their inability to produce and/or secrete α-factor.

In the pheromone response assay, *MAT***a** cells of the *YNL119w* mutant 505 showed supersensitivity to α-factor in the halo assay, suggesting that further analysis of this mutant should focus on the pheromone response pathway. The *YOL087c* mutant (2) was also supersensitive to α-factor in the halo assay and it displayed significantly reduced *FUS1-lacZ* expression in response to the pheromone. However, the mutant showed no obvious change in the percentage of shmoos formed. These properties suggest that the gene might be related to the pheromone response pathway. The *SFH5* mutant (425) formed fewer shmoos and showed reduced pheromone-induced *FUS1-lacZ* expression, suggesting that Sfh5 is also related to the pheromone response pathway. The *ecm33* mutant (349) showed a

significant reduction in the percentage of shmoos formed, whereas no obvious change in pheromone induced *FUS1-lacZ* expression was observed. These findings raise the possibility that Ecm33 might affect polarized growth during the mating process.

Measurement of the kinetics of zygote formation revelaed a significant discrepancy between the efficiency of zygote formation and that of diploid formation in the *ssh1* deletion mutant (380). In addition, simultaneous detection of GFP and nuclear staining with DAPI demonstrated that the *ssh1* mutant exhibited a defect in nuclear fusion. It is possible that Ssh1 functions in nuclear fusion during mating. In the following sections four of these mutants which showed strong phenotypes are discussed in detail.

Deletion mutants like *itc1*, which is defective in α-factor production, may affect the transcriptional silencing program

S. cerevisiae has two haploid mating types, **a** and α can mate to form a third cell type, the diploid **a**/α cell. The differences among the three cell types are reflected in differences in their gene transcription profiles. α-specific genes (αsg) are expressed only in α cells. Conversely, **a**-specific genes (**a**sg) are expressed in **a** cells, but repressed in the *MAT*α haploid and *MAT***a**/α diploid cell types. Either mating type can switch to the other mating type by a programmed genetic rearrangement (review Sprague and Thorner, 1992; see above).

In this study, the *itc1* deletion mutant 303 showed a significant reduction in mating efficiency in the *MAT*α *mut* × *MAT***a** WT cross and in the bilateral mutant cross. In the α-factor production assay, mutant 303 was almost totally defective in α-factor production. Victoria and Mazon (2000) have shown that disruption of the *ITC1* gene in *MAT*α cells leads to an aberrant cell morphology which resembles the polarized mating projection formed by cells that are responding to pheromone. Ruiz *et al*. (2003) then showed that Itc1 is a component of the ATP-dependent Isw2-Itc1 chromatin remodelling complex, and is required for the repression of **a**-specific genes. These properties suggest that the **a**-specific genes are derepressed in the *MAT*α *itc1* deletion mutant, and that this results in the mating type interconversion. This is consistent with my findings that the *MAT*α *itc1* deletion mutant is defective in α-factor production, and shows significantly reduced mating efficiency in the *MAT*α *mut* X *MAT***a** WT cross and in the bilateral mutant cross.

SSH1 may function in both protein translocation and nuclear fusion

Nuclear fusion (karyogamy) is the last step in the mating pathway, which culminates in the formation of a diploid cell. The pathway of karyogamy in yeast proceeds by at least two major steps. First, cytoplasmic microtubules emanating from the spindle pole body (SPB) are required to bring the nuclei into close proximity, a process called congression. The second step in karyogamy entails the fusion of the nuclear membranes. Two membranes, the inner and outer nuclear envelopes, surround each

nucleus. Therefore, the establishment of nuclear continuity requires that the two outer and two inner membranes become fused in register. Membrane fusion is coupled to the fusion of the two SPBs, resulting in the formation of a single, large, microtubule-organizing center (for review, see Rose, 1996).

SSH1 was first identified as a member of the heat shock protein (Hsp70) multigene family of *S. cerevisiae* (Schilke *et al*., 1996). *SSH1* (Sec 61 homolog) encodes a protein that is ~30% identical to Sec61, which is localized in the endoplasmic reticulum (Finke *et al*., 1996). Ssh1 has ten predicted transmembrane segments, is a component of the Ssh1-Sss1-Sbh2 complex, and is involved in protein translocation into the endoplasmic reticulum (South *et al*., 2001). Several ER–nuclear envelope proteins were recently shown to be required for the fusion of the nuclear envelope during the conjugation of *S. cerevisiae* (Brizzio *et al*., 1999). Two of these proteins, Kar2 and Kar5, are clearly required for nuclear fusion, both in vitro and in vivo. Kar2 is the yeast homologue of the mammalian BIP/GRP78, a member of the Hsp70 chaperone family (Rose *et al.*, 1989). Kar5 is a novel integral ER–nuclear envelope membrane protein. The *KAR5* gene is induced by pheromone and its product localizes near the SPB (Beh *et al.*, 1997; Erdman *et al*., 1998; Brizzio *et al*., 1999), which is consistent with a role in nuclear fusion.

Like *kar2* and *kar5* mutants, the *ssh1* deletion mutant was found in my study to be impaired in nuclear fusion. The *ssh1* deletion mutant 380 also showed a significant discrepancy between the efficiency of zygote formation and that of diploid formation. In addition, simultaneous visualization of GFP and nuclei (stained with DAPI) during zygote formation revealed a defect in nuclear fusion in the *ssh1* deletion mutant. However, the biochemical function of Ssh1 during nuclear fusion is not yet known. Like Kar2p, Ssh1 may have a dual role in protein translocation and nuclear fusion. Further studies should concentrate on identifying the step(s) in nuclear fusion in which Ssh1 functions.

Karyopherin Kap122 is a putative Kapβ homologue that may affect nuclear protein transport and morphogenesis

The karyopherins (also termed importins, exportins, or transportins) are a family of structurally related proteins that function in transporting proteins, nucleic acids, and nucleoproteins into and out of the nucleus (Pemberton *et al*., 1998). Comparative sequence analysis has revealed that, in *S. cerevisiae*, the Kap family is composed of one Kapα and 14 structurally related Kapβ proteins. Kapβ-related proteins carry cargo molecules into or out of the nucleus by binding to them, to the NPC (nuclear pore complex) and to RanGTP. Kapα (Kap60 in yeast) functions as an adaptor protein which is able to bind substrate and Kapβ1 (Kap95 in yeast). Recent studies have shown that Kap142 (Msn5) has multiple functions, including the regulation of carbohydrate metabolism, stress responses, the mating response, the control of signal transduction, cell cycle control, and pseudohyphal differentiation of diploid cells (Yoshida and Blobel, 2001) It was shown recently that Kap142 functions as a nuclear

exportin for Ste5, the protein that serves as a scaffold for the assembly of the MAPK cascade that relays the pheromone signal to the nucleus (Mahanty *et al.*, 1999). *KAP122* (*PDR6*) was previously classified as a member of a gene family that is involved in pleiotropic drug resistance and was only later found to function as a karyopherin in nuclear import. Kap122 is found both in the cytoplasm and the nucleus, and is the major Kap responsible for the import of Toa1 and Toa2 (subunits of the transcription activator TFIIA) into the nucleus (Titov and Blobel, 1999). In this study, the *kap122* deletion mutant exhibited a significantly reduced mating efficiency; however, it showed no defect in pheromone production and was not affected in the pheromone response. The only obvious phenotype obtained was a significantly reduced rate of shmoo formation, which implies a function in polarized growth, perhaps involving the cytoskeleton. Interestingly, Kap122 has been identified in association with Arp2 using an affinity precipitation assay (Ho *et al.*, 2002). Arp2 is an essential component of the actin cytoskeleton that is involved in membrane growth and polarity, as well as in endocytosis (Moreau *et al.*, 1996). The mechanism of its function in shmoo formation and mating is not known. Further study of Kap122 is likely to yield significant insights into the link between nuclear transport and polarized morphogenesis during mating.

Ecm33 is a putative GPI-anchored cell surface protein that might affect polarized growth during mating

Glycosylphosphatidylinositol-anchored (GPI) proteins are widely found in lower and higher eukaryotic organisms (Eisenhaber *et al.*, 2001). GPI proteins are known to be either covalently incorporated into the cell wall network or to remain attached to the plasma membrane. Various functions have been suggested for them. They may be involved in cell wall biosynthesis and cell wall remodelling, they may determine surface hydrophobicity and antigenicity, and they are also thought to have a role in adhesion (Hoyer, 2001; Klis *et al.*, 2001; Sundstrom, 2002).

The *ECM33* gene of *S. cerevisiae* encodes a GPI-anchored protein. In this study, the *ECM33* deletion mutant (349) exhibited significantly reduced mating efficiency in all three mating situations. It was found that the *ECM33* deletion mutant showed no defect in pheromone production, and pheromone induced *FUS1-LacZ* expression was normal. However, the *ECM33* deletion mutant displayed a significant defect in shmoo formation. A recent study has reported that the shift in the localization of Ecm33 from the plasma membrane to the cell wall affects its cellular function (Tohe and Oguchi, 1999; Terashima *et al.*, 2003). These properties suggest that Ecm33, like other cell wall components such as chitin synthase I (encoded by *CHS1*), probably functions to provide structural support to the newly deposited cell wall of the growing mating projection (Appeltauer and Achstetter, 1989). Further investigation of the role of Ecm33 in mating cells might provide insights into how cell surface components are coupled to polarized growth processes in the underlying cell cortex, and how these components affect cell-cell communication events.

4.3 Functional analysis of *MDY2* in mating of *S. cerevisiae*

The *MDY2* gene, which was identified in the first part of this study, was chosen for detailed analysis because it showed a strong mutant phenotype and the gene contains an ubiquitin-like domain (the *UBL* domain). The closest homologue of Mdy2 is the human ubiquitin-like protein GdX, which consists of 157 amino acids. Residues 74-212 of Mdy2 share 34% identity with the N-terminal 123 residues of GdX. These regions are homologous (sharing about 30% identity) to ubiquitin (Fig 4.1).


```
                    *        20        *        40        *        60
GdX        1: MQLIVKALQGRECSLQ---VPEDELVSTLKQLVSEKLNVPVRQQRLLFKGKALADGKRLSDYSIGP : 63
Ubiquitin  1: MQIFVKTLTGKTITLE---VESSDTIDNVKSKIQDKEGIPPDQQRLIFAGKQLEDGRTLSDYNIQK : 63
Mdy2      74: VHLTLKKIQAPKFSIBHDFSPSDTILQIKQHLISEEKASHLSEIKLLLKGKVLHDNLFLSDLKVTP : 139


                    *        80        *       100        *       120        *
GdX       64: N-SKLNLVVKPLEKVLIEEGEAQRLADSPPEQVWQLISKVLARHFSAADASRVLEQLQRDYERSLS : 128
Ubiquitin 64: E-STLHLVLR-----LRGG---------------------------------------------- : 76
Mdy2     140: ANSTITVMIKP-NPTISKEPEAEKSTNSPAPAPPQ----BLT----VP-WDDIEALLKNNFENDQ- : 194


                   140        *       160
GdX      129: RLTLDDIERLASRFLHPEVTETMEKGFSK-- : 157
Ubiquitin   : ----------------------------- :   -
Mdy2     195: ----AAVR---------QVMERLQKGWSLAK : 212
```

Fig 4.1 Alignment of predicted Mdy2 sequences from residues 74-212 with *S. cerevisiae* ubiquitin and human GdX. Residues identical are shaded in dark gray; similar residues are shaded in light gray. Sequences homology to *S. cerevisiae* Mdy2. Residues 74-212 of Mdy2 are homologous to ubiquitin and human GdX

Ubiquitin is a small protein found in eukaryotic cells, either free or covalently attached to a variety of cytoplasmic, nuclear, and integral membrane proteins. Ubiquitination, like phosphorylation, plays a regulatory role in a wide variety of processes in cells; DNA repair, cell cycle control, and the stress response all require the participation of specific ubiquitinating enzymes. Whereas the phosphorylation of proteins is often used to change their functional state, ubiquitination appears mainly to serve as a marker that targets a protein for degradation. However, since not all ubiquitinated proteins are selectively degraded, ubiquitin may play other roles as well (Finley, 1992). A growing family of ubiquitin-like proteins is being uncovered in yeast, such as Rub1, Dsk2, Rad23, Apg12, Smt3 and Hub1 (Hochstrasser, 1996; Hochstrasser, 2000; Dittmar *et al*., 2002), and strikingly, the functional consequences of modification by ubiquitin-like proteins appear to be distinct from those associated with ubiquitination, in that ubiquitin-like modifiers do not typically signal the degradation of their protein targets. Ubiquitin-like modifiers may thus serve as reversible modulators of protein function, and have been implicated in autophagy and nuclear transport (Dittmar *et al*., 2002). The functional analysis of *MDY2* in this study clearly shows that it is required for mating in *S. cerevisiae*.

4.3.1 *MDY2* is required for regulation of the mating pheromone response pathway

In our quantitative mating assay *mdy2* mutants showed an approximately 8-fold reduction in mating efficiency. In the presence of α-factor, *MAT***a** *mdy2* mutant cells underwent some morphological changes but exhibited a servere defect in the formation of shmoos as compared with the wild-type strain. Furthermore, the *mdy2* deletion mutant exhibited a partial defect in the ability to arrest the cell cycle in response to pheromone, as indicated by the decreased percentage of unbudded cells observed after α-factor treatment, and the mutant cells also recovered much more rapidly from α-factor induced G_1 arrest than the wild-type strain. In the halo assay for pheromone response the *mdy2* mutant showed slightly reduced growth inhibition only at a low concentrations of pheromone. The mutant also showed a slight delay in activating the *FUS1-lacZ* reporter gene (monitored by measuring β-galactosidase activity), whereas the peak level of β-galactosidase activity was nearly the same as that attained by the wild-type strain but showed a faster recovery upon removal of the pheromone. These data suggest that *MDY2* is involved in the mating of *S. cerevisiae* and mainly influences the pheromone-induced formation of the mating projection formation and, to a lesser extent, pheromone-induced G_1 arrest.

Overexpression of the *MDY2* gene also caused several phenotypes. In the assay for diploid formation, the *mdy2* deletion mutant harbouring *MDY2* on a high-copy-number plasmid showed a higher efficiency of diploid formation than the wild-type strain bearing the empty vector. A similar tendency was also observed in the analysis of zygote formation (data not shown). Overexpression of *MDY2* improved the abnormally low rate of shmoo formation displayed by the *mdy2* mutant and promoted cell cycle arrest in G_1 upon treatment with α-factor. In addition, overexpression of *MDY2* complemented the defect in α-factor production observed in the *mdy2* mutant. Overexpression of *MDY2* under the control of the *GAL1* promoter in *MAT***a** cells led to an increase in the level of induction of *FUS1* in the presence of pheromone, suggesting that Mdy2 acts upon the transcriptional response to mating pheromone. All these phenotypes are fully compatible with the conclusion that *MDY2* plays an important role in the regulation of the mating pheromone response pathway.

4.3.2 Mdy2 interacts with components of the mating pathway and localizes in the nucleus

To determine how *MDY2* functions within the signal transduction pathway, I set out to identify the proteins in the mating pheromone response pathway with which Mdy2 interacts, using a two-hybrid assay. The results indicated that Mdy2 may interact *in vivo* with Fus3, Ste5, Ste7, Kss1, and Cdc24. Investigation of the subcellular localization of Mdy2 showed that GFP-Mdy2 is localized in the nucleus in vegetatively growing cells. In cells treated with α-factor, GFP-Mdy2 was also predominantly nuclear, but a very small fraction of the protein was dispersed in the mating

projections. The subcellular localization of components of the yeast pheromone MAPK pathway showed that, during vegetative growth, Fus3-GFP was predominantly nuclear, but a fraction was dispersed throughout the cytoplasm; Ste5-GFP expressed from the *GAL1* promoter was predominantly nuclear with some cytoplasmic staining. Ste7-GFP was uniformly distributed throughout the cytoplasm. In cells treated with α-factor, Ste5-GFP, Ste7-GFP and Fus3-GFP localized to the tips of mating projections, and Ste5 and Fus3 were also found in the cell nucleus (Van Drogen *et al.*, 2001). Kss1 is predominately nuclear (Ma *et al.*, 1995) and Cdc24 was found to reside largely in the nucleus in the absence of pheromone and was exported to the cytosol together with Far1 after exposure to pheromone (Blondel *et al.*, 1999; Shimada *et al.*, 2000; Nern and Arkowitz, 2000). Taken together, these data suggest that Mdy2 may interact with Fus3, Ste5, Ste7, Kss1, and Cdc24 in the nucleus.

A major function of Ste5 is to recruit the various components of the signaling pathway to the right place at the right time, and presumably to optimize their relative orientation in a way that enhances their sequential interaction, thereby maximizing the efficiency of signalling (Feng *et al.*, 1998; Elion, 2001, Dohlman and Thorner, 2001). Genetic and biochemical evidence indicates that Ste5 functions as a dimer or higher-order oligomer (Elion, 2001). Recently it has been found that only a minor fraction of the total pool of Ste5 is oligomerized in dilute whole cell extracts, and the formation of a Ste5 oligomer is a key rate-limiting step in determining the ability of Ste5 to be recruited to the plasma membrane and to activate the pathway (Wang and Elion, 2003). The fusion protein Ste5-GST forms homo-oligomers due to interactions between the GST moieties, and Ste5-GST is also more efficiently recruited to the plasma membrane than Ste5-Myc during both vegetative growth and in the presence of α-factor (Wang and Elion, 2003). Ste5-GST must pass through the nucleus and be recruited by Ste4 in order to activate the pathway, and is more efficiently exported from the nucleus, and retained by Ste11 in the cytoplasm.

In this study it could be shown that the level of GST-Ste5 in the *mdy2* mutant is higher than that in the wild-type strain, both in the absence and presence of α-factor. However, there was no detectable difference in the amounts of Myc-Ste5 observed in the *mdy2* mutant and the wild-type strain after pheromone treatment. Both results are in agreement with the data of Wang and Elion, who showed that the majority (>95%) of Myc-Ste5 is monomeric and that α-factor does not affect the level of Myc-Ste5 oligomers (Wang and Elion, 2003). The higher level of GST-Ste5 in *mdy2* cells is consistent with the fact that fusing GST to Ste5 greatly increases the pool of oligomers, because Ste5-GST is more efficiently exported and is retained and stabilized by Ste11 in the cytoplasm. These properties raise two interesting possibilities. One possibility is that Mdy2, an ubiquitin-like protein, might play a direct role in the turnover of Ste5 oligomers in the nucleus. The second possiblity is that in the presence of pheromone the relatively high level of GST-Ste5 in the *mdy2* mutant is a consequence of the decreased level of phosphorylated Fus3 in *mdy2* mutant, and this suggests that the link between Mdy2 and Ste5 might play an indirect role in the mating pheromone response pathway. Further studies should concentrate on the possible modification of Ste5 by Mdy2.

In *S. cerevisiae*, MAPK activation pathways transmit signals involved in five processes: mating, responses to nutrient limitation and osmotic stress, cell wall biosynthesis and sporulation. Some signals are transduced via the same MAPK cascade but give rise to different responses. For example, signal transduction through a common MAPK cascade can induce either mating (in response to mating pheromones) or invasive growth/pseudohyphal filamentous growth (in response to nutrient limitation) (review Herskowitz, 1995). How this is accomplished remains one of the central unsolved problems in signal transduction.

Recently a genome-wide binding assay that combines chromatin immunoprecipitation with DNA microarray technology was used to study the binding behavior of Ste12 during mating and filmentation. It was found that Ste12 binds to distinct promoters *in vivo* under different conditions, and that the different sets of genes specify distinct developmental programs. The global switch in target gene specificity of Ste12 depends on the transcription factor Tec1 during filamentation and is differentially regulated by the two MAPKs (Fus3 and Kss1). Both MAPKs have the ability to induce mating genes in response to pheromone, but Fus3 has an additional activity that inhibits Ste12 binding to filamentation specific genes during mating (Zeitlinger, *et al.*, 2003).

In this study we have shown in a two hybrid assay that Mdy2 interacts with both Fus3 and Kss1. These results raise the interesting possibility that Mdy2 may also play a role in the invasive growth pathway. Indeed, compared to the wild-type strain and *ste11* and *ste50* mutants, the *mdy2* deletion strain showed a partial defect in invasive growth. This implies that Mdy2 might influence both MAPKs (Fus3 and Kss1) and therefore affect invasive growth as well as mating.

4.3.3 Mdy2 and the dynamics of Fus3 modification

Based on the results of the two-hybrid assay and pull down analysis, Mdy2 was shown to interact specifically with Fus3. The difference in the modification of the Myc-Fus3 fusion protein observed in *mdy2* mutant relative to the wild-type strain suggests that Mdy2 might be required for the proper phosphorylation of Fus3. It has been proposed that, upon activation, MAPKs must be transported from the cytoplasm into the nucleus. However, the dynamics of the localization of components of the mating pathway suggested that Fus3 constitutively shuttles between the cytoplasm and the nucleus, and that its translocation is not regulated by pheromones (Van Drogen *et al.*, 2001). It is possible that Mdy2 interacts with the phosphorylated and activated Fus3 in the nucleus to sustain the pheromone-induced response by stabilizing the activity of the phosphorylated MAPK Fus3.

Both activation and inactivation of MAPKs are necessary for the regulated response of cells to a variety of extracellular stimuli. In *S. cerevisiae*, stimulation by mating pheromone induces specific gene expression and cell cycle arrest at the G_1 stage to prepare cells for subsequent morphological changes. After prolonged stimulation, however, cells recover from G_1 arrest. The recovery involves down-regulation of the MAPK cascade. *fus3* null mutants are defective in G_1 arrest, whereas *kss1* null

mutants are not, suggesting that Fus3 plays a more important role in the control of G_1 arrest than Kss1 (Elion *et al*., 1990, 1991; Cherkasova *et al*., 1999). The defect of *fus3* null mutants with respect to G_1 arrest is due to the nearly complete dependence of the cyclin-dependent kinase inhibitor Far1 on phosphorylation by Fus3, and consequently a major requirement for Fus3 for the repression of G_1/S cyclin genes (Peter *et al*., 1993; Tyers and Futcher, 1993; Cherkasova *et al*., 1999). Fus3 also plays essential roles in projection formation, partner selection, and cell fusion that are not shared by Kss1 (Elion *et al*., 1990; Farley *et al*., 1999). That Fus3 is more critical than Kss1 for many responses to mating pheromone is consistent with the fact that the *FUS3* gene is expressed predominantly in haploids and is induced by mating pheromone (Elion *et al*., 1990), whereas the *KSS1* gene is constitutively expressed in both haploids and diploids (Ma *et al*., 1995). A reduction in Fus3 activity in the *mdy2* mutant could also explain the fall in shmoo formation and the slight defect in G_1 arrest. Overexpression of *MDY2* slightly increased the efficiency of both shmoo formation and G_1 arrest after α-factor treatment. A *kss1* mutant is not defective in G_1 arrest, but *mdy2kss1* double mutants exhibited a slight defect in G_1 arrest. These results support the idea that Mdy2 functionally interacts with Fus3 and is required for the regulation of Fus3 MAPK activity, and also suggest that the interaction between Kss1 and Mdy2 plays a less important role in the G_1 arrest and polarized cell growth. In addition, the functional analysis of a series of *fus3* point mutants has demonstrated that Fus3 is specifically required to promote formation of the mating projection (shmoo) and that it promotes polarized growth independently of its ability to promote transcription (Farley *et al*., 1999). Furthermore, catalytically inactive Fus3 prevents active Fus3 from activating Ste12 (Farley *et al*., 1999). These properties raise the possibility that, in the absence of Mdy2, inactive Fus3 blocks the ability to promote shmoo formation and G_1 arrest, and finally blocks further differentiation by restoring mitotic growth, thus resulting in the mating defect. Further experiments will be required to clarify whether the deletion of *MDY2* interferes with the proper phosphorylation of Far1.

Once Fus3 is activated by Ste7-dependent phosphorylation, a number of factors help to limit the active lifetime of the MAPK. One particularly important mechanism involves the dephosphorylation of either Tyr or Thr, which inactivates Fus3. Two phosphotyrosine-specific phosphoprotein phosphatases, Ptp3 and Ptp2, regulate this process (Zhan *et al*., 1997). Mutations in Ptp3 or Fus3 that abolish their interaction lead to unregulated kinase activity and delay recovery after pheromone stimulation (Zhan and Guan, 1999). In addition, a dual-specificity phosphatase, Msg5, also contributes to inactivating Fus3. The *MSG5* gene is highly pheromone inducible, and cells carrying an *msg5* mutation display increased pheromone sensitivity and increased steady-state Fus3 phosphorylation, both before and after pheromone treatment (Doi *et al*., 1994), which suggests that Msg5 action contributes to adaptation and recovery. Furthermore, it has been shown that Gpa1, the α-subunit of the G-protein associated with the pheromone receptor, binds directly to the MAPK Fus3 (Metodiev *et al*., 2002). Disruption of this interaction by mutation confers increased sensitivity to pheromone and causes a defect in Gpa1-mediated adaptation. It has recently been observed that Gpa1

and Msg5 work in concert to down-regulate the mating signal, and that they do so by inhibiting the pheromone-induced increase in the level of Fus3 in the nucleus.
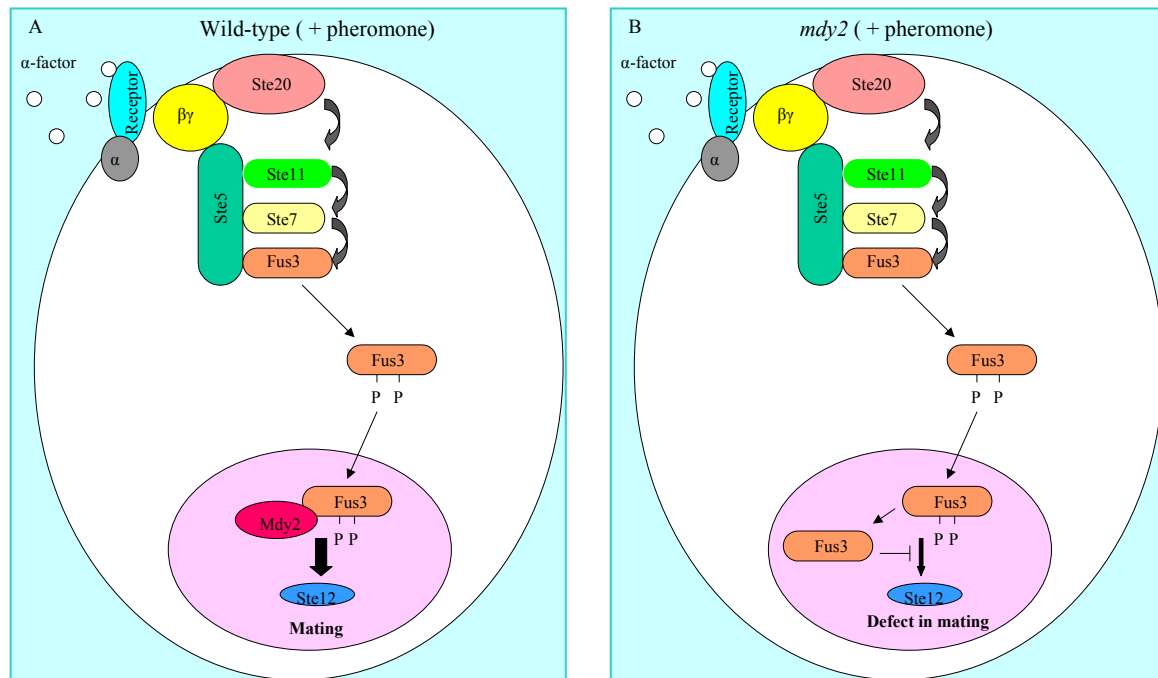

Fig 4.2 A model for the interaction between Mdy2 and MAPK Fus3 and its role in the mating pathway. (A) In the presence of pheromone, the interaction between Mdy2 and Fus3 is probably required for the stabilization of phosphorylated Fus3 and promotes the proper mating in the wild-type cells. (B) In the presence of pheromone, the deletion of *MDY2* results in the defect in the stabilization of phosphorylation of Fus3 in the nucleus and finally results in the defect in mating.

Kap104 is required for the Gpa1/phosphatase-mediated effect on Fus3 localization (Blackwell *et al*., 2003). In this study it was found that Mdy2 interacts with Fus3, but does not interact with Gpa1 in the two-hybrid assay. Mdy2 is localized predominantly in the nucleus. As shown in Fig 4.1, in the central portion of the molecule (74-149 amino acids), Mdy2 shares homology to ubiquitin and human GdX, and it is an ubiquitin-like protein. Dittmar *et al*. (2002) suggest that the functional consequences of protein modification by ubiquitin-like proteins are distinct from that of ubiquitination, in that ubiquitin-like modifiers do not typically signal the degradation of their protein targets. A growing family of ubiquitin-like proteins are being uncovered in yeast (Hochstrasser, 2000; Dittmar *et al*., 2002), and ubiquitin-like proteins have been implicated in autophagy, nuclear transport and polarized morphogenesis (Hochstrasser, 2001; Ichimura *et al*., 2000; Dittmar, 2001).   In this study, the difference seen in modification of the Myc-Fus3 fusion protein between wild-type and the *mdy2* mutant suggests that Mdy2, an ubiquitin-like protein, is most probably required for the stabilization of the phosphorylated form of the MAPK Fus3 in the pheromone response pathway (Fig 4.2).

Summary

The cytological events of yeast mating have been well described but, in comparison with our knowledge of the components of the mating signal transduction cascade and their interactions, relatively few components are known to be specifically involved in the later events in the mating process. The limited number of genes currently identified as functioning in these processes suggested that a search for new genes required for mating might yield additional components of the mating pathway, and thereby help to determine the molecular and cellular mechanism involved in the mating process.

In the first part of this study, a semi-quantitative mating analysis and complementation tests were performed to identify new genes required for mating in the yeast *S. cerevisiae*. 38 out of 64 single gene deletion mutants selected during EUROFAN project for reduced mating efficiency indeed showed significantly reduced mating efficiency in the mating assay. More detailed characterization of 15 of these mutants with respect to pheromone production, pheromone response, morphogenesis, cell fusion and nuclear fusion yielded insight into the precise steps affected by these mutations.

MDY2, one of genes identified in the first part of study, was then characterized in more detail. *MDY2* is located on chromosome XV and encodes a protein of 212 amino acids. It contains an ubiquitin-like domain (*UBL*-domain). The closest homologue of *MDY2* is the 157 amino acid human protein GdX. Phenotypic analysis of *mdy2* deletion mutants suggests that *MDY2* is required for mating in *S. cerevisiae* and mainly influences the pheromone induced formation of the mating projection and, to a lesser extent, the pheromone-dependent arrest of the cell cycle in G_1. The phenotypic analysis of the effects of overexpression of *MDY2* confirmed that *MDY2* plays an important role in the regulation of the pheromone response pathway.

To determine whether and where *MDY2* functions within the signal transduction pathway, possible protein-protein interactions between Mdy2 and proteins involved in the mating pheromone response pathway were investigated using two-hybrid assays. The results indicated that Mdy2 may interact *in vivo* with the MAPKs Fus3 and Kss1, the scaffold protein Ste5, the MAPKK Ste7, and Cdc24. In a pull down analysis, Mdy2 was shown to interact specifically with the MAPK Fus3. An analysis of the modification of the Myc-Fus3 fusion protein in response to pheromone in the *mdy2* mutant suggests that Mdy2 probably influences the stability of the phosphorylated form of Fus3. Investigation of the subcellular localization of Mdy2 showed that GFP-Mdy2 is localized in the nucleus of vegetative growing cells. In cells treated with α-factor, GFP-Mdy2 is predominantly nuclear, but a very small fraction is dispersed in the mating projections. These results suggest that Mdy2 may interact with Fus3 in the nucleus.

References

1. Anderegg, R.J., Betz, R., Carr, S.A., Crabb, J.W., and Duntze, W. (1988). Structure of *Saccharomyces cerevisiae* mating hormone a-factor. Identification of S-farnesyl cysteine as a structural component. J Biol. Chem. 263:18236-18240.

2. Andrews, B.J., and Herskowitz, I. (1990). Regulation of cell cycle-dependent gene expression in yeast. J Biol. Chem. 265:14057-14060.

3. Appeltauer, U., and Achstetter, T. (1989). Hormone-induced expression of the *CHS1* gene from *Saccharomyces cerevisiae*. Eur. J Biochem. 181:243-247.

4. Arkowitz, R.A. (1999). Responding to attraction: chemotaxis and chemotropism in Dictyostelium and yeast. Trends Cell Biol. 9:20-27.

5. Bahr, A., Hankeln, T., Fiedler, T., Hegemann, J., and Schmidt, E.R. (1999). Molecular analysis of *METTL1*, a novel human methyltransferase-like gene with a high degree of phylogenetic conservation. Genomics 57:424-428.

6. Bardwell, L., Cook, J.G., Inouye, C.J., and Thorner, J. (1994). Signal propagation and regulation in the mating pheromone response pathway of the yeast *Saccharomyces cerevisiae*. Dev Biol. 166:363-379.

7. Beh, C.T., Brizzio, V., and Rose, M.D. (1997). *KAR5* encodes a novel pheromone-inducible protein required for homotypic nuclear fusion. J Cell Biol. 139:1063-1076.

8. Blackwell, E., Halatek, I.M., Kim, H.J., Ellicott, A.T., Obukhov, A.A., and Stone, D.E. (2003) Effect of the pheromone-responsive G(alpha) and phosphatase proteins of *Saccharomyces cerevisiae* on the subcellular localization of the Fus3 mitogen-activated protein kinase. Mol. Cell. Biol. 23:1135-1150.

9. Blinder, D., Bouvier, S., and Jenness, D.D. (1989). Constitutive mutants in the yeast pheromone response: ordered function of the gene products. Cell 56:479-486.

10. Blondel, M., Alepuz, P.M., Huang, L.S., Shaham, S, Ammerer, G., and Peter, M. (1999). Genes Dev. 13:2284-2300.

11. Boyartchuk, V.L., and Rine, J. (1998). Roles of prenyl protein proteases in maturation of *Saccharomyces cerevisiae* a-factor. Genetics 150:95-101.

12. Brachmann, C.B., Davies, A., Cost, G.J., Caputo, E., Li, J., Hieter, P., and Boeke, J.D. (1998). Designer deletion strains derived from *Saccharomyces cerevisiae* S288C: a useful set of strains and plasmids for PCR-mediated gene disruption and other applications. Yeast 14:115-132.

13. Brake, A.J. (1989). Secretion of heterologous proteins directed by the yeast alpha-factor leader. Biotechnology. 13:269-280.

14. Breitkreutz, A., Boucher, L., and Tyers, M. (2001). MAPK specificity in the yeast pheromone response independent of transcriptional activation. Curr. Biol. 11:1266-71.

15. Brizzio, V., Khalfan, W., Huddler, D., Beh, C.T., Andersen, S.S., Latterich, M., and Rose M.D. (1999). Genetic interactions between *KAR7/SEC71*, *KAR8/JEM1*, *KAR5*, and *KAR2* during nuclear fusion in *Saccharomyces cerevisiae*. Mol. Biol. Cell. 10:609-626.

16. Burkholder, A. C., and Hartwell, I. (1985). The yeast alpha-factor receptor: structural properties deduced from the sequence of the *STE2* gene. Nucleic Acids Res. 13:8463-8475.

17. Capozzo, C., Sartorello, F., Dal Pero, F., D'Angelo, M., Vezzi, A., Campanaro, S., and Valle, G. (2000) Gene disruption and basic phenotypic analysis of nine novel yeast genes from chromosome XIV. Yeast 16:1089-1097.

18. Chang, F., and Herskowitz, I. (1990). Identification of a gene necessary for cell cycle arrest by a negative growth factor of yeast: *FAR1* is an inhibitor of a G_1 cyclin, *CLN2*. Cell 63:999-1011.

19. Chant, J. (1999). Cell polarity in yeast. Annu. Rev. Cell Dev. Biol. 15:365-391.

20. Cherkasova, V., and Elion, E.A. (2001). far4, far5, and far6 define three genes required for efficient activation of MAPKs Fus3 and Kss1 and accumulation of glycogen. Curr. Genet. 40:13-26.

21. Cherkasova, V., Lyons, D.M., and Elion, E.A. (1999). Fus3p and Kss1p control G_1 arrest in *Saccharomyces cerevisiae* through a balance of distinct arrest and proliferative functions that operate in parallel with Far1p. Genetics. 151:989-1004.

22. Chien, C., Bartel, P.L., Sternglanz, R., and Fields, S. (1991). The two-hybrid system: a method to identify and clone genes for proteins that interact with a protein of interest. Proc. Natl. Acad. Sci. USA 88: 9578-9582.

23. Choi, K.Y., Kranz, J.E., Mahanty, S.K., Park, K.S., and Elion, E.A. (1999). Characterization of Fus3 localization: active Fus3 localizes in complexes of varying size and specific activity. Mol Biol Cell. 10:1553-1568.

24. Choi, K.Y., Satterberg, B., Lyons, D.M., and Elion, E.A. (1994). Ste5 tethers multiple protein kinases in the MAP kinase cascade required for mating in *S. cerevisiae*. Cell 78:499-512.

25. Christianson, T.W., Sikorski, R.S., Dante, M., Shero, J.H., and Hieter, P. (1992). Multifunctional yeast high-copy-number shuttle vectors. Gene 110:119-122.

26. Clark, K.L., Dignard, D., Thomas, D.Y., and Whiteway, M. (1993). Interactions among the subunits of the G protein involved in *Saccharomyces cerevisiae* mating. Mol. Cell. Biol. 13:1-8.

27. Cook, J.G., Bardwell, L., and Thorner, J. (1997). Inhibitory and activating functions for MAPK Kss1 in the *S. cerevisiae* filamentous-growth signalling pathway. Nature 390:85-88.

28. Cullen, P.J., Schultz, J., Horecka, J., Stevenson, B.J., Jigami, Y., and Sprague, G.F. Jr. (2000). Defects in protein glycosylation cause *SHO1*-dependent activation of a *STE12* signaling pathway in yeast. Genetics. 155:1005-1018.

29. Cullen, P.J., and Sprague, G.F.Jr. (2000). Glucose depletion causes haploid invasive growth in yeast. Proc Natl Acad Sci USA. 97:13619-13624.

30. Cullen, P.J., and Sprague, GF. Jr. (2002). The roles of bud-site-selection proteins during haploid invasive growth in yeast. Mol. Biol. Cell 13:2990-3004.

31. Dittmar, G.A., Wilkinson, C.R., Jedrzejewski, P.T., Finley, D. (2002). Role of a ubiquitin-like modification in polarized morphogenesis. Science 295:2442-2446.

32. Dohlman, H.G., and Thorner, J.W. (2001) Regulation of G protein-initiated signal transduction in yeast: paradigms and principles. Annu. Rev. Biochem. 70:703-754.

33. Doi, K., Gartner, A., Ammerer, G., Errede, B., Shinkawa, H., Sugimoto, K., and Matsumoto, K. (1994). *MSG5*, a novel protein phosphatase promotes adaptation to pheromone response in *S. cerevisiae*. EMBO J. 13:61-70.

34. Dorer, R., Boone, C., Kimbrough, T., Kim, J., and Hartwell, L.H. (1997). Genetic analysis of default pathway to select a mate in the absence of pheromone gradients. J. Cell Biol. 130: 1283-1296.

35. Drogen, F., O'Rourke, S.M., Stucke, V.M., Jaquenoud, M., Neiman, A.M., and Peter, M. (2000). Phosphorylation of the MEKK Ste11p by the PAK-like kinase Ste20p is required for MAP kinase signaling in vivo. Curr. Biol. 10:630-639.

36. Eisenhaber, B., Bork, P., and Eisenhaber, F. (2001). Post-translational GPI lipid anchor modification of proteins in kingdoms of life: analysis of protein sequence data from complete genomes. Protein Eng. 14:17-25.

37. Elion, E.A. (1995). Ste5: a meeting place for MAP kinases and their associates. Trends Cell Biol. 5:322-327.

38. Elion, E.A. (2001). The Ste5p scaffold. J Cell Sci. 114:3967-78.

39. Elion, E.A., Brill, J.A., and Fink, G.R. (1991) *FUS3* represses *CLN1* and *CLN2* and in concert with *KSS1* promotes signal transduction. Proc Natl Acad Sci USA 88:9392-9396.

40. Elion, E.A., Brill, J.A., and Fink, G.R. (1991). Functional redundancy in the yeast cell cycle: *FUS3* and *KSS1* have both overlapping and unique functions. Cold Spring Harb Symp Quant Bio. 56:41-49.

41. Elion, E.A., Grisafi, P.L., and Fink, G.R. (1990). *FUS3* encodes a $cdc2^+/CDC28$-related kinse required for the transition from mitosis into conjugation. Cell 60:649-664.

42. Elion, E.A., Satterberg, B., and Kranz, J.E. (1993). *FUS3* phosphorylates multiple components of the mating signal transduction cascade: evidence for *STE12* and *FAR1*. Mol. Biol. Cell 4: 495-510.

43. Erdman, S., Lin, L., Malczynski, M., and Snyder, M. (1998). Pheromone-regulated genes required for yeast mating differentiation. J Cell Biol. 140:461-483.

44. Errede, B., Gartner, A., Zhou, Z., Nasmyth, K., and Ammerer, G. (1993). MAP kinase-related *FUS3* from *Saccharomyces cerevisiae* is activated by *STE7* in vitro. Nature 362:261-264.

45. Esch, R.K., and Errede, B. (2002). Pheromone induction promotes Ste11 degradation through a MAPK feedback and ubiquitin-dependent mechanism. Proc. Natl. Acad. Sci. USA 99: 9160-9165.

46. Farley, F.W., Satterberg, B., Goldsmith, E.J., and Elion, E.A. (1999). Relative dependence of different outputs of the *Saccharomyces cerevisiae* pheromone response pathway on the MAP kinase Fus3p. Genetics 151:1425-1444.

47. Feng, Y.Y., Song, L.Y., Kincaid, E., Mahanty, S.K., and Elion, E.A. (1998). Functional binding between G-beta and the LIM domain of Ste5 is required to activate the MEKK Ste11. Curr. Biol. 8:267-278.

48. Finke, K., Plath, K., Panzner, S., Prehn, S., Rapoport, T.A., Hartmann, E., and Sommer, T. (1996). A second trimeric complex containing homologs of the Sec61p complex functions in protein transport across the ER membrane of *S. cerevisiae*. EMBO J. 15:1482-1494.

49. Finley, D. (1992) The molecular and cellular biology of the yeast *Saccharomyces*. Volume 2. Gene expression. Cold Spring Harbor Laboratory Press.

50. Fuller, R.S., Sterne, R.E., and Thorner, J. (1988). Enzymes required for yeast prohormone processing. Annu. Rev. Physiol. 50:345-362.

51. Gartner, A., Nasmyth, K., and Ammerer, G. (1992). Signal transduction in Saccharomyces cerevisiae requires tyrosine and threonine phosphorylation of *FUS3* and *KSS1*. Genes Dev. 6:1280-1292.

52. Georgatsou, E., and Alexandraki, D. (1999). Regulated expression of the Saccharomyces cerevisiae Fre1p/Fre2p Fe/Cu reductase related genes. Yeast 15:573-584.

53. Gimeno, C.J., and Fink, G.R. (1994). Induction of pseudohyphal growth by overexpression of *PHD1*, a Saccharomyces cerevisiae gene related to transcriptional regulators of fungal development. Mol. Cell. Biol. 14:2100-2112.

54. Gimeno, C.J., Ljungdahl, P.O., Styles, C.A., and Fink, G.R. (1992). Unipolar cell divisions in the yeast S. cerevisiae lead to filmentous growth: regulation by starvation and RAS. Cell 68:1077-1090.

55. Grava, S., Dumoulin, P., Madania, A., Tarassov, I., and Winsor, B. (2000). Functional analysis of six genes from chromosomes XIV and XV of *Saccharomyces cerevisiae* reveals *YOR145c* as an essential gene and *YNL059c/ARP5* as a strain-dependent essential gene encoding nuclear proteins. Yeast 16:1025-1033.

56. Güldener, U., Heck, S., Fiedler, T., Beinhauer, J., and Hegemann, J.H. (1996). A new efficient gene disruption cassette for repeated use in budding yeast. Nucleic Acids Res. 24: 2519-2524.

57. Gustin, M.C., Albertyn, J., Alexander, M., and Davenport, K. (1998). MAP kinase pathways in the yeast *Saccharomyces cerevisiae*. Microbiol. Mol. Biol. Rev. 62:1264-1300.

58. Hanahan. (1983). Studies on transformation of Escherichia coli with plasmids. J Mol. Biol. 166:557-580.

59. Harper, J.W., Adami, G.R., Wei, N., Keyomarsi, K., and Elledge, S.J. (1993). The p21 Cdk-interacting protein Cip1 is a potent inhibitor of G1 cyclin-dependent kinase. Cell 75:805-816.

60. Hartwell, L.H. (1980). Mutants of *Saccharomyces cerevisiae* unresponsive to cell division control by polypeptide mating hormone. J Cell Biol. 85:811-822.

61. Hasson, M.S., Blinder, D., Thorner, J., and Jenness, D.D. (1993). Mutational activation of the *STE5* gene product bypasses the requirement for G protein β and γ subunits in the yeast pheromone response pathway. Mol. Cell. Biol. 14:1054-1065.

62. Heiman, M.G., and Walter, P. (2000). Prm1p, a pheromone-regulated multispanning Membrane protein, facilitates plasma membrane fusion during yeast mating. J Cell Biol. 151:719-730.

63. Herskowitz, I. (1995). MAP kinase pathways in yeast: for mating and more. Cell 80:187-197.

64. Hicke, L. (1999). Getting' down with ubiquitin: turning off cell-surface receptors, transporters and channels. Trends Cell Biol. 9:107-112.

65. Ho, Y., Gruhler, A., Heilbut, A., Bader, G.D., Moore, L., Adams, S.L., Millar, A., Taylor, P., Bennett, K., Boutilier, K., Yang, L., Wolting, C., Donaldson, I., Schandorff, S., Shewnarane, J., Vo, M., Taggart, J., Goudreault, M., Muskat, B., Alfarano, C., Dewar, D., Lin, Z., Michalickova, K., Willems, A.R., Sassi, H., Nielsen, P.A., Rasmussen, K.J., Andersen, J.R., Johansen, L.E., Hansen, L.H., Jespersen, H., Podtelejnikov, A., Nielsen, E., Crawford, J., Poulsen, V., Sorensen, B.D., Matthiesen, J., Hendrickson, R.C., Gleeson, F., Pawson, T., Moran, M.F., Durocher, D., Mann, M., Hogue, C.W., Figeys, D., and Tyers, M. (2002). Systematic identification of protein complexes in Saccharomyces cerevisiae by mass spectrometry. Nature. 415:180-183.

66. Hochstrasser, M. (1996). Ubiquitin-dependent protein degradation. Annu. Rev. Genet. 30:405-39.

67. Hochstrasser, M. (2000). Evolution and function of ubiquitin-like protein-conjugation systems. Nat. Cell Biol. 2:153-157.

68. Hoyer, L.L., Fundyga, R., Hecht, J.E., Kapteyn, J.C., Klis, F.M., and Arnold, J. (2001). Characterization of agglutinin-like sequence genes from non-albicans Candida and phylogenetic analysis of the ALS family. Genetics 157:1555-1567.

69. Ichimura, Y., Kirisako, T., Takao, T., Satomi, Y., Shimonishi, Y., Ishihara, N., Mizushima, N., Tanida, I., Kominami, E., Ohsumi, M., Noda, T., and Ohsumi, Y. (2000). A ubiquitin-like system mediates protein lipidation. Nature 408:488-492.

70. Ito, H., Fukuda, Y., Murata, K., and Kimura, A. (1983). Transformation of intact yeast cells treated with alkali cations. J Bacteriol. 153:163-168.

71. Iwanejko, L., Smith, K.N., Loeillet, S., Nicolas, A., and Fabre, F. (1999). Disruption and functional analysis of six ORFs on chromosome XV: *YOL117w*, *YOL115w* (*TRF4*), *YOL114c*, *YOL112w* (*MSB4*), *YOL111c* and *YOL072w*. Yeast 15:1529-1539.

72. Jansen, G., Bühring, F., Hollenberg, C.P., and Ramizani Rad, M. (2001) Mutations in the SAM domain of *STE50* differentially influence the MAPK-mediated pathways for mating, filamentous growth and osmotolerance in *Saccharomyces cerevisiae*. Mol. Genet. Genomics 265: 102-117.

73. Kaffmann, A., and O'Shea, E.K. (1999). Regulation of nuclear localization: a key to a door. Annu. Rev. Cell. Dev. Biol. 15:291-339.

74. Ketchum, C.J., Schmidt, W.K., Rajendrakumar, G.V., Michaelis, S, and Maloney, P.C. (2001). The yeast a-factor transporter Ste6p, a member of the ABC superfamily, couples ATP hydrolysis to pheromone export. J Biol. Chem. 276:29007-19011.

75. Kieran, M.W., Katz, S., Vail, B., Zon, L.I., and Mayer, B.J. (1999). Concentration-dependent positive and negative regulation of a MAP Kinase by a MAP kinase kinase. Oncogene 18:6647-6657.

76. Klis, F.M., de Groot, P., and Hellingwerf, K. (2001). Molecular organization of the cell wall of Candida albicans. Med. Mycol. 1: 1-8.

77. Kolling, R., and Hollenberg, C. P. (1994). The ABC-transporter Ste6 accumulates in the plasma membrane in a ubiquitinated form in endocytosis mutants. EMBO J 13:3261-3271.

78. Kolling, R., and Losko, S. (1997). The linker region of the ABC-transporter Ste6 mediates ubiquitination and fast turnover of the protein. EMBO J 16:2251-2261.

79. Kranz, J.E., Satterberg, B., and Elion, E.A. (1994). The MAP kinase Fus3 associates with and phosphorylates the upstream signaling component Ste5. Genes Dev. 8:313-327.

80. Kuchler, K., Dohlman, H.G., and Thorner, J. (1993). The a-factor transporter (*STE6* gene product) and cell polarity in the yeast *Saccharomyces cerevisiae*. J Cell Biol. 120:1203-1215.

81. Kunzler, M., Trueheart, J., Sette, C., Hurt, E., and Thorner, J. (2001). Mutations in the *YRB1* gene encoding yeast ran-binding-protein-1 that impair nucleocytoplasmic transport and suppress yeast mating defects. Genetics. 157:1089-1105.

82. Leberer, E., Dignard, D., Harcus, D., Hougan, L., Whiteway, M., and Thomas, D.Y. (1993). Cloning of *Saccharomyces cerevisiae STE5* as a suppressor of a Ste20 protein kinase mutant: structural and functional similarity of Ste5 to Far1. Mol. Gen. Genet. 241:241-254.

83. Leberer, E., Thomas, D.Y., and Whiteway, M. (1997). Pheromone signalling and polarized morphogenesis in yeast. Curr. Opin. Genet. Dev. 7:59-66.

84. Leberer, E., Wu, C.L., Leeuw, T., Fourestlieuvin, A., Segall, J.E., and Thomas, D.Y. (1997). Functional characterization of the Cdc42p binding domain of yeast Ste20 protein kinase. EMBO J. 16:83-97.

85. Lee, K.S., Irie, K., Gotoh, Y., Watanabe, Y., Araki, H., Nishida, E., Matsumoto, K., and Levin, D.E. (1993). A yeast mitogen-activated protein kinase homolog (Mpk1p) mediates signalling by protein kinase C. Mol. Cell. Biol. 13:3067-3075.

86. Lee, B.N., Elion, E.A. (1999). The MAPKKK Ste11 regulates vegetative growth through a kinase cascade of shared signaling components. Proc Natl Acad Sci USA. 96:12679-12684.

87. Leeuw, C., Leeuw, T., Leberer, E., Thomas, D.Y., and Whiteway, M. (1998). Cell cycle- and Cln2p-Cdc28p-dependent phosphorylation of the yeast Ste20p protein kinase. J Biol Chem. 273:28107-28115.

88. Leeuw, T., Fourest-Lieuvin, A., Wu, C., Chenevert, J., Clark, K., Whiteway, M., Thomas, D.Y., and Leberer, E. (1995). Pheromone response in yeast: association of Bem1p with proteins of the MAP kinase cascade and actin. Science 270:1210-1213.

89. Lillo, J.A., Andaluz, E., Cotano, C., Basco, R., Cueva, R., Correa, J., and Larriba, G. (2000). Disruption and phenotypic analysis of six open reading frames from the left arm of *Saccharomyces cerevisiae* chromosome VII. Yeast 16:365-375.

90. Lustig, A.J. (1998). Mechanisms of silencing in *Saccharomyces cerevisiae*. Curr. Opin. Genet. Dev. 8:233-239.

91. Ma, D., Cook, J.G., and Thorner, J. (1995). Phosphorylation and localization of Kss1, a MAP kinase of the *Saccharomyces cerevisiae* pheromone response pathway. Mol. Biol. Cell. 6:889-909.

92. Mackay, V., and Manney, T.R. (1974). Mutations affects sexual conjugation and reated processes in *Saccharomyces cerevisiae* pheromone response pathway. Mol. Biol. Cell 16:4095-4106.

93. Mahanty, S.K., Wang, Y., Farley, F.W., and Elion, E.A. (1999). Nuclear shuttling of yeast scaffold Ste5 is required for its recruitment to the plasma membrane and activation of the mating MAPK cascade. Cell 98:501-512.

94. Metodiev, M.V., Matheos, D., Rose, M.D., and Stone, D.E. (2002). Regulation of MAPK function by direct interaction with the mating-specific Galpha in yeast. Science. 296:1483-1486.

95. Michaelis, S and Herskowitz, I. (1988). The a-factor pheromone of *Saccharomyces cerevisiae* is essential for mating. Mol. Cell. Biol. 8:1309-1318.

96. Michaelis, S. (1993). *STE6*, the yeast a-factor transporter. Semin. Cell Biol. 4:17-27.

97. Moreau, V., Madania, A., Martin, R.P., Winson, B. (1996). The *Saccharomyces cerevisiae* actin-related protein Arp2 is involved in the actin cytoskeleton. J Cell Biol. 134:117-132.

98. Mukai, Y., Harashima, S., and Oshima, Y. (1993). Function of the Ste signal transduction pathway for mating pheromones sustains *MAT*a1 transcription in *Saccharomyces cerevisiae*. Mol. Cell. Biol. 13:2050-2060.

99. Mumberg, D., Muller, R., and Funk, M. (1994). Regulatable promoters of *Saccharomyces cerevisiae*: comparsion of transcriptional activatity and their use for heterologous expression. Nucleic Acids Res. 22: 5767-5768.

100. Nern, A., and Arkowitz, R.A. (2000). Nucleocytoplasmic shuttling of the Cdc42p exchange factor Cdc24p. J Cell Biol. 148:1115-1122.

101. Nishida, E., and Gotoh, Y. (1993). The MAP kinase cascade is essential for diverse signal transduction pathways. Trends Biochem. Sci. 18:128-131.

102. Pemberton, L.F., Blobel, G., and Rosenblum, J.S. (1998). Transport routes through the nuclear pore complex. Curr. Opin. Cell. Biol. 10:392-399.

103. Peter, M., Gartner, A., Horecka, J., Ammer, G. and Herskowitz, I. (1993). *FAR1* links the signal transduction pathway to the cell cycle machinery in yeast. Cell 73:747-760.

104. Printen, J.A., and Sprague, G.F., Jr. (1994). Protein-protein interactions in the yeast pheromone response pathway: Ste5p interacts with all members of the MAP Kinase cascade. Genetics 138: 609-619.

105. Pryciak, P.M., and Huntress, F.A. (1998). Membrane recruitment of the kinase cascade scaffold protein Ste5 by the Gbetagamma complex underlies activation of the yeast pheromone response pathway. Genes Dev. 12:2684-2697.

106. Ramezani-Rad, M. (2003). The role of adaptor protein Ste50-dependent regulation of the MAPKKK Ste11 in multiple signalling pathways of yeast. Curr. Genet. 43:161-70.

107. Reiser, V., Ruis, H., and Ammerer, G. (1999). Kinase activity-dependent nuclear export opposes stress-induced nuclear accumulation and retention of Hog1 mitogen-activated protein kinase in the budding yeast *Saccharomyces cerevisiae*. Mol. Biol. Cell 10:1147-1161.

108. Roberg, K.J., Rowley, N., Kaiser, C.A. (1997). Physiological regulation of membrane protein sorting late in the secretory pathway of *Saccharomyces cerevisiae*. J Cell Biol. 137:1469-1482.

109. Roberts, C.J., Nelson, B., marton, M.J., Stoughton, R., Meyer, M.R., Bennett, H.A., He, Y.D. D., Dai, H.Y., Walker, W.L., and Hughes, T.R. (2000). Signaling and circuitry of multiple MAPK pathways revealed by a matrix of global gene expression profiles. Science 287:873-880.

110. Robinson, M.J., Stippec, S.A., Goldsmith, E., White, M.A., and Cobb, M.H. (1998). A constitutively active and nuclear form of the MAP kinase ERK2 is sufficient for neurite outgrowth and cell transformation. Curr. Biol. 8:1141-1150.

111. Rodriguez-Navarro, S., Estruch, F., and Perez-Ortin, J.E. (1999) Functional analysis of 12 ORFs from *Saccharomyces cerevisiae* chromosome II. Yeast 15:913-919.

112. Roemer, T., Madden, K., Chang, J., and Snyder M. (1996). Selection of axial growth sites in yeast requires Axl2p, a novel plasma membrane glycoprotein. Genes Dev. 10:777-793.

113. Roemer, T., Vallier, L., and Snyder, M. (1996). Selection of polarized growth sites in yeast. Trends Cell Biol. 6:434-441.

114. Rose, M.D. (1996). Nuclear fusion in the yeast *Saccharomyces cerevisiae*. Annu. Rev. Cell Dev. Biol. 12:663-695.

115. Rose, M.D., Misra, L.M., and Vogel, J.P. (1989). *KAR2*, a karyogamy gene, is the yeast homolog of the mammalian BiP/GRP78 gene. Cell 57:1211-1221.

116. Ruiz, C., Escribano, V., Morgado, E., Molina, M., Mazon, M.J. (2003). Cell-type-dependent repression of yeast a-specific genes requires Itc1p, a subunit of the Isw2p-Itc1p chromatin remodelling complex. Microbiology. 149:341-351.

117. Sambrook, J., Fritsch, E.F., and Maniatis, T. (1989). Molecular Cloning: A laboratory Manual. Cold Spring Harbor, NY: Cold Spring Harbor Laboratory.

118. Schilke, B., Forster, J., Davis, J., James, P., Walter, W., Laloraya, S., Johnson, J., Miao, B., and Craig, E. (1996). The cold sensitivity of a mutant of *Saccharomyces cerevisiae* lacking a mitochondrial heat shock protein 70 is suppressed by loss of mitochondrial DNA. J Cell Biol. 134:603-613.

119. Schmidt, W.K., Tam, A., Michaelis, S. (2000). Reconstitution of the Ste24p-dependent N-terminal proteolytic step in yeast a-factor biogenesis. J Biol. Chem. 275:6227-6233.

120. Schnabl, M., Oskolkova, O.V., Holic, R., Brezna, B., Pichler, H., Zagorsek, M., Kohlwein, S.D., Paltauf, F., Daum, G., and Griac, P. (2003). Subcellular localization of yeast Sec14 homologues and their involvement in regulation of phospholipid turnover. Eur. J Biochem. 270:3133-3145.

121. Shen, X., Ranallo, R., Choi, E., and Wu, C. (2003). Involvement of actin-related proteins in ATP-dependent chromatin remodelling. Mol. Cell. 12:147-155.

122. Shimada, Y., Gulli, M.P., and Peter, M. (2000). Nuclear sequestration of the exchange factor Cdc24 by Far1 regulates cell polarity during yeast mating. Nat. Cell Biol. 2:117-124.

123. South, S.T., Baumgart, E., and Gould, S.J. (2001). Inactivation of the endoplasmic reticulum protein translocation factor, Sec61p, or its homolog, Ssh1p, does not affect peroxisome biogenesis. Proc Natl Acad Sci USA. 98:12027-12031.

124. Sprague, G.f, Jr., and Thorner, J. (1992). Pheromone response and signal transduction during the mating Process of *Saccharomyces cerevsiae*. Genetics. 122:19-27.

125. Sprague, G.F. Jr., Jensen, R., and Herskowitz, I. (1983). Control of yeast cell type by the mating type locus: positive regulation of the alpha-specific *STE3* gene by the *MAT* alpha 1 product. Cell. 32:409-415.

126. Sundstrom, P. (2002). Adhesion in Candida spp. Cell Microbiol. 4:461-469.

127. Tedford, K., Kim, S., Sa, D., Stevens, K., and Tyers, M. (1997). Regulation of the mating pheromone and invasive growth responses in yeast by two MAP kinase substrates. Curr. Biol. 7:228-238.

128. Terashima, H., Hamada, K., and Kitada, K. (2003). The localization change of Ybr078w/Ecm33, a yeast GPI-associated protein, from the plasma membrane to the cell wall, affecting the cellular function. FEMS Microbiol Lett. 218:175-180.

129. Titov, A.A., and Blobel, G. (1999). The karyopherin Kap122p/Pdr6p imports both subunits of the transcription factor IIA into the nucleus. J Cell Biol. 147:235-246.

130. Tohe, A., and Oguchi, T. (1999). Las21 participates in extracellular/cell surface phenomena in *Saccharomyces cerevisiae*. Genes Genet. Syst. 74:241-256.

131. Toniolo, D., Martini, G., Migeon, B.R., and Dono, R. (1988). Expression of the G6PD locus on the human X chromosome is associated with demethylation of three CpG islands within 100 kb of DNA. EMBO J. 7:104-406.

132. Trueheart, J., Boeke, J.D., and Fink, G.R. (1987). Two genes required for cell fusion during yeast conjugation: evidence for a pheromone-induced surface protein. Mol. Cell. Biol. 7:2316-2328.

133. Tyers, M., and Futcher, B. (1993). Far1 and Fus3 link the mating pheromone signal transduction pathway to three G1-phase Cdc28 kinase complexes. Mol. Cell. Biol. 13:5659-5669.

134. Van Drogen, F., Stucke, V.M., Jorritsma, G., and Peter, M. (2001). MAP kinase dynamics in response to pheromones in budding yeast. Nat. Cell Biol. 3:1051-1059.

135. Victoria, E., M., and Mazon, M.J. (2000). Disruption of six novel ORFs from *Saccharomyces cerevisiae* chromosome VII and phenotypic analysis of the deletants. Yeast 16:621-630.

136. Wang, Y., and Elion, E.A. (2003). Nuclear export and plasma membrane recruitment of the Ste5 scaffold are coordinated with Oligomerization and association with signal transduction components. Mol. Biol. Cell 14:2543-2558.

137. Whiteway, M.S., Wu, C., Leeuw, T., Clark, K., Fourest-Lieuvin, A., Thomas, D.Y., and Leberer, E. (1995). Association of the yeast pheromone response G protein beta gamma subunits with the MAP kinase scaffold Ste5p. Science 269:1572-1575.

138. Wu, C., Whiteway, M., Thomas, D.Y., and Leberer, E. (1995). Molecular characterization of Ste20p, a potential mitogen-activated protein or extracellular signal-regulated kinase kinase (MEK) kinase kinase from *Saccharomyces cerevisiae*. J Biol. Chem. 270:15984-15992.

139. Yoshida, K., and Blobel, G. (1996). The karyopherin Kap142p/Msn5p mediates nuclear import and nuclear export of different cargo proteins. J Cell Biol. 152:729-740.

140. Zeitlinger, J., Simon, I., Harbison, C.T., Hannett, N.M., Volkert, T.L., Fink, G.R., and Young, R.A. (2003). Program-specific distribution of a transcription factor dependent on partner transcription factor and MAPK signaling. Cell 113:395-404.

141. Zhan, X.L., and Guan, K.L. (1999). A specific protein-protein interaction accounts for the in vivo substrate selectivity of Ptp3 towards the Fus3 MAP kinase. Genes Dev. 13:2811-2827.

142. Zhan, X.L., Deschenes, R.J., and Guan, K.L. (1997). Differential regulation of *FUS3* MAP kinase by tyrosine-specific phosphatases *PTP2/PTP3* and dual-specificity phosphatase *MSG5* in *Saccharomyces cerevisiae*. Genes Dev. 11:1690-1702.

143. Zhang, N., Merlotti, C., Wu, J., Ismail, T., El-Moghazy, A.N., Khan, S.A., Butt, A., Gardner, D.C., Sims, P.F., and Oliver, S.G. (2001). Functional Analysis of six novel ORFs on the left arm of Chromosome XII of *Saccharomyces cerevisiae* reveals three of them responding to S-starvation. Yeast 18:325-334.

Abbreviations

aa	amino acid
AD	activation domain
amp	ampicillin
APS	adenosine phosphosulfate
bp	base pair
BCIP	5-bromo-4-chloro-3-indolylphosphate
BD	binding domain
BSA	bovine serum albumin
°C	grad celsius
CIP	calf intestinal alkaline phosphatase
DAPI	4', 6-diamidino-Z-phenylindole
DIC	differential interference-contrast microscopy
DMF	dimethylformamide
DNA	deoxyribonucleic acid
dNTP	deoxyribonucleoside triphosphate
DOC	deoxycorticosterone
DTT	dithiothreitol
EDTA	ethylene diaminetetra-acetic acid
EUROFAN	European functional analysis
GFP	green fluorescence protein
g	gram
h	hour
His	histidine
IPTG	isopropylthio-β-D-galactoside
kb	kilobase
kD	kilodalton
l	liter
LB	Luria-Bertani
Leu	leucine
M	mole
MAPK	mitogen-activated protein kinase
mA	milliampere
m.c.	multicopy
mg	miligram
min	minute
ml	milliliter
mM	millimolar
μg	microgram
μl	microliter
NBT	4-nitro-blue tetrazolium
OD	optical density
oligo	oligonucleotide
ONPG	o-nitrophenl-β-D-galactopyranoside
ORF	open reading frame
PBS	phosphate-buffered saline
PCR	polymerase chain reaction
PEG	polyethylene glycol
PMSF	phenylmethylsulfonylfluoride
RNase	ribonuclease
rpm	round per minute
RT	room temperature
s.c.	single copy
SDS	sodium dodecyl sulfate
SDS-PAGE	SDS-polyacrylamide gel electrophoresis
sec	second
TEMED	N, N, N´, N´-tetra-methylethylenediamine
Tris	tris(hydroxymethyl)aminomethane
TRP	tryptophan

U	unit
URA	uracil
UV	ultravolt
V	volt
x	times
X-gal	5-bromo-4-chloro-3-indolyl-ß -D-galactoside
YNB	Yeast Nitrogen Base
YPD	Yeast Extract/Peptone/Dextrose

Eidesstattliche Erklärung

Ich erkläre an Eides statt, dass ich die vorliegende Arbeit selbständig verfasst habe und keine anderen als die angegebenen Hilfsmittel verwendet habe.

Düsseldorf, Feb 2004

Acknowledgements

Firstly, I would like to deeply thank my advisor Prof. Dr. Cornelis P. Hollenberg for giving me the opportunity to purse the Doctor degree at the institution. These new fields of molecular genetics and genomics have challenged myself. I am very grateful to him for many discussions and suggestions in my work. I would like to thank for his trust, encouragement, and the supervision he gave me throughout the entire period of my study.

Immeasurable thanks go to PD Dr. Massoud Ramizani Rad who accepted me into his laboratory and provided all the necessary practical advice, effective supervision as well as many constructive discussions. His many discussions and advice were very helpful for my work. His concern about my progress in these studies and their completion are evident throughout the thesis. I would also like to thank him for proof-reading of my work.

I would like to thank DAAD for the financial support they gave me during my study in Germany and their support towards my family as well. Special thanks to Ms. Schädlich and other members of Referat 423 of DAAD for their efficient work, which enabled me to pursue my study and research sucessfully. I would like to thank Prof. Dr. J.H. Hegemann for the writing of recommend letter for the annual extension of scholarship. I would also like to thank my mentors in China Prof. Guoqing He, Prof. Jingpeng Wu and Prof. Yufang Xi for their recommendations and encouragement.

I would like to thank Dr. Paul A. Hardy for his critical reading of my thesis and his valuable comments. Many thanks to my colleagues: Claudia Hopp, Sven Kluge, Igo Spode, Casten Amuel, Anja Saran, Nicolas Bernsmeier for their help in writing and telephone in German, and their help in solving logistical problems. Extended thanks goes to Ms. Anna Nagy and Ms. Hannelore Gurk for their help at the institute.

Finally, the deepest thanks go to my wife Miaoying Fan and my lovely daughter Jiarui Hu, who have always given me their best support which allowed me to concentrate on my research. I will always be indebted to them. The same deepest thanks goes to my parents, my brother and my sister in China for their understanding, support and encouragement.

Lebenslauf

Name: Zheng HU
Geburtsdatum: 25.08.1970
Geburtsort: Zhejiang, China

Schulbildung:

1978-1982	Grundschule in Zhejiang, China
1982-1988	Mittelschule in Zhejiang, China

Studium:

9/1988-7/1992   Studium der lebensmittel-wissenschaften

Zhejiang University, Huajiachi Campus, Hangzhou, China

1992   Bachelor of Science

9/1992-7/1995   Magister-Studium der Mikrobiologie und Fermentation

Zhejiang University, Hua-jia-chi Campus, Hangzhou, China

1995   Master of Science

10/2000-2/2004 Doktorarbeit am Institut für Mikrobiologie

der Heinrich-Heine-Universität Düsseldorf

unter der Anleitung von Prof. Dr. Cornelis P. Hollenberg

"Functional analysis of *MDY2*, a novel gene required

for mating of the yeast *S.cerevisiae*"

Berufstätigkeiten:

8/1995- 8/1999 Wissenschaftlicher Mitarbeiter

Fakultät für Biosystem und Lebensmittel

Zhejiang University, Hua-jia-chi Campus, Hangzhou, China

Ausbildung:

9/1999-7/2000   Deutschkurs am Deutsch Kollege der Tong-Ji

Universität, Shanghai, China

8/2000-9/2000   Deutschkurs am Goethe Institut Konstanz, Deutschland